UNIVERSIDAD AUTÓNOMA DE NUEVO LEÓN

Facultad de Ingeniería Civil

FILLER EFFECT OF MINERAL POWDERS
ON ULTRA HIGH PERFORMANCE CONCRETE

Por:

MSc. GUILLERMO HERNÁNDEZ CARRILLO

Como requisito parcial para obetener el Grado de Doctor en Ingenierìa con Orientaciòn en Materiales de Conctrucciòn

Abril 2021

UNIVERSITÉ DE SHERBROOKE

Faculté de génie

Département de génie civil

EFFET DE REMPLISSAGE DES POUDRES MINÉRALES SUR LE BÉTON À ULTRA HAUTE PERFORMANCE

FILLER EFFECT OF MINERAL POWDERS ON ULTRA HIGH PERFORMANCE CONCRETE

Thèse de doctorat Spécialité génie civil

Guillermo Hernández Carrillo

A dissertation submitted in partial fulfillment of the requirements for the degree of Doctor of Philosophy
(Civil Engineering)

Jury : Arezki Tagnit-Hamou, directeur de thèse

Alejandro Durán Herrera, co-directeur de thèse

Richard Gagné, rapporteur

Luca Sorelli, évaluateur

Ismael Flores-Vivian, évaluateur

Sherbrooke (Québec), Canada **Avril 2021**

Table of content

List of Figures

List of Tables

Summary

Ultra High Performance Concrete (UHPC) design has been being refined since its conception in the 90's. Due to its very good performance in both structural and durability scenarios more and more investigations are being made around the optimization of the components needed to achieve such properties.

In the early definition of the UHPC researchers proposed that without using very large quantities of cement (between 800 and 1000 kg/m^3) and 25% addition of silica fume at water to cement (w/c) ratios below 0.25 it was impossible to obtain a compressive strength of 150 MPa, twenty years after this first proposal it has been shown that upon optimization, large quantities of cement can be replaced by other powders without decreasing the mechanical performance. The possibility of this replacement could have an explanation on the fact that cement at w/c below of around 0.4 does not reach full hydration and works like a hard inclusion in a hydrated matrix, therefore reactive or non-reactive materials could replace the cement if they can make a continuous paste by means of packing density or partial topochemical hydration.

This work has two main objectives:

- Try to explain why the unhydrated clinker still gives good properties to the binding matrix in low w/c environments
- Explain the mechanism in which metakaolin and silica fume improve the performance in Ultra High Performance Concrete systems

Key words: UHPC, Hydration, Filler effect

Résumé

La conception du béton à ultra-haute performance (BUHP) a été affinée depuis sa conception dans les années 90. En raison de ses très bonnes performances dans les scénarios de structure et de durabilité, de plus en plus de recherches sont menées sur l'optimisation des composants nécessaires pour obtenir ces propriétés.

Dans la première définition du BUHP, les chercheurs ont proposé que sans l'utilisation de très grandes quantités de ciment (entre 800 et 1000 kg/m^3) et l'ajout de 25% de fumée de silice à des rapports eau/ciment (w/c) inférieurs à 0,25, il était impossible d'obtenir une résistance à la compression de 150 MPa. Vingt ans après cette première proposition, il a été démontré qu'après optimisation, de grandes quantités de ciment peuvent être remplacées par d'autres poudres sans diminuer les performances mécaniques. La possibilité de ce remplacement pourrait avoir une explication sur le fait que le ciment à rapports eau/ciment inférieures d'environ 0,4 n'atteint pas une hydratation complète et fonctionne comme une inclusion dure dans une matrice hydratée, donc des matériaux réactifs ou non réactifs pourraient remplacer le ciment s'ils peuvent faire une pâte continue au moyen d'une densité de compactage ou d'une hydratation topochimique partielle.

Ce travail a deux objectifs principaux :

- Essayer d'expliquer pourquoi le clinker non hydraté donne encore de bonnes propriétés à la matrice de liaison dans des environnements à faible w/c

- Expliquer le mécanisme par lequel le métakaolin et les fumées de silice améliorent les performances des systèmes de béton à ultra haute performance

Mots-clés: Béton à ultra-haute performance, hydratation, effet de remplissage.

1 Introduction

The durability of building materials has been one of the main concerns along the last decades, mainly because its assurance comes with a high economic and ecologic price. As an approach to solve this issue, Ultra-High Performance Concretes (UHPC) have been under development during the last two decades with the main objective of pushing concrete to its limits in terms of structural and durability properties. UHPC is highly resilient, but its constituents (cement, silica fume, quartz sand, chemical admixtures, etc.) and their relative high volumes used during its production set the UHPC as an expensive alternative at this point of its development.

The optimization paradigm of Low Cement UHPC, with some exceptions, is to determine the portland cement quantity that can be replaced keeping the compressive strength constant without a real understanding of the mechanism that drives this mechanical property. It is known that a reactive powder can change the concrete's binder phase hydration. However, up to now it is still unclear if the improvements brought by the addition of Supplementary Cementitious Materials (SCM) come only from the chemical reactions between them and the cement hydration products. In fact, any fine particle will produce to some extent a "filler effect" that could enhance the properties of a paste regardless of its reactivity.

1.1 Problem statement

There is a consensus that cement consumption should be reduced due to its high environmental impact. In this regard, two approaches have been developed to reduce the carbon footprint of Portland Cement based concretes:

- Enhancing the concrete performance, so the durability and mechanical properties are improved. Therefore, the concrete consumption in the long term can be reduced.
- Reducing the Portland Cement consumption in concrete, replacing it with latent hydraulic or pozzolanic materials.

From the first approach, the UHPC emerges as a portland cement based concrete with large additions of Silica Fume (25% weight of cement) and low water-to-cement ratio (< 0.25). These concretes are characterized by a well packed and dense matrix, allowing them to have very long life spans if used in the same quantities as in High Performance Concrete (HPC). The high mechanical strength of this UHPC can reduce around five times the cross-sections of concrete without compromising the structural requirements (regarding axial loads) [1].

This advantage can be used in high rise buildings to increase the renting area. Though it has been already proved that in Monterrey, Mexico it is possible to attain the 150 MPa UHPC requirement, using the locally available limestone crushed aggregates, the cost per cubic meter remains high for the local construction industry [2].

Regarding the second approach, the possibility to reduce the amount of silica fume and Portland Cement in UHPC mixes in order to reduce its cost and environmental impact, is still a major topic of research around the world.

As the environmental concerns arise, the two approaches need to merge and produce a concrete with better performance in comparison with HPC, maintaining the cement and silica fume contents low to reduce the cost and carbon footprint.

It has been known since the beginning of the UHPC design, that some of the cementitious materials will remain as dry powders embedded into the dense cementitious matrix [1]. The negative effects of those large amounts of dry powders include, but are not limited to, increase of shrinkage and heat of hydration, rapid loss of workability, cracking, etc. Large replacements of both cementitious materials and quartz aggregates, have been made in order to reduce energy and consumption of materials to overcome the drawbacks previously mentioned [3]–[5]. However, the microstructural investigation of this type of studies is usually limited to observe the microstructural morphology without detailed quantification. While there are some studies dealing with the quantification of UHPC hydration degree by thermogravimetric analysis or back scattered electron image processing, these studies dealt only with the cement part and not with the SCM per-se[6]–[8]. Silica fume is one of the most expensive materials within the UHPC formulations, but its reaction has not been often quantified in UHPC as it has been in regular pastes [9], this quantification can lead to its optimization in the concrete.

The anhydrous powder within cement pastes has been replaced with calcium carbonate or quartz indistinctly [10], although the mechanical properties of those materials are different among them and from the cement. The intrinsic properties of the inert materials replacing binders are usually obviated when the replacement is made, although this is not the case when an aggregate on the conventional concrete is to be selected [11]. If the mechanical properties of the inert large aggregates have influence on the concrete strength (such as bonding, tensile

strength, etc.), these effects have to be present to some extent on the microscale of mortars and pastes too.

It does not seem that the mechanism of hydration or the mechanical properties of the inert fillers and SCM's are sufficient to explain the compressive response of the UHPC. Therefore, the quantification of powders and the cement hydration itself is important and could help with the comprehension of this phenomenon and allow UHPC designers to make optimized mixes with a wider range of powders increasing the sustainability and performance, while reducing the cost and carbon foot-print.

This project will study the effects of replacing the anhydrous clinker by different inert fillers with different hardness and hydration on ITZ structuration through analysis of back scattered electrons images (BSEI), Thermogravimetric and X-ray Diffraction Analysis (TGA, XRD). This study will help to explain the macro properties such as compressive and tensile strength, chloride diffusion coefficient and surface electrical resistivity.

Because this work is a joint research project, the research work will be conducted in both, Mexican and Canadian facilities at the University of Sherbrooke (Quebec, Canada) and the Universidad Autónoma de Nuevo León (Monterrey, México). The definition of the project and some trials and the final writing of the thesis will be done in México, while the core experimentation will be conducted in Canadian facilities. It is expected that the proposed experimental program will be concluded within three years (January 2016- December 2018).

1.2 Hypothesis

The replacement of unhydrated binding particles from UHPC by inert fillers with lower mechanical properties is possible if the porosity of the interfacial transition zone (ITZ) can be kept constant, those mixes with lower binder amounts will have a good mechanical and durability properties while reducing the costs and increasing the sustainability.

1.3 General Objective

The general objective of this thesis is the study the mechanism that gives the UHPC its mechanical strength. The investigation will be performed at microstructural and macrostructural levels through the testing of binary and ternary systems with inert fillers

.

1.4 Specific objectives

This thesis will be divided in the following stages:

- The metakaolin, silica fume and cement hydration will be quantified in binary systems along with the ITZ structuration. This data will be compared with the mechanical performances and durability indices.
- The unhydrated cement in the previous study will be replaced by limestone and quartz powder and the same hydration figures will be obtained to determine which changes in the microstructure affect the mechanical and durability performance
- An ITZ analysis will be performed by coupling the porosity obtained by BSEI to determine the evolution of porosity and unhydrated material as you move away from the aggregates.

2 State of the Art

2.1 The Ultra High Performance Concrete (UHPC)

Since the human being started to build his first permanent constructions, probably with straws and adobe or with large boulders, he has always had the interest of developing a better material, more resilient, more durable. This human restlessness of always wanting to surpass the achievements of the previous generations has taken him to the moon, to the depths of the ocean and all of this has been possible through the development of materials science and technology.

The use of concrete and mortar goes back to the year 2000 B.C. when the Minoic culture used lime based mortars [12]. Many civilizations made attempts to develop hydraulic binders, some try with gypsum, nevertheless, gypsum and lime based binders are not durable and it was not until the roman empire discovered the pozzolanic reaction that it was possible to build construction that could resist the attack of water.

Portland cement is first produced at the beginning of the XIX century [13] and with its production and mix with rock aggregates and water a material that sets even under water is made, and more importantly the raw materials for its conception is widely available throughout the world at a relative low cost. Among the main advantages of the Portland cement based hydraulic concrete as an building material we can find: the compressive strength, durability and the low need for maintenance; however, the modern construction industry demands for concrete that is more easily placed, with higher ductility, lower permeability and even higher compressive strength.

The UHPC emerges as a response to such demands and is defined according to the Federal Highway Administration of the United States [14] as a cementitious composite material with discontinuous fiber reinforcement, compressive strength above 150 MPa, pre and post cracking tensile strength higher than 5 MPa, and an enhanced durability through a discontinuous pore structure.

The progress of UHPC has allowed to narrow his basic mix design of the material to the following points [15]:

- Water to cement ratio (w/c) between 0.16 and 0.27.

- Use of high range water reducers based on polycarboxylate technology
- Mini cone slump flow between 30 y 35 cm.
- Moderate fineness cement with a C_3A content significantly lower than 8%.
- Silica fume with a low carbon content dosed in addition to the cement at 25% per weight
- Steel micro fiber addition up to 2.5% of concrete's volume.

Once the basic mix design of UHPC has been seen, it would be easy to think of it as a luxury material, nevertheless, people should not cloud its vision at first sight due to the high price, there are other factors to be taken into account to evaluate a material beyond its unitary cost, such as the effective quantity of the material used in the construction, the service life, the architectonic impact, etc.

An ordinary concrete is in general specified to have 30 MPa of compressive strength whilst an UHPC should lie between 130 and 170 MPa of compressive strength, taking this change in strength it should be possible to reduce the size of the section of an structural element 5 times, multiplying this by the length of such element it would be possible to considerably decrease the weight of the structure gaining as well more renting space and reducing the amount of workforce needed for its placement since it can be considered self-compacting as well.

Several first world countries (Canada, Germany, France, Japan) have started research programs oriented to the development and application of UHPC. At least 26 bridges have been built in Canada using UHPC in one or more components [14].

With respect to the advantages of using this type of compounds it is possible to enumerate the following:

- Better investment return
- Increased design alternatives
- New architectonic possibilities
- Higher concrete's volume efficiency
- Decrease of dead loads
- Much higher durability

The development of UHPC technology has allowed several companies around the world to develop binders and aggregate combinations that comply with the UHPC definition, such

combinations have become proprietary and are sold as ready mix packages, some examples are the following:

- BSI® developed by the Eiffage group in France,
- Ductal® developed by Lafarge, Bouyges and Rhodia in Francia.
- Fortis® developed by CEMEX in Mexico.
- CRC® developed by Aalborg Portland in Denmark.

In comparison with the ordinary concrete that cost around 130 USD/m^3, the proprietary UHPC can be around 20 times more costly, because of this it is important to understand the underlying mechanism that allows such good performance in UHPC in order to allow the democratization of the material.

2.1.1 STATE OF THE ART OF UHPC WITH REDUCED TRADITIONAL CEMENTITIOUS CONTENTS

The designers of UHPC usually use the design guidelines made by Richards and Cheyrezy [1]. These recommendations are summarized in the Table 2.1.

This type of mix design usually uses at least 800 kg/m^3 of cement and 200 kg/m^3 of silica fume. These two cementitious materials joined with the high prices of the quartz sand and powder; make the democratization of the material a highly hard to accomplish task.

The amount of cement that is proposed in Richard and Cheyrezy does not reach a complete hydrated state. According to the Powers model, the minimum w/c ratio that can completely hydrated in a closed system is 0.42 [16]. Even Richard and Cheyrezy stated that the silica fume added in its design is more than the amount needed to consume all the CH, because the cement was not supposed to be completely hydrated. So, on one hand, there is a large amount of unhydrated cement, and on the other hand there is certain amount of silica fume being used only for its filling capacities and not for its chemical performance. This opens a door to replace those inactive materials by others with similar mechanical and physical properties (even if they are not reactive).

The need of quartz sand and powder has also been debated, as its main intention of use was to prevent the strength retrogression of the cement when subjected to high temperature treatments [1][17]. Nevertheless, multiple reports have shown that 150 MPa compressive strength can be achieved without heat treatments. Studies have shown that the use of well-graded limestone sand can replace both [18]. Moreover, there are reports around the world

about the use of different pozzolans to replace the standard cementitious materials on UHPC (silica fume and cement).

Some of them are summarized in Table 2.2, which also includes the composition of the most popular UHPC, Ductal [19], some observations are worth mention from this literature review:

- The material that has been more successful as partial cement replacer is the slag. This may be due to the fact that the slag is a latent binder.
- The silica fume has been only completely replaced by materials with very high specific surface area such as rice husk ash or metakaolin.
- Because of the high speed of reaction of the silica fume, the pozzolanic reaction could be attributed mainly to the silica fume, and to a lesser extent, to the other pozzolans in the mixes, although the contribution of the secondary pozzolans can't be neglected. A better understanding of the mechanism given the strength to UHPC matrixes can be achieved by following the hydration of both micro and ultra-fine pozzolans.

Table 2.1 Composition of an UHPC according to Richards and Cheyrezy [1]

Material	**Quantity by weight**
Portland cement	1
Silica Fume	0.25
Quartz Sand 150-600 um	1.1
Quartz Powder d_{50}=10 um	0.39
Superplasticizer	0.019
Water	0.17

Table 2.2 Reports of UHPC with cement and or silica fume replacements

Materials of the paste	**Ductal** [19]	**Rougeau P. (2004)** [20]				**Yun-sheng Z. (2008)**[4]	**Yang S.L (2009)** [21]	**Yazici H. (2009)**[22]	**Ta-fraoui A. (2009)**[23]	**Van Tuan N. (2011)** [24]	**Wang C. (2012)** [25]	**Ha-ssan (2012)** [26]	**Fadzil A. (2013)** [27]	**Yu R. (2014)** [6]	**Soliman N.A (2016)**[28]
Cement (kg/m^3)	712	903	903	903	903	400	657	498	824	885	450	657	724	612	392
Silica Fume (kg/m^3)	231					100	119.4	141			90	119		43.7	217
Glass Powder (kg/m^3)															392
Slag (kg/m^3)						250	429.8	83			180	418			
Fly ash (kg/m^3)		181 (ultra fine)				250		249							
Limestone (kg/m^3)			181 (ultra fine)								180			262.5	
Metakaolin (kg/m^3)				181 (ultra fine)					206				88 (Nano particles)		
Rice Husk Ash (kg/m^3)										221					
Phonolith (kg/m^3)					181 (ultra fine)										
Compressive strength	180-225	145	163	150	170	158	140	230	192	172	150	151	145	142	145

2.2 Materials in Ultra High Performance Concrete

In the following subsections it will be presented the effect of the constituent materials on the properties of UHPC based on the collected information of research around the world with the idea of allowing a better understanding of the specific role of each element on the mix design.

2.2.1 AGGREGATES

The aggregate's hardness is usually higher to the one found in the cementitious paste. An example of this is the elastic modulus of the silica which is around 70 GPa, compared to the 18 or 22 MPa of the cement paste [1].

Despite the usual usage of high performance aggregates in this type of concrete such as: granite, diabase, crushed quartz, siliceous sand, basalt, sintered bauxite or in some cases crushed steel, there are some studies that report the possibility of using limestone or crushed glass as replacement for that type of aggregates [21], [29]–[31].

According to Richards and Cheryrezi, one of the main problems of the concrete is the lack of homogeneity for what he propose the following [1]:

- Elimination of the coarse aggregate by fine sand at a maximum aggregate size of 600 micrometers
- Improvement of the mechanical properties of the paste by heat treatment and addition of silica fume
- Reduction of the aggregate/matrix ratio

In accordance with them, the aggregates in concrete form a set of hard inclusion on the matrix. When a compression force is applied, tensile and shear stresses appear in the interfacial transition zone between the aggregates and the paste which then generates cracks in the matrix. The size of such cracks is related to the size of the zone under shear or tensile stress. In the case of a spherical inclusion, the size of the cracking is directly related to diameter of the inclusion. In the case of the UHPC, a reduction in the size of the biggest aggregate by a factor of 50 (400 micrometers instead of 20 mm), can reduce in an important manner the micro fissuring coming from the following origins:

- Mechanical (external loads)
- Chemical (autogenous shrinkage)

- Thermo-mechanical (differential expansion between the paste and aggregate under heat treatment).

Despite that the hypothesis of Richard and Cheyrezy stablishes a prohibiting maximum size of the aggregates, researchers have managed to produce UHPC without removing the coarse section of the aggregates reaching even 20 mm of maximum aggregate size [25]
Collepardi [30] showed that the use of a well graded aggregate of 8 mm maximum size can replace the fine quartz sand proposed by Richard and Cheyrezy. Nevertheless, in general, for all UHPC formulation better results are obtained with finer aggregates despite their origin [32] as can be seen in the Figure 2.1.

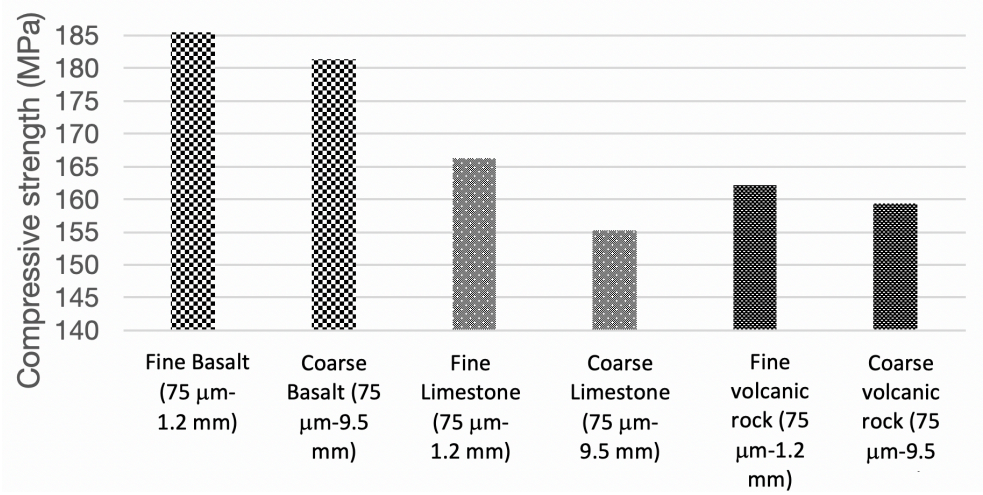

Figure 2.1 Influence of the aggregates size on compressive strength of the UHPC.

On the optimization of the granular skeletons for UHPC there are two popular models:

- Andreasen and Andersen modified model and the
- Compressible Packing Model

Andreasen and Andersen model (A&A)

The A&A model is widely used in the fabrication of UHPC, Self compacting concrete, and refractory castables [6], [33]–[36], the model suggest an granulometric curve given by the equation 2.1

$$P(D) = \frac{D^q - D^q min}{D^q max - D^q min} \qquad 2.1$$

Where:

P (D): is a fraction of the total solids that are smaller than the D size,

D: is the size of the particle in micrometers

Dmax: is the maximum aggregate size in micrometers

Dmin: is the minimum aggregate size in micrometers

q: is the distribution modulus

Higher values of the q modulus than 0.5 yield coarse mixes, lower values than 0.25 yield mixes that are rich in fine particles.

Although according to the literature the q modulus that gives the optimum packing is 0.37 [35], apparently the maximum packing density is not the more recommended, but a slightly lower number that still has a high packing density in a way that allows the mix to have a good workability and be less coarsy [37]. It has been showed [6][36], that a q between 0.22 and 0.25 is the must recommended for the mixes with high fine contents and silica fume can flow and have high strength.

The optimization of the materials quantities is made by the minimization of the eq. 2.2

$$Min(\sum_{i=1}^{n}((P_{mix}(D_i) - P_{objetive}(D_i))^2 \quad 2.2$$

Where:

P_{mix}= Percentage of the passing material at a size Di in the mixture to optimize

$P_{objective}$= Percentage of the passing material that passes at a size Di according to the A&A model

Compressible Packing Model (CPM)

Developed by François de Larrard [38], it allows to predict several characteristics of the concrete in both fresh and hardened state.

The first concept that is introduced by this model is the one called Virtual packing density, which refers to the highest packing density that a granular mix can reach if the particles where ordered one by one, scenario that only occurs theoretically.

The second concept is the dominant class. A granular class of big grains is dominant when fills the space in a way that adding a little amount of tiny grains would only fill the interstices without forcing the particles to move away from each other. A granular class of tiny grains

is dominant when consumes more space than the interstices available between big particles Figure 2.2

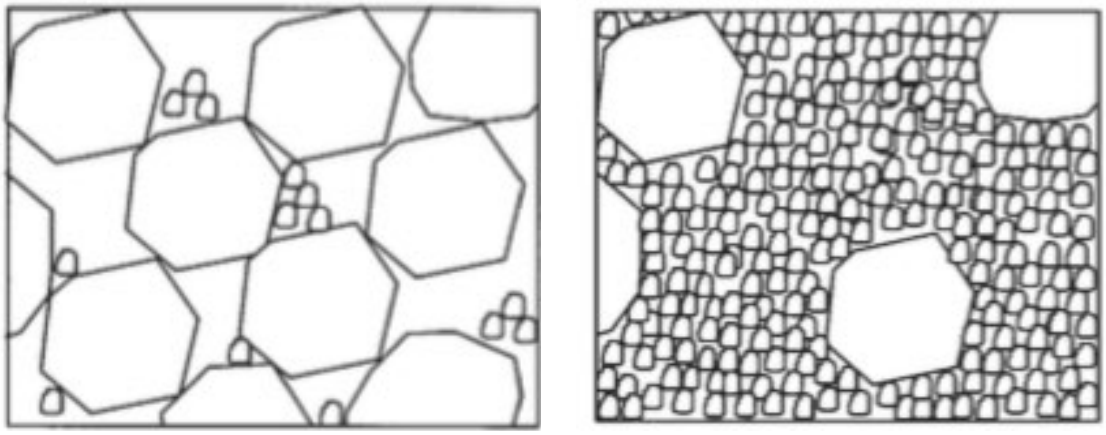

Figure 2.2. a) Granular mix with big dominant grains, b) Granular mix with tiny dominant grains

The virtual packing density of a mix having any quantity of particle sizes with a dominant class i, is given by the equation 2.3

$$\gamma_i = \frac{\beta_i}{1 - \sum_{j=1}^{i=1}\left[1 - \beta_i + b_{i,j}\beta_i\left(1 - \frac{1}{\beta_j}\right)\right]y_j - \sum_{j=i+1}^{n}\left[1 - a_{i,j}\left(1 - \frac{\beta_i}{\beta_j}\right)y_i\right]} \qquad 2.3$$

Where:

γ_i= Is the virtual packing density of a mix with a dominant class i

β_i= is the virtual packing density of the class i

y_i= Is the volumetric fraction of the class i

a_{ij}= Is the loosening effect that the class j exerts over the class i

b_{ij}= Is the Wall effect that the class j exerts over the class i

The coefficients a_{ij} and b_{ij} are given by the equations 2.4 and 2.5:

$$a_{i,j} = \sqrt{1-\left(1-\frac{d_j}{d_i}\right)^{1.02}} \quad 2.4$$

$$b_{i,j} = 1-\left(1-\frac{d_i}{d_j}\right)^{1.50} \quad 2.5$$

Since the virtual packing is only theoretical, the model takes into account the compaction methods of the particles to convert the virtual packing in real.

The compaction index K relates the real packing (φ) with the virtual one (γ) through the equation 2.6:

$$K = \sum_{i=1}^{n} K_i = \sum_{i=1}^{n} \frac{\frac{y_i}{\beta_i}}{\frac{1}{\varphi} - \frac{1}{\gamma_i}} \quad 2.6$$

The K indices are given in the Table 2.3 and are designated according to the energy of compaction.

Table 2.3 Compaction indices K

Compaction method	**K**
Simple pouring	4.1
Rodding	4.5
Vibration	4.75
Vicat probe	6.7
Vibration+compaction	9

Knowing the values of y_i, β_I, γ_I, and K, the only unknown value is φ which should be maximized changing the percentages yi in the equation 2.6 by iterations.

The CPM model has been successfully used in UHPC mix design according to [38]–[40]

2.3 Binders

The binders play a vital role in the concrete mixes, they are the glue that joins the aggregates. A difference is made between two types of binders:

- Hydraulic and latent hydraulic binders: They are conformed by the Portland cement and some slags, due to their chemical characteristics can react directly with the water and form hydrated products
- Supplementary cementitious materials (SCM): They are the ones that depend upon a source of calcium hydroxide to form hydrated, which can come from the cement reaction as a sub product, this kind of reaction is often known as pozzolanic,

In the following subsections information about the hydraulic reaction of portland cement and pozzolanic reaction of SCM'sm as well as information on the filler effect which is a phenomenon exerted by the physical interaction of fine particles on the cement hydration regardless of their ability to form compounds.

2.3.1 PORTLAND CEMENT HYDRATION

According to the ASTM C 219 [41], Portland cement is "a cementitious material produced by pulverizing clinker, consisting essentially of crystalline hydraulic calcium silicates, and usually containing one or more of the following: water, calcium sulfate, up to 5% material limestone, and processing additions".

The main compounds of the Portland cement are the following:

- Tricalcium Silicate,
- Dicalcium Silicate,
- Tricalcium Aluminate,
- Tetracalcium aluminoferrite and
- Gypsum

Each compound has a different role in the hydration mechanism of cement. A simplified explanation regarding to the mineral function of the crystalline phases in the cement is presented in the Table 2.4, accompanied with the short notation used in the cement texts and

the percentages usually found in the composition of an ordinary Portland cement. The main hydration reactions of the cement phases are summarized in the Table 2.5

From water sorption isotherms and non-evaporable water experiments on various cements, T.C Powers made in 1984 an empirical model that provides quantitative calculations of the volumetric distribution of the hydration products on the hydrated cement pastes [16]. The Powers model describes the cement hydration based on the following:

- Water can be found in three forms in a water/cement paste: chemically bounded to the different phases of the cement, physically adsorbed to sheets of hydrated products or free within capillary pores.
- The chemically bounded and physically adsorbed water are not usually available for further reaction, the hydration takes place preferably with the capillary water.
- The adsorbed water is proportional to the chemically bounded water.
- There is a volumetric change in the paste product of the density change between the anhydrous components and the hydrated products, this is called chemical shrinkage.

Table 2.4 Typical composition of an Ordinary Portland cement [42]

Chemical name	**Chemical formula**	**Short Notation**	**% in weight**	**Mineral function**
Tricalcium Silicate	$3CaO{\cdot}SiO_2$	C_3S	50	Hydrates rapidly and gives high strength and setting to the cement
Dicalcium Silicate	$2CaO{\cdot}SiO_2$	C_2S	25	Hydrates slowly and gives long term strength
Tricalcium silicate	$3CaO{\cdot}Al_2O_3$	C_3A	12	Hydrates almost instantaneously and very exothermally. Contributes to the setting and early strength
Tetracalcium aluminoferrite	$4CaO{\cdot}Al_2O_3{\cdot}Fe_2O_3$	C_4AF	8	Hydrates rapidly. Acts as melting agent in the manufacture of clinker. Gives griseous appearance to the cement.
Gypsum	$CaSO_4{\cdot}2H_2O$	$C\ \bar{S}\ H_2$	3.5	It's inter-grounded with the clinker to control the C_3A reaction.

Table 2.5 Main hydration reactions of cement Phases [43]

$2(3CaO{\cdot}SiO_2)+ 11\ H_2O$	$=3CaO{\cdot}2SiO_2{\cdot}8\ H_2O$ Calcium silicate hydrate (C-S-H) + 3 ($CaO{\cdot}\ H_2O$) Calcium Hydroxide
$2(3CaO{\cdot}SiO_2)+ 9\ H_2O$	$=3CaO{\cdot}2SiO_2{\cdot}8\ H_2O$ (C-S-H) + $CaO{\cdot}\ H_2O$ Calcium Hydroxide
$3CaO{\cdot}Al_2O_3+ 3\ (CaO{\cdot}SO_3{\cdot}2H_2O) + 26\ H_2O$	$=6CaO{\cdot}Al_2O_3{\cdot}SO_3{\cdot}12H_2O$ Ettringite (Aft)
$2(3CaO{\cdot}Al_2O_3)+ CaO{\cdot}Al_2O_3{\cdot}3SO_3{\cdot}32{\cdot}H_2O+ 4\ H_2O$	$=3(4CaO{\cdot}Al_2O_3{\cdot}SO_3{\cdot}12H_2O)$ Calcium monosulfoaluminate (AFm)
$3CaO{\cdot}Al_2O_3+CaO{\cdot}H_2O+12H_2O$	$=4CaO{\cdot}Al_2O_3{\cdot}13H_2O$ Tetracalcium aluminate hydrate
$4CaO{\cdot}Al_2O_3{\cdot}Fe_2O_3+ 10\ H_2O+ 2\ (CaO{\cdot}H_2O)$	$=6CaO{\cdot}Al_2O_3{\cdot}Fe_2O_3{\cdot}12H_2O$ Tetracalcium aluminate hydrate

With this, potential hydration of the cement can be predicted, to some extent, knowing the water to cement ratio and the type of curing. The model has been used to successfully reduce autogenous shrinkage through internal curing or to increase cement hydration through the filler effect [44], [45].

A graphical way to see the Powers Model was develop by Jensen and it is presented in the Figure 2.3. In this example of a paste with w/c 0.25, it can be seen that the cement does not have enough water to get fully hydrated.

A variety of methods to assess the hydration degree of cement have been developed, some of them are the following:

- Isothermal calorimetry.
- Chemically bound water.
- Reduction of the characteristic crystalline peaks of cement phases on X ray diffraction studies and Rietveld analysis.
- Back Scattered Electron Imaging on polished sections.
- Chemical shrinkage.

If some assumptions are made, these methods can present strong correlations among them [46].

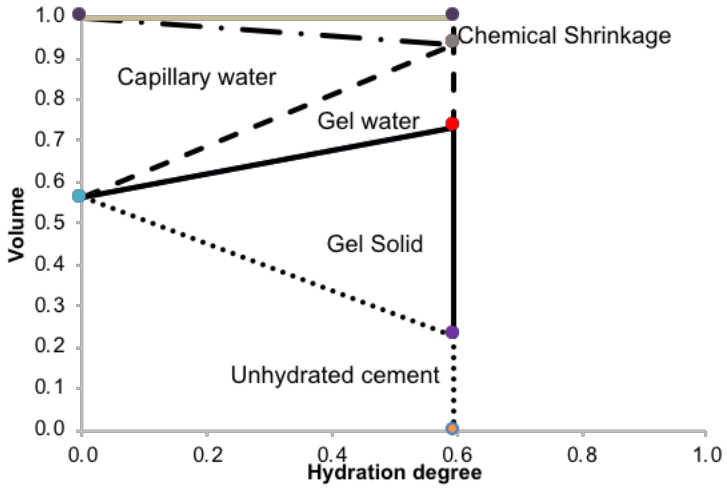

Figure 2.3 Volume distribution of a cement paste with a w/c of 0.25

2.4 Supplementary Cementitious Materials (SCM's)

It is well known that during the production of portland cement high amounts of carbon dioxide are released to the atmosphere. This fact has pushed concrete users and cement makers to reduce the cement in their mixes to diminish the impact on the environmental regulations [47].

The American Society for Testing and Materials (ASTM) defines a pozzolan as "a siliceous or siliceous and aluminous material, which in itself possesses little or no cementitious value but will, in finely divided form and in the presence of moisture, chemically react with calcium hydroxide at ordinary temperatures, to form compounds possessing cementitious properties"[48]. Currently, the use of pozzolans as partial cement replacers is widespread. Even some cement standards allow (depending on the nature of the material) the replacement of cement in percentages ranging from 5 to 50% by pozzolans [49].

SCM's can be classified into two categories: natural and artificial. Volcanic tuffs, pumices and diatomaceous earths are sorted as natural pozzolans while the second category includes fly ashes, silica fume and blast furnace ground granulated slags.

However, the effects of an active pozzolan are not limited to its reaction with the calcium hydroxide. There is also a complimentary phenomenon named "filler effect", so the mechanism of action of a pozzolan can be divided into the following:

2.4.1 FILLER EFFECT:

According to Lothenbach, the reactivity of a SCM highly depends on the alkalinity of the pore solution, which is developed during the first days of reaction [50]. Nevertheless, the strength increases in pastes with silica fume are shown from the first day, even though according to Nuclear Magnetic Resonance tests the silica fume shows almost no reaction. Therefore, the increase on strength at early ages is attributed to the filler effect.

The filler effect is driven by these two mechanisms:

- Extra space: As the filler powder is not reacting, the space for the clinker particles to react is increased.
- Enhanced nucleation: Usually the SCM's are finely grounded or fine in its nature, so the greater specific area allows the materials to act as a heterogeneous nucleation cites for the clinker phases.

2.4.2 POZZOLANIC REACTION:

The hydration of the calcium silicates of the cement produces Calcium Hydroxide (CH) and Calcium Silicate Hydrates (C-S-H) (see Table 2.5). The actual composition of the C-S-H varies. The Ca/Si ratio lies within 1.5 to 2 in Portland cement pastes. The pozzolanic reaction occurs between the CH, an amorphous silica source (S) and water (H), and it is represented in this way [51]:

$$_xCH + _yS + _zH \Longrightarrow C_xS_yH_z$$

When silica fume is used the C/S ratio of this reaction is lower than the one of Portland cement pastes, reaching values of around 1.1. The pozzolans are highly different in composition, so the hydration product changes as well. For example, pozzolans with high Alumina (A) content like metakaolin will produce beside C-S-H, a C-A-S-H type hydrate, increasing the complexity of the reaction and its study.

In the case of metakaolin additionally to the C-S-H, stratlingite may precipitate (C_2ASH_8) as well as hemi and monocarbonate when limestone is present in the cement [52][53]. Metakaolin reaction could be heavily influenced by the alkalinity of the pore solution. In [52] two cements of normal and low C_3A contents were tested, in the case of the low C_3A cement the reaction of the metakaolin was greatly hindered by the reduction of the pH of the solution product of its reaction, this phenomenon was not observed in the normal C_3A cement.

Thomas in [51] establish that the total amount of CH which can react with the pozzolan depend on the following factors:

- Nature of the pozzolan reactive phases.
- Content of reactive phases.
- SiO_2 content of reactive phases.
- CH/pozzolan ratio of the mix.
- Duration of curing.

Thomas also stated that the kinetics of the reaction would depend upon:

- Specific surface area of the pozzolan
- Water/solid ratio of the mix
- Temperature

It is important to mention that the pH of the pore solution is another factor controlling the amount of CH that can be consumed by the pozzolanic reaction. Little changes in the pH can change drastically the amount of silicon in dissolution. According to [54] for the fly ash a change from 13.99 to 13.70 produced a reduction from 16 ppm to 5 ppm of Si in solution.

2.5 Techniques to characterize hydration products

The quantity of unhydrated powders are very high in UHPC, therefore, it is necessary to use methodologies that could discern between the hydration products from the anhydrous ones and to quantify its content, composition and properties. In the following a description of the techniques that will be used in this project will be presented.

2.5.1 -BACK SCATTERED ELECTRONS (BSE) IMAGE ANALYSIS

Back scattered electron imaging of polished sections is a method to study cement and concrete microstructures that allows quantification of the hydration of the pastes in addition to the morphology of the products. This technique has shown to be in good agreement with more complex techniques, such as the X-ray diffraction with Rietveld analysis [55] (Figure 2.4).

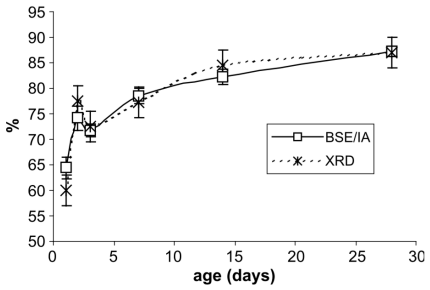

Figure 2.4 Relation between the Degree of Reaction on cement Paste obtained from BSE imaging and XRD analysis [56].

According to Scrivener [57] , the advantages of the technique are the following:

- Wide range of magnifications from 20x to 10000x allows the features to be seen in context.
- Reproducible contrast which allows quantification by image analysis of the different microstructural constituents.
- Possibility to combine BSE imaging with information from local chemical microanalyses

The intensity of a BSE signal is function of the atomic number of the affected area, if the sample is polished the topography of the sample can be neglected. It is possible to reproduce the contrast of a sample if the operational conditions are maintained. The combination of cement with water leads to products with lower atomic number than the anhydrous materials, making a contrast between the both, this contrast allows to quantify the amount of hydrates per volume of paste.

From the histogram of the image a quantification of the unhydrated volume can be done. A statistical study found that a magnification of 200x can give good results for the anhydrous phase and that a measurement of 30 fields is sufficient to get a mean error of <0.2% in pastes of mortars [57].

The BSE technique allows the study of the ITZ in context. It permits quantitative analysis of the porosity, the amount hydrates fractions and sometimes some specific phases can be de-convoluted from the histogram [58]. It has to be noted that to get reliable results from this kind of tests, a very good procedure o polishing has to be done. A description of an example of this can be found in [59].

The methodology for this technique has been discussed in [60], the technique consists in the segmentation of a 200 or 400 x BSE image, each segment made with the contour of the aggregate and a width of 3 micrometers .

Each band will yield a histogram showing distinctive peaks for anhydrous materials and C-S-H (Figure 2.5). The porosity threshold is taken arbitrary as the first inflexion point of the first peak (Figure 2.6). It is recommended to analyze at least 30 images to reduce the error.

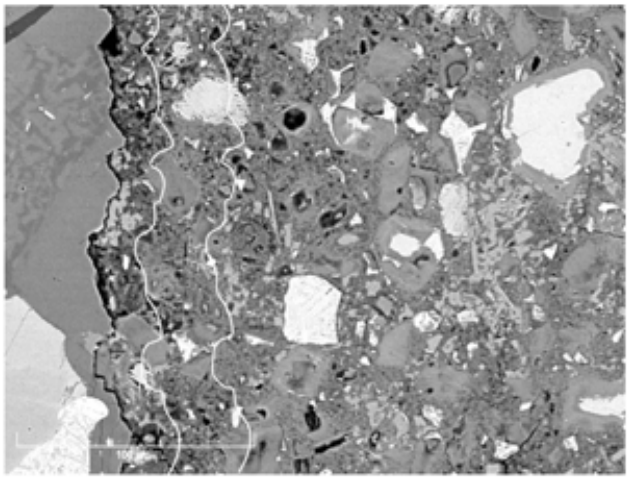

Figure 2.5 BSE image of concrete, what is seen on the left is the aggregate [61].

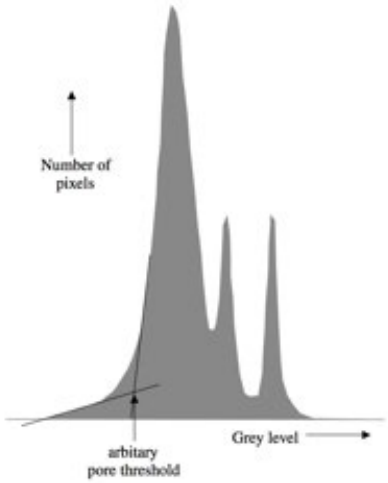

Figure 2.6 Histogram of a cement paste, the peaks to the right are attributed to unhydrated material and calcium hydroxide, while the widest peak corresponds to C-S-h, there is no peak for porosity [57].

2.5.2 -THERMOGRAVIMETRIC ANALYSIS (TGA)

Two values obtained from TGA tests can indicate the degree of reaction of a SCM, the bound water and the calcium hydroxide content.

The amount of bound water can be extracted from the weight loss between 105ºC and 1000 ºC, this measurement has been reported to be related to the results obtained from quantitative XRD [9] (Figure 2.7). The calcium hydroxide content comes from the weight loss between 410 and 480ºC that is due to water vaporization. To quantify the amount of reacted pozzolan a method of comparison between the maximum production of calcium hydroxide of the cement and the maximum consumption of the pozzolan has been proposed in the literature [55]

These calculations can be used to stablish trends in the hydration process, but are associated to the following sources of error:

- Neglecting the filler effect
- Small changes in the portlandite content can be related to large increments in the reaction of certain materials, so the sampling has to be good.
- The C-S-H composition is variable and hard to quantify
- Some pozzolans react with both portlandite and the C-S-H product of the cement reaction so an overall reduction of the C/S ratio has to be considered
- The formation of other phases like the ones with alumina can affect the portlandite consumption.

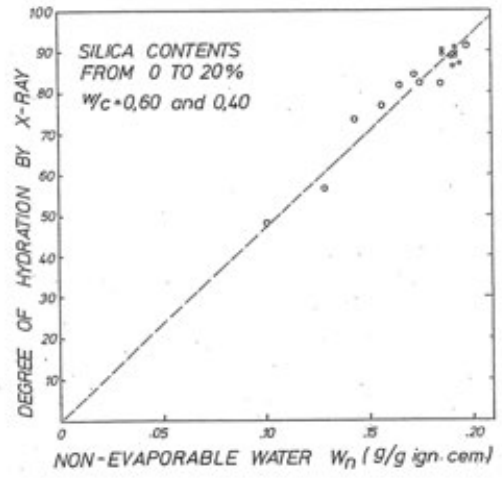

Figure 2.7 Correlation between non-evaporable water and the degree of hydration by X-Ray analysis [9]

2.5.3 X-RAY DIFFRACTION (XRD)

The X-ray diffraction (XRD) technique allows the identification of the presence of crystalline phases through reflections produced by a material at a given angle when impacted by X Rays. The position of the peaks are related to the symmetry and size of the unit cell and derived from the Bragg's law, while the intensities are product of the nature and disposition of the atoms of the crystal [59]. When different phases are present in a diffractogram, the relative intensities are indication of a mass percentage in the mixture. When the technique is used on cementitious materials, it allows the following of the hydration by the quantification of both amorphous or crystalline materials detected on the systems.

The Rietveld method uses the least squares method to reduce the differences between the observed XRD pattern and the calculated diffraction profile[62]:

$$S_y = \sum_i w_i \, ½ y_i(obs) - y_i(cal) ½^2$$

Where:

S_y= Is the function to be minimized

Y_i (obs and cal)= are the observed (obs) and calculated (cal) intensities for the "i" point of the pattern, respectively.

The intensity at an "i" point is given by the sum of the contribution of the reflections p of all the phases j and the background bkg_i[59]:

$$y_i(cal) = \sum_{j=1}^{N\ phases} S_j \sum_{p=1}^{N\ peaks} m_{p,j} Lp_p \, ½ F_{p,j} ½^2 G_{p,j}\left(2\theta_i - 2\theta_{p,j}\right) P_{p,j} + bkg_i$$

Where:

S_j= is the scale factor,

$M_{p,j}$= is the reflextion multiplicity factor,

Lp_p= is the Lorentz polarization factor,

$F_{p,j}$= is the structure factor,

$G_{p,j}(2\theta_i\text{-}2\theta_{p,j})$= is the peak shape function and

$P_{p,j}$= is the preferred orientation correction

The structure factor F_p comes from the summation over all atoms n in the unitary cell:

$$F_p = \sum_n f_n o_n \exp(2\pi i\{hx_n + ky_n + Iz_n\}) \exp(-B_n)$$

Where:

F_n= is the atomic X-ray factor that depends on the source of X-rays,

O_n= is the fractional site occupancy,

X_n, y_n, z_n= are the fractional coordinates of the atom n in the unit cell and

B_n= stands for the atomic displacement parameter.

The position of the peaks in relation to the angle θ is given by the Bragg's law:

$$\lambda = 2 d_{hkl} sin\theta$$

Where:

λ= is the wavelength of the incident X ray radiation

D_{hkl}= is the spacing between crystalline planes given by the symmetry group and the unit cell.

When only crystalline phases are present in the sample the phase weight fraction is calculated with:

$$w_j = \frac{S_j \rho_j {V_j}^2}{\sum_j^{N\ phases} S_j \rho_j {V_j}^2}$$

Where:

ρ_j= corresponds to the density of the unit cell density of the phase,

V_j= is the volume of the unit cell.

The reproducibility and accuracy of the XRD analyses depends on sample preparation, data acquisition conditions, complete identification of the crystalline phases in the sample and the control of the Rietvel quatitative phase analysis [63].

As the Rietveld analysis can only give information on the crystalline phases relative mass quantities, two methods have been developed to overcome this problem and give the results in an absolute manner:

Internal standard method: A crystalline material with known composition is blended with sample in a known quantity and the test is perform normally.

External standard: A material with known crystallinity is examined with the same conditions as the unknown target and from this a calibration "G factor" is obtained according to:

$$G = \frac{S_s \rho_s {V_s}^2 \mu_s}{C_s}$$

Where:

G= is the "G factor"

S_s= is the scale factor of the standard,

ρ_s= corresponds to the density of the unit cell density of the standard,

V_s= is the volume of the unit cell.

μ_s= is the mass attenuation coefficient (MAC) of the standard and

C_s= is the crystallinity percentage of the standard

Following the calculation of the G factor, the masses of the phases are corrected for the differences between the MAC of the sample and the standard with the following:

$$w_j = \frac{S_j \rho_j {V_j}^2 \mu_j}{G}$$

Where:

μ_s= is the mass attenuation coefficient (MAC) of the sample.

The internal standard has some known issues that could come from the lack of homogeneity of the mix, big differences between the MAC of the materials that could lead to microabsorption problems as well as problems derived by the wrong choosing of the amount of standard in the mix.

On the other hand, the external standard avoids those two problems, and the precision of the method does not depend on the amount of the amorphous material.

While the external standard method can give the absolute amounts of the phases present on the sample and quantify the unknown or amorphous content by difference, it can not separate the contribution of different amorphous species on the sample.

When the structural data is incomplete or no structural data is present at all for a given material within a sample, the Partially or not Known Crystalline Structure (PONCKS) method can allow to differentiate between such phases [64].

Amorphous materials form humps instead of well-defined narrow peaks in the XRD analyses, such humps can be fitted with a peak phase, which consist in a series of peaks and a background [65]. Such peaks can be characterized by the empirical structure factor calculated via Pawley or Le Bail curve-fitting methods to create a pseudo structure. The number of formula units per unit cell (Z), the mass of the formula unit (M) and the unit-cell volume (V) of this phase can be determined using an internal or external standard together with a pure sample [66].

When a base pattern is used to do the Pawley or Le Bail fitting, the value of V is known, leaving only the term ZM unknown. This value can be obtained with the help of the G factor method with the following expression:

$$ZM = \frac{w_a}{\frac{S_a {V_a}^2 \mu_a}{G}}$$

Where:

ZM= is the pseudo mass

w_a= weight percentage of the amorphous phase

S_a= is the scale factor of the amorphous phase,

V_s= is the pseudo volume of the unit cell of the amorphous phase and

μ_a= is the mass attenuation coefficient (MAC) of the sample containing the amorphous.

While the ZMV value of the amorphous phase does not have a physical meaning, it can be used for the quantification of its presence in mixes containing it.

The quantification of the amorphous contents with the PONCKS technique has shown to be accurate to the 3% content when 5-10% materials is replaced according to [65], while [66] states that disregarding the amount of amorphous material present in the sample the method gives a precision of about 1%.

2.5.4 QUANTITATIVE ENERGY DISPERSIVE SPECTROSCOPY

A powerful tool to examine the chemical characteristics of the phases present within a cementitious matrix is the Quantitative Energy Dispersive Spectroscopy. This technique consists of detecting the radiation emitted in the form of X-rays product of the bombarding of a solid sample with a beam of electrons.

This technique often complimentary to the SEM imaging takes advantage of the following phenomena. When an electron hits an atom of a given material, it undergoes various collisions of elastic and inelastic type, if the hit has sufficient energy an inner shell electron can be ejected. In order for the atom to gain the lowest energy state, an electron coming from an outer shell takes its place, by doing so energy is released in form of either X-ray or Auger electrons [67]. To facilitate quantification and allow high resolution, the quantitative chemical analysis can only be made on polished samples in high vacuum.

A problem that is often phased when cementitious materials are examined is the intermixing of the phases, when the electron beam is directed it affects an area of a few microns that is called “interaction volume” [59].

To overcome the problem of intermixing of phases, usually a plot of atomic ratios is made in order to make scatter plots that allow an interpretation of the compositions of the phases and

zones of intermixing. This tool is specially useful when trying to describe the C-A-S-H which usually contains inclusions of various elements.

In [68], the authors used such plots to identify big differences between the C-A-S-H formed in an OPC paste and a paste that had metakaolin and limestone additions, from this an average composition can be derived for unknown reaction products.

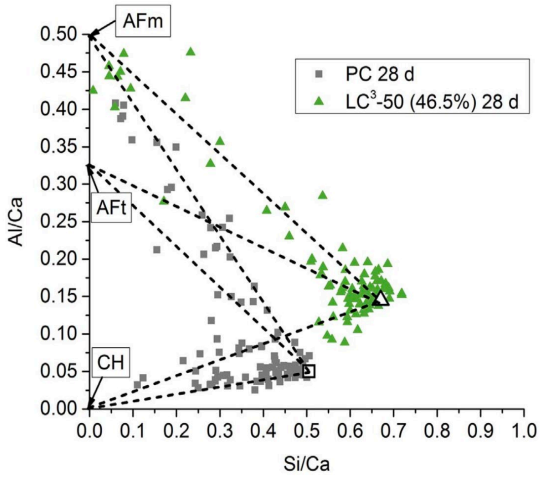

Figure 2.8 Use of scatter plots of elemental ratios to identify the C-A-S-H composition [68].

2.5.5 NANO INDENTATION:

Even though this technique will not be used in the development of this project, it gives a good insight about the reason of having unhydrated clinker particles. The basics of its application will be presented, and a literature review based on this technique will be used to choose the inert materials that will replace the cement on this thesis.

As a big quantity of cement in UHPC is unhydrated, some part of the mechanical performance of the cement pastes could come from the anhydrous clinker. This technique consists in establishing contact between an indenter and a sample, and subsequently measuring a load, and the penetration depth [69].

This test provides two characteristics of the material, the indentation hardness “H” and an indentation modulus “M”. From this kind of tests, we can know the mechanical properties of the C-S-H and the clinker (Table 2.6).

The nano indentation results from [69], show the great difference between the mechanical properties of the clinker and the C-S-H, being the first about ten times harder than the later

and having a much greater elastic modulus. Since the C-S-H is the product that binds the materials it can't be replaced, but the inert cement that remains in the concrete should be able to be replaced to some extent by a material with similar mechanical characteristics.

Given that the nano indentation is a powerful to determine the mechanical characteristics at a nano scale it can be used to characterize powders that could be used to replace the cement in terms of hardness. A literature review about the subject is presented in the Table 2.7.

Table 2.6 Nano indentation results from an UHPC [69]

Phase	Hardness (GPa)	Elasticity modulus (GPa)
Low density C-S-H	**0.55±0.03**	**19.7±2.5**
High density C-S-H	**1.36±0.35**	**34.2±5.0**
Cement Clinker	**9.12±0.90**	**141.1±34.8**

Table 2.7 Nano indentation data of possible powders to be used in concrete.

Powder	Hardness (GPa)	Elastic Modulus (GPa)
Calcite [70]	**2.21± 0.16**	**78.1±5.2**
Quartz [70], [71]	**14.54 ±0.42, 14.6**	**117.6 ± 2.7, 124 ± 0.54**
Fused silica [71]	**9**	**69.3 ± .39**
Slag [72]	**5.06±1.18**	**72.4±8.7**
Fly ash [73] [74]	**2.54-9.24, 10.128 ±3.875**	**43.8-79.1, 78.314±14.049**
Soda lime glass [71],[75],	**6.3, 5.5**	**69.9 ± 0.22, 71**
Borosilicate glass [75]	**6.4**	**63**
Kaolin [76], [77]	**0.019±0.009, 0.042±0.006**	**2.59±.008,1.3±0.5**
MetaKaolin [77]	**0.36±.017**	**6.0±0.8**

From the literature review, it can be seen that the commonly used pozzolans have about the same hardness (6 GPa), which is roughly the same as the one in soda lime glass. The fly ash according to [73] can be found in two strength classes, the weak and the strong, but the range is large between the both. The mechanical properties of the metakaolin are very low compared to the other materials, nevertheless the Table 2.2 shows mixes with metakaolin attaining very high compressive strengths.

Research on the importance of the chosen aggregates for UHPC mixes have shown that stronger aggregates yield in general better results [29][32], The Figure 2.9 shows clearly this effect. If this trend continues in a smaller scale, harder powders could replace more successfully the cement even if they are not reactive.

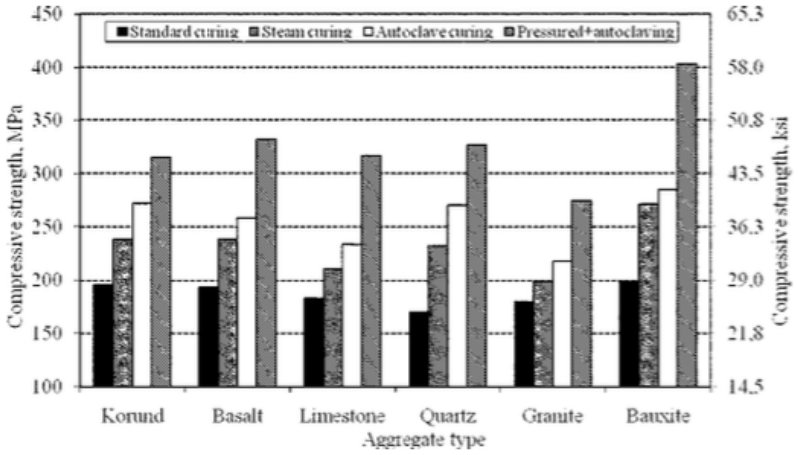

Figure 2.9 Influence of the aggregate type on compressive strength [29]

If the binding paste of the UHPC can be seen as continuous matrix of hydration products that covers certain volume of anhydrous materials, the paste of the UHPC is like a micro concrete where effects that are seen in the concrete could take place. There is an interfacial transition zone within the anhydrous particle of clinker or silica fume and the C-S-H, the roughness and the hydration products on the surface of the particle may have an effect in the strength of the paste.

2.6 The Interfacial Transition Zone (ITZ)

The concrete composition involves mainly three phases: the aggregates, the paste, and a transition phase called the interfacial transition zone which differ in properties from the formers. Both aggregates and cement paste have an elastic behavior before fracture, whereas concrete shows an inelastic behavior (Figure 2.10). In the case of concrete, the deformation is not controlled by the interatomic forces like in the case of homogenous materials, but the porosity of the ITZ, which is usually the weaker part of the concrete.

There are plenty of reasons that can explain why the ITZ is weaker than the bulk paste, but the main one is that there is an effective higher water to cement ratio (w/c) on the vicinity of

the aggregate, this increase of the w/c has been found to be proportional to the size of the aggregate Figure 2.11.

The effect of the increase of the water to cement ratio on the strength is well explained in the Figure 2.12 extracted from [78]. The higher the amount of water in a cement paste the larger the distance the hydrates must go through to find another particle to form a percolation path. The higher porosity and lower mechanical properties of the ITZ makes the study of it very important when the design of low permeability or high strength concrete is pursued.

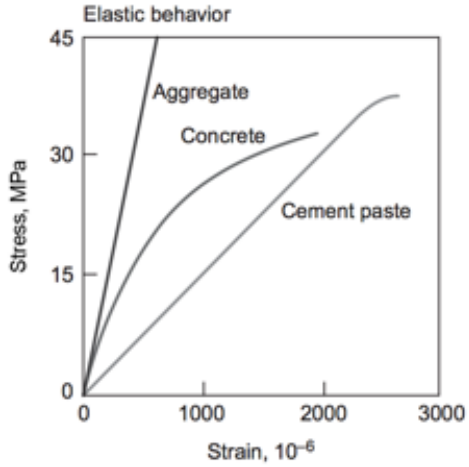

Figure 2.10 Behavior under stress of the concrete vs its components [79]

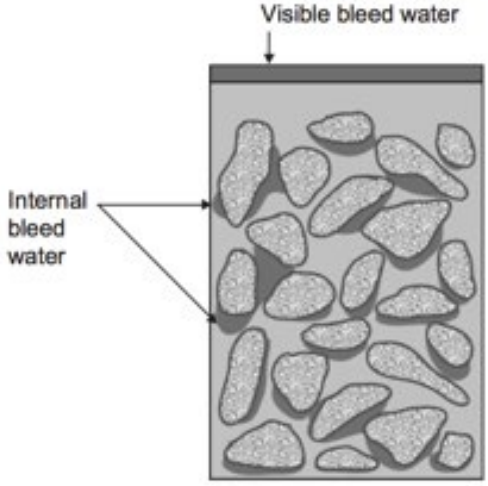

Figure 2.11 Internal bleeding of the concrete leading to higher w/c around the aggregate [79]

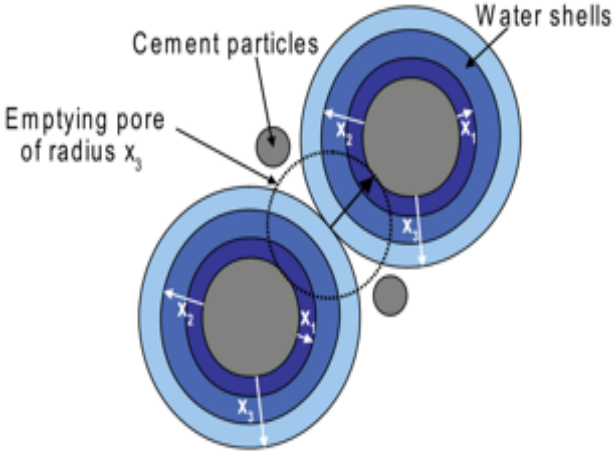

Figure 2.12 Effect of the water layers in the distance between cement Particles [78].

2.6.1 -THE SILICA FUME EFFECT ON THE CEMENT PASTE-AGGREGATE INTERFACE

The discovery of the advantages of the use of silica fume in concrete formulations gave birth to a new class of concrete, the high strength concrete, however the causes of the strength increase of silica fume-portland cement concretes were not clear.

The amorphous and very fine nature of the silica fume affects concrete in two very different ways [10]:

- Upon reacting with the calcium hydroxide, it forms a C-S-H that resembles the one coming from the alite increasing the amount of the binding phase.
- The very fine nature allows it to serve as good site for heterogeneous nucleation of the cement products.

These two effects affect directly the strength and transport properties of the concrete. The silica fume increases the pace of the reactions and reduces the volumetric fraction of large porosity, nevertheless the total porosity remains unchanged.

It is suggested in [80] that the contribution of the silica could be related to the densification of the aggregate transition zone improving the aggregate/paste matrix bond. To prove this asseveration, they compared the ITZ of a reference concrete made at 0.33 w/c with a mix having a 15% replacement of silica fume, to keep the workability at the same level a superplasticizer was used.

Some remarks from that work are the following:

- The amount of silica fume used does not affect the packing density of the cement, leaving the same spatial distribution of unhydrated cement.
- Although the porosity gradients still exist in the silica fume mix, there is a dramatic reduction of the porosity when silica fume is present, this was attributed to the ability of the silica fume to fill the cement voids. This decrease of porosity is present from the first day but does not affect the strength until the silica fume has enough time to react (Figure 2.13).

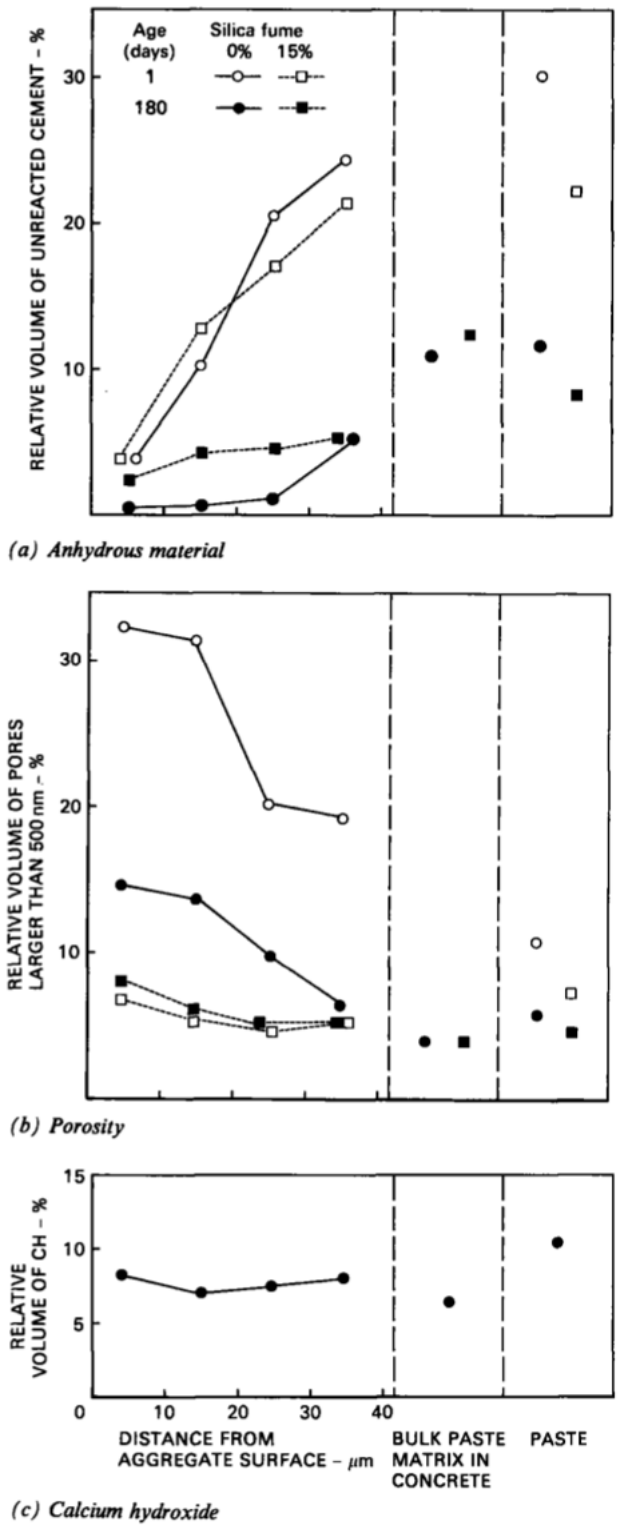

Figure 2.13 Effects of the silica fume in the ITZ, a) andhydrous material, b) porosity c) calcium hydroxide

3 Experimental methodology

3.1 Characterization of the materials

The characterization of the raw materials is described in the Table 3.1. The limestone and quartz powders will have a mean size similar to the cement one and the fine aggregate will be natural Canadian river sand.

Table 3.1 Characterization of the materials

Material / Test	Natural river sand (75um-4.75mm)	Cement with high resistance to sulfates	Limestone Powder	Quartz Powder	Silica fume	Silica Sand	Metakaolin
PSD from laser diffraction/sieving	√	√	√	√	√	√	√
Density	√	√	√	√	√	√	√
Surface area (Blaine/BET)					√	√	√
CH consumption/production		√			√		√
Oxides composition (XRF)		√	√	√	√	√	√
Phases composition (XRD)		√	√	√	√	√	√

3.2 First experimental stage: "Effect of the hardness of inert fillers as cement replacement materials on UHPC mechanical, durability and hydration properties"

The first stage deals with silica fume-opc-filler systems, both in binary and ternary mixes. It is the main goal of this paper to show how the hardness of the anhydrous particles affect the mechanical and durable properties of the composite.

Correlations between the calcium hydroxide per gram of cement, compressive strength and resistivity will be done to define to which extend the effect of such pozzolanic materials is physical.

To avoid differences in entrapped air for mortars, the superplasticizer dosage will be adjusted to get a fluid consistency and if needed, vibration will be applied.

The first part of this experiment consists in testing how the increase of silica fume affects the performance of the matrix the systems tested both in mortars or pastes are described in the Table 3.2.

The second part will consist in replacing 300 kg/m^3 of cement of the first presented systems in order to reach a 0.4 w/c to try to get the highest degree of hydration of the mixes. The cement will be replaced by either quartz or limestone, to test if the unhydrated cement can be subtracted from the matrix without deleterious consequences, the description of such systems can be found on the Table 3.3.

Both binary and ternary systems will be evaluated as mortars as described in the Table 3.4. The durability assessment of the mixes will be done with the help of electrical resistivity measurements.

The pastes of the defined systems will be studied to see if there is a correlation between the hydration of the bulk paste and the performance indicators (resistivity, compressive strength). The experiments to be performed on the pastes are defined on the Table 3.5.

Table 3.2 Binary systems to be explored in the first experimental stage

Cement content	**Silica fume addition (kg/m^3)**
800 kg/m^3 w/c 0.25	**0**
	40
	80
	120

Table 3.3 Ternary systems to be explored on second part of the first experimental stage

Cement content	**Quartz Powder**	**Limestone**	**Silica fume**
500 kg/m^3 w/c 0.4	**Volume of 300 kg of cement**		**0,40, 80, 120, and 240 kg/m^3**
		Volume of 300 kg of cement	

Table 3.4 Test to be performed on mortars of the first experimental stage

Test	Age
Volumetric weight, spread, entrapped air content	**Fresh state**
Compressive strength	**7, 28, 91 days**
Resistivity	**7, 28, 91 days**
ITZ porosity and unhydrated part determination by SEM, BSE	**91 days**

Table 3.5 Tests to be performed on pastes for the first experimental stage

Test	Age
XRD	**91 days**
TGA	**7, 28, 91 days**
EDS	**91 days**

3.3 Second experimental stage "Filler effect in Cement-Limestone-Calcined clays systems in UHPC"

Within this is second stage there is an evaluation on how metakaolin affects the properties of cementitious Portland cement matrices. The first part deals with the increase dosage of metakaolin to an ordinary Portland cement system at a w/c of 0.25 as described in the Table 3.6

For the second stage, the unhydrated cement will be replaced with either limestone or quartz powder until reaching a w/c of 0.4. The reasoning behind this replacement comes from the well-studied idea that the system Portland cement-metakaolin-limestone yields monocarboaluminate compounds that could enhance the mechanical properties of the systems, to have a comparison with an inert filler a set of cement replaced by quartz powder mixes are proposed in the Table 3.7

The test to be done on mortars are shown in the Table 3.8 while the test to be done in pastes in Table 3.9.

Table 3.6 Binary systems to be tested in the first part of the second experimental stage

Cement content	Metakaolin addition (kg/m^3)
800 kg/m^3 w/c 0.25	0
	40
	80
	120
	240

Table 3.7 Ternary systems to be explored in the second part of the second experimental stage

Cement content	Quartz Powder	Limestone	Metakaolin
500 kg/m^3 w/c 0.4	Volume of 300 kg of cement		0, 40, 80, 120, and 240 kg/m^3
		Volume of 300 kg of cement	

Table 3.8 Test to be performed on mortars of the second experimental stage

Test	Age
Volumetric weight, spread, air content	Fresh state
Compressive strength	7, 28, 91 days
Electrocal resistivity	7, 28, 91 days

Table 3.9 Tests to be done on Pastes for the second experimental stage

Test	Age
XRD	91 days
TGA	91 days

4 References

[1] P. Richard and M. Cheyrezy, "Composition of reactive powder concretes," *Cem. Concr. Res.*, vol. 25, no. 7, pp. 1501–1511, 1995.

[2] G. Hernández Carrillo, A. Durán Herrera, and P. L. Valdez Tamez, "ULTRA HIGH PERFORMANCE CONCRETE (UHPC) WITH LOW SILICA FUME CONTENTS AND

LIMESTONE AGGREGATES," *Proc. RILEM Int. Conf. Mater. Syst. Struct. Civ. Eng. Conf. Segm. Concr. with Suppl. Cem. Mater.*, pp. 349–358, 2016.

[3] Z. Rong, W. Sun, and Y. Zhang, "Dynamic compression behavior of ultra-high performance cement based composites," *Int. J. Impact Eng.*, vol. 37, no. 5, pp. 515–520, 2010.

[4] Z. Yunsheng, S. Wei, L. Sifeng, J. Chujie, and L. Jianzhong, "Preparation of C200 green reactive powder concrete and its static-dynamic behaviors," *Cem. Concr. Compos.*, vol. 30, no. 9, pp. 831–838, 2008.

[5] J. Camiletti, A. M. Soliman, and M. L. Nehdi, "Effects of nano- and micro-limestone addition on early-age properties of ultra-high-performance concrete," *Mater. Struct.*, vol. 46, no. 6, pp. 881–898, 2013.

[6] R. Yu, P. Spiesz, and H. J. H. Brouwers, "Mix design and properties assessment of Ultra-High Performance Fibre Reinforced Concrete (UHPFRC)," *Cem. Concr. Res.*, vol. 56, pp. 29–39, 2014.

[7] W. Xu *et al.*, "Effect of rice husk ash fineness on porosity and hydration reaction of blended cement paste," *Constr. Build. Mater.*, vol. 89, pp. 90–101, 2015.

[8] N. Van Tuan, G. Ye, K. Van Breugel, and O. Copuroglu, "Hydration and microstructure of ultra high performance concrete incorporating rice husk ash," *Cem. Concr. Res.*, vol. 41, no. 11, pp. 1104–1111, 2011.

[9] E. J. Sellevold, B. D.H, E. Klitgaard Jensen, and T. Knudsen, "Silica fume - cement pastes; hydration and pore structure," Trondheim, 1982.

[10] B. Lothenbach, K. L. Scrivener, D. Hooton, B. Lothenbach, K. Scrivener, and R. D. Hooton, "Supplementary Cementitious Materials Supplementary cementitious materials," vol. 74, no. October 2015, pp. 211–278, 2011.

[11] H. Beshr, A. . Almusallam, and M. Maslehuddin, "Effect of coarse aggregate quality on the mechanical properties of high strength concrete," *Constr. Build. Mater.*, vol. 17, no. 2, pp. 97–103, 2003.

[12] P.-C. Aitcin, *Binders for Durable and Sustainable Concrete*. 2018.

[13] M. Tang, *High performance Concrete – Past, Present and Future*. 2004.

[14] H. Russel, G and B. a. Graybeal, "Ultra-High Performance Concrete : A State-of-the-Art Report for the Bridge Community," no. June, p. 171, 2013.

[15] K. Wille, A. E. Naman, and G. J. Parra-Montesinos, "Ultra - High Performance Concrete with Compressive Strength Exceeding 150 MPa (22ksi) : A Simpler Way," *ACI Mater. J.*, vol. 108, no. 1, pp. 46–53, 2011.

[16] O. M. Jensen and P. F. Hansen, "Water-entrained cement-based materials I . Principle and

theoretical background," *Cem. Concr. Res.*, vol. 31, no. 4, pp. 647–654, 2000.

[17] B. Iverson, J. Maxson, and D. Bour, "Strength Retrogression in Cements Under High-Temperature Conditions," *Thirty-Fifth Work. Geotherm. Reserv. Eng.*, 2010.

[18] "Mechanical Properties of Modified Reactive Powder Concrete By S. Collepardi, L. Coppola, R. Troli, M. Collepardi."

[19] B. Graybeal, "Material Property Characterization of Ultra-High Performance Concrete," Georgetown Pike McLean, VA, 2006.

[20] P. Rougeau and B. Borys, "Ultra high performance concrete with ultrafine particles other than silica fume.," in *International symposium on ultra high performance concrete. Kassel: University of Kassel*, 2004, pp. 213–226.

[21] S. L. Yang, S. G. Millard, M. N. Soutsos, S. J. Barnett, and T. T. Le, "Influence of aggregate and curing regime on the mechanical properties of ultra-high performance fibre reinforced concrete (UHPFRC)," *Constr. Build. Mater.*, vol. 23, no. 6, pp. 2291–2298, 2009.

[22] H. Yazıcı, M. Y. Yardımcı, S. Aydın, and A. Ş. Karabulut, "Mechanical properties of reactive powder concrete containing mineral admixtures under different curing regimes," *Constr. Build. Mater.*, vol. 23, no. 3, pp. 1223–1231, Mar. 2009.

[23] A. Tafraoui, G. Escadeillas, S. Lebaili, and T. Vidal, "Metakaolin in the formulation of UHPC," *Constr. Build. Mater.*, vol. 23, no. 2, pp. 669–674, 2009.

[24] V. T. Nguyen, "Rice husk ash as a mineral admixture for Ultra High performance Concrete," Delft University of Technology, 2011.

[25] C. Wang, C. Yang, F. Liu, C. Wan, and X. Pu, "Preparation of Ultra-High Performance Concrete with common technology and materials," *Cem. Concr. Compos.*, vol. 34, no. 4, pp. 538–544, 2012.

[26] A. M. T. Hassan, S. W. Jones, and G. H. Mahmud, "Experimental test methods to determine the uniaxial tensile and compressive behaviour of Ultra High Performance Fibre Reinforced Concrete(UHPFRC)," *Constr. Build. Mater.*, vol. 37, pp. 874–882, 2012.

[27] A. Mohd Fadzil *et al.*, "Alteration of Nano Metakaolin for Ultra High Performance Concrete," no. SEPTEMBER 2013, pp. 5–7, 2013.

[28] N. A. Soliman and A. Tagnit-Hamou, "Development of ultra-high-performance concrete using glass powder Towards ecofriendly concrete," *Constr. Build. Mater.*, vol. 125, pp. 600–612, 2016.

[29] S. Aydin, H. Yazici, M. Y. Yardimci, and H. Yigiter, "Effect of aggregate type on mechanical properties of reactive powder concrete," *ACI Mater. J.*, vol. 107, no. 5, pp. 441–449, 2010.

[30] S. Collepardi, L. Coppola, R. Troli, and M. Collepardi, "Mechanical Properties of Modified

Reactive Powder Concrete," 1997.

[31] M. M. Reda, N. G. Shrive, and J. E. Gillott, "Microstructural investigation of innovative UHPC," *Cem. Concr. Res.*, vol. 29, no. 3, pp. 323–329, 1999.

[32] K. Wille and C. Boisvert-Cotulio, "Material efficiency in the design of ultra-high performance concrete," *Constr. Build. Mater.*, vol. 86, pp. 33–43, 2015.

[33] K. Wille and A. E. Naaman, "The path to ultra-high performance fiber reinforced concrete (UHP-FRC): five decades of progress.," *Proc. Hipermat 2012 3rd Int. Symp. UHPC Nanotechnol. high Perform. Constr. Mater.*, pp. 3–13, 2012.

[34] J. J. H. and R. Brouwers H.J., "Self-compacting concrete: the role of the particle size distribution," *First Int. Symp. Des. Perform. Use Self-Consolidating Concr.*, vol. 0, no. May, pp. 109–118, 2005.

[35] B. Sealey, *Elkem Materials Mixture Analyser "EMMA" User Guide", Versión 2, Elkem*. .

[36] B. Myhre, "The effect of particle-size distribution on flow of refractory castables," *Elkem Refractories*. pp. 3–17, 1994.

[37] P. N. Quiroga and D. W. Fowler, "Guidelines for proportioning optimized concrete mixtures with high microfines," *Int. Cent. Aggregates Res. Rep. 104-2.*, 2004.

[38] F. de Larrard, "Concrete Mixture Proportioning - A Scientific Approach. Modern Concrete Technology Series," *Mod. Concr. Technol.*, vol. 9, p. 421, 1999.

[39] R. D. Toledo Filho, E. A. B. Koenders, S. Formagini, and E. M. R. Fairbairn, "Performance assessment of Ultra High Performance Fiber Reinforced Cementitious Composites in view of sustainability," *Mater. Des.*, vol. 36, pp. 880–888, 2012.

[40] N. A. Soliman and A. Tagnit-Hamou, "Partial substitution of silica fume with fine glass powder in UHPC: Filling the micro gap," *Constr. Build. Mater.*, vol. 139, pp. 374–383, 2017.

[41] ASTM International, "ASTM C219-07a, Standard Terminology Relating to Hydraulic Cement." West Conshohocken, PA., pp. 24–26, 2007.

[42] H. G. van Oss, "Background Facts and Issues Concerning Cement and Cement Data," *U.S. Geol. Surv.*, 2005.

[43] S. H. Kosmatka, B. Kerkhoff, and W. C. Panarese, *Design and control of concrete mixtures*. 2002.

[44] D. P. Bentz, E. F. Irassar, B. E. Bucher, and W. J. Weiss, "Limestone Fillers Conserve Cement - Part 1: An analysis based on Powers' model," *Concr. Int.*, vol. 3, no. November, pp. 41–46, 2009.

[45] M. T. Hasholt, O. M. Jensen, K. Kovler, and S. Zhutovsky, "Can superabsorent polymers mitigate autogenous shrinkage of internally cured concrete without compromising the

strength?," *Constr. Build. Mater.*, vol. 31, pp. 226–230, 2012.

[46] V. Kocaba, E. Gallucci, and K. L. Scrivener, "Methods for determination of degree of reaction of slag in blended cement pastes," *Cem. Concr. Res.*, vol. 42, no. 3, pp. 511–525, 2012.

[47] N. Chatziaras, C. S. Psomopoulos, and N. J. Themelis, "Use of waste derived fuels in cement industry: a review," *Manag. Environ. Qual. An Int. J.*, 2016.

[48] ASTM International, "ASTM C 125-09a Standard Terminology Relating to Concrete and Concrete Aggregates." West Conshohocken, PA, 2009.

[49] Industria de la construcción –cementos hidráulicos– especificaciones y métodos de prueba, "NMX-C-414 ONNCCE." 2004.

[50] B. Lothenbach, K. Scrivener, and R. D. Hooton, "Supplementary cementitious materials," *Cem. Concr. Res.*, vol. 41, no. 12, pp. 1244–1256, 2011.

[51] M. Thomas, *Supplementary Cementing Materials in Concrete*. 2013.

[52] M. Mirzahosseini and K. A. Riding, "Effect of curing temperature and glass type on the pozzolanic reactivity of glass powder," *Cem. Concr. Res.*, vol. 58, pp. 103–111, Apr. 2014.

[53] W. Huang, H. Kazemi-Kamyab, W. Sun, and K. Scrivener, "Effect of replacement of silica fume with calcined clay on the hydration and microstructural development of eco-UHPFRC," *Mater. Des.*, vol. 121, pp. 36–46, 2017.

[54] a. L. a. Fraay, J. M. Bijen, and Y. M. de Haan, "The reaction of fly ash in concrete a critical examination," *Cem. Concr. Res.*, vol. 19, no. 2, pp. 235–246, 1989.

[55] K. L. Scrivener *et al.*, "TC 238-SCM: hydration and microstructure of concrete with SCMs," *Mater. Struct.*, vol. 48, no. 4, pp. 835–862, 2015.

[56] K. L. Scrivener, T. Füllmann, E. Gallucci, G. Walenta, and E. Bermejo, "Quantitative study of Portland cement hydration by X-ray diffraction/Rietveld analysis and independent methods," *Cem. Concr. Res.*, vol. 34, no. 9, pp. 1541–1547, 2004.

[57] K. L. Scrivener, "Backscattered electron imaging of cementitious microstructures: Understanding and quantification," *Cem. Concr. Compos.*, vol. 26, no. 8, pp. 935–945, 2004.

[58] F. Deschner, B. Münch, F. Winnefeld, and B. Lothenbach, "Quantification of fly ash in hydrated, blended Portland cement pastes by backscattered electron imaging," *J. Microsc.*, vol. 251, no. 2, pp. 188–204, 2013.

[59] K. Scrivener, R. Snellings, and B. Lothenbach, *A Practical Guide to Microstructural Analysis of Cementitious Materials*. 2016.

[60] M. G. Alexander, *Engineering and Transport Properties of the Interfacial Transition Zone in Cementitious Composites*. RILEM Publications, 1999.

[61] K. L. Scrivener and D. B. Technik, "The Interfacial Transition Zone (ITZ) Between Cement

Paste and Aggregate," pp. 411–421, 2004.

[62] M. A. G. Aranda, A. G. De la Torre, and L. Leon-Reina, "Rietveld Quantitative Phase Analysis of OPC Clinkers, Cements and Hydration Products," *Rev. Mineral. Geochemistry*, vol. 74, no. 1, pp. 169–209, 2012.

[63] R. Snellings, A. Bazzoni, and K. Scrivener, "The existence of amorphous phase in Portland cements: Physical factors affecting Rietveld quantitative phase analysis," *Cem. Concr. Res.*, vol. 59, pp. 139–146, 2014.

[64] N. V. Y. Scarlett and I. C. Madsen, "Quantification of phases with partial or no known crystal structures," *Powder Diffr.*, vol. 21, no. 04, pp. 278–284, 2006.

[65] R. Snellings, A. Salze, and K. L. Scrivener, "Use of X-ray diffraction to quantify amorphous supplementary cementitious materials in anhydrous and hydrated blended cements," *Cem. Concr. Res.*, vol. 64, pp. 89–98, 2014.

[66] Y. P. Stetsko, N. Shanahan, H. Deford, and A. Zayed, "Quantification of supplementary cementitious content in blended Portland cement using an iterative Rietveld-PONKCS technique," *J. Appl. Crystallogr.*, vol. 50, pp. 498–507, 2017.

[67] J. J. Friel, R. Terborg, S. Langner, T. Salge, M. Rohde, and J. Berlin, "X-ray and image analysis in electron microscopy, 2nd Edition," *Ref_EDS*, 2003. .

[68] F. Avet, X. Li, and K. Scrivener, "Determination of the amount of reacted metakaolin in calcined clay blends," *Cem. Concr. Res.*, vol. 106, no. February, pp. 40–48, 2018.

[69] L. Sorelli, G. Constantinides, F. J. Ulm, and F. Toutlemonde, "The nano-mechanical signature of Ultra High Performance Concrete by statistical nanoindentation techniques," *Cem. Concr. Res.*, vol. 38, no. 12, pp. 1447–1456, 2008.

[70] M. E. Broz, R. F. Cook, and D. L. Whitney, "Microhardness, toughness, and modulus of Mohs scale minerals," *Am. Mineral.*, vol. 91, no. 1, pp. 135–142, 2006.

[71] W. C. Oliver and G. M. Pharr, "An improved technique for determining hardness and elastic modulus using load and displacement sensing indentation experiments," *Journal of Materials Research*, vol. 7, no. 06. pp. 1564–1583, 1992.

[72] C. Hu, Z. Li, Y. Gao, Y. Han, and Y. Zhang, "Investigation on microstructures of cementitious composites incorporating slag," *Adv. Cem. Res.*, vol. 26, no. 4, pp. 222–232, 2014.

[73] C. Hu, "Microstructure and mechanical properties of fly ash blended cement pastes," *Constr. Build. Mater.*, vol. 73, pp. 618–625, 2014.

[74] J. Němeček, P. Kabele, and Z. Bittnar, "Nanoindentation based assessment of micro-mechanical properties of fiber reinforced cementitious composite," *6th Int. RILEM Symp. Fibre-Reinforced Concr. (FRC*, no. September, pp. 401–410, 2004.

[75] A. Chorfa, M. A. Madjoubi, M. Hamidouche, N. Bouras, J. Rubio, and F. Rubio, “Glass hardness and elastic modulus determination by nanoindentation using displacement and energy methods,” *Ceram. - Silikaty*, vol. 54, no. 3, pp. 225–234, 2010.

[76] a P. Bathija, “Elastic properties of clays,” vol. PhD, p. Ph.D. thesis, 2009.

[77] a Mikowski, P. Soares, F. Wypych, J. E. F. C. Gardolinski, and C. Lepienski, “Mechanical properties of kaolinite ‘macro-crystals,’” *Philos. Mag.*, vol. 87, no. 29, pp. 4445–4459, 2007.

[78] D. P. Bentz and P. C. Aitcin, “The Hidden Meaning of Water- Cement Ratio Distance between cement particles is fundamental,” *Concr. Int.*, vol. 30, no. 5, pp. 51–54, 2008.

[79] P. J. M. M. P. M. Paulo Monteiro, *Concrete: Microstructure, Properties, and Materials: 3rd (Third) edition: Paulo Monteiro, Paulo J.M. Monteiro P. Mehta: 8580000010992: Amazon.com: Books*. 1993.

[80] K. L. Scrivener, A. Bentur, and P. L. Pratt, “Quantitative characterization of the transition zone in high strength concretes,” *Adv. Cem. Res.*, vol. 1, no. 4, pp. 230–237, 1988.

5 *Effect of the hardness of inert fillers as cement replacement materials on UHPC mechanical, durability, and hydration properties*

5.1 Introduction

Ultra High Performance Concrete constitutes a major milestone in concrete technology, its mechanical and durable properties are being more and more studied and the mechanism that allows such properties is being unveiled progressively.

Still the big problem of the UHPC is its high usage of Portland cement (800 kg/m^3) at a w/c of 0.25, such low w/c do not allow the cement to reach its higher hydration potential, therefore leaving high amounts of cement without a binding task in the matrix. This first stage points towards describing how the unhydrated particles in the cementitious matrices work to give such high properties in silica fume ternary systems.

Various silica fume additions were tested from 0 to 120 kg/m^3 at a w/c of 0.5. Subsequently, the cement of the UHPC was replaced until reaching a w/c of 0.4 by both a soft and a hard-inert inclusions, limestone and quartz powder respectively, in order to define whether the hardness of the unhydrated clinker is necessary to reach the performance of UHPC.

Several microstructural techniques were used to describe how hydration affects mechanical and durable properties on UHPC mixtures. Finally a sustainable point of view is added to the discussion showing that ternary type mixes are a good alternative for UHPC mixture design even if the materials hold do not reactivity.

5.2 Optimization of UHPC by the use of limestone and quartz fillers.

by Guillermo Hernández-Carrillo, Alejandro Durán-Herrera, and Arezki Tagnit-Hamou

Biography:

Guillermo Hernández-Carrillo: His research interests include mixture optimization and durability of ultra-high performance and characterization of pozzolanic reaction

Alejandro Durán-Herrera, Professor and Head of Concrete Technology at the Civil Engineering School, Universidad Autónoma de Nuevo León (UANL), Monterrey, Nuevo León, México. Fellow Member of ACI International. Research interests: High and Ultra-high performance concrete, internal curing of concrete, self consolidating concrete.

Arezki-Tagnit Hamou FACI, is a Professor in the Civil Engineering Department at the Université de Sherbrooke, QC, Canada. He is also the Head of the cement and concrete group and industrial chair holder on valorization of glass in materials. He is a member of ACI Committees 130, Sustainability of Concrete, and 555, Concrete with Recycled Materials.

ABSTRACT

Ternary systems Cement-Limestone-Silica Fume and Cement-Quartz-Silica Fume are studied to disclose whether the hardness has to be taken into account when choosing a filler in an UHPC type mix design. The results showed no difference between quartz and limestone systems, both with an adequate silica fume dosage where able to keep both compressive strength and bulk resistivity performance at a 37.5% cement replacement. Studies of Back Scattered Electrons, X ray diffraction and Quantitative Energy Dispersive Spectroscopy were done to propose that the cement replacement by fillers of any source is possible due to a higher dissolution of both cement and silica fume that allows the formation of lower Ca/Si ratio C-S-H, if enough silica fume is present to keep porosity next to the aggregate constant, finally the replaced mixes had a 37% lower carbon footprint than the reference.

Keywords: Durability, Filler effect, Microstructure, UHPC, sustainability.

INTRODUCTION

Ultra High Performance Concrete (UHPC) have been under development during the last two decades with the main objective of pushing concrete to its limits in terms of structural and durability properties. UHPC is highly resilient, but its constituents (cement, silica fume, quartz sand, chemical admixtures, etc.) and their relative high volumes used during its production, set the UHPC as an expensive alternative at this point of its development.

Because an UHPC typically requires water/cement ratios (w/c) below 0.25 [1], the low water availability will prevent a certain fraction of the binder to reach full hydration. According to the Powers model, the minimum w/c ratio that can get completely hydrated in a closed system is 0.42 [2], therefore a lower w/c ratio system like a UHPC mixture has approximatively 40% of the cement volume unhydrated. This scenario represents a significant area of opportunity to identify materials that could be used as inert fillers in UHPC in substitution of unhydrated Portland cement that in terms of cost and sustainability will result expensive.

Many researchers have worked in the reduction of cement contents in UHPC replacing it by supplementary cementitious materials (SCM's) such as blast furnace slag, fly ash, glass powder, etc.[3]–[6]. However, the presence of a very high pozzolanic material such as silica fume and the lower water availability might hinder the possibility of coarser, less reactive materials, to react in UHPC mixes, where even the silica fume reaction rate decreases with the lack of water [7]–[9].

According to an UNEP report [10]; in regions where they are available, the common pozzolans (fly ash, slag) are currently being used at its maximum potential as replacement of cement, furthermore quantities of such materials are constantly being decreased, especially the fly ash which is being eradicated by governments initiatives to force carbon power plants to close. On the other hand, limestone powder is a product that can be find in almost every place in the world at a low cost and due to its softness, it is easy to grind it to an appropriate fineness for concrete production.

As a cement replacement the quality of limestone is well understood, leading to its adoption in standards around the world [11], [12]. However, some concerns have arisen from the possible thaumasite formation with large replacements of cement by limestone on cold environments [13], [14]. Nevertheless, the combination of limestone cement with pozzolans

(silica fume, fly ash, etc.) hinder the appearance of the attack [15], [16] through the overall reduction of permeability .

Another concern for the limestone replacement is the large difference in hardness between the calcite (2.21 GPa [17]) and the clinker (9.12 GPa [18]). This comes from the idea of some researchers that the hard anhydrous inclusions within a cement paste are partially responsible for the mechanical performance of the compound [18], [19].

In order to challenge the idea of the hardness of the anhydrous inclusions affecting the mechanical performance, this work will replace 37.5% of the cement volume by a softer and harder material that is not reactive, being limestone at 2.21 GPa and quartz at 14.6 GPa [17], [20] the softer and harder material respectively.

With the cement replacement it is expected an increase of the porosity due to the increase of distance that the hydrates have to travel to reach another particle of cement, and with that a decrease of strength [21]. In this case the effect of different silica fume additions in the microstructure, the bulk resistivity and compressive strength will be studied. The silica fume addition should help to increase the amount of calcium-silicate hydrates required to compensate the increase of porosity [22], and to produce a better performing C-S-H with lower Ca/Si ratio [23].

In this work the paste fraction of the mortars that presented the best performance were studied by X Ray Diffraction coupled with rietveld refinement. Bulk electrical resistivity (BER) and compressive strength of the mortars were determined at different ages to assess the durability and mechanical performance.

Finally, polished samples mounted in resin of the mortars were observed by scanning electron microscope (SEM) coupled with the Back Scattered Electron Imaging (BSEI) to study the Interfacial Transition Zone (ITZ) and Quantitative Energy Dispersive Spectroscopy (QEDS) to obtain the C-S-H composition of the different samples.

RESEARCH SIGNIFICANCE

Two mostly inert materials were used as cement replacement on Ultra High Performance Concrete mixes in order to determine their suitability as fillers. The choosing of limestone and quartz will allow to assess whether the cement hard inclusions play a role on UHPC properties. Both macrostructural and microstructural analysis were done in order to define

how the filler effect works on very low water to cement ratios, furthermore a quantitative study on the hydration of the mixes allows a better understanding of the contribution of silica fume and fillers on the compressive strength, and electrical resistivity of the mixes. The authors believe that the contribution of this work will add knowledge on strategies to greatly decrease the clinker factor on UHPC while maintaining both durable and mechanical properties and at the same time decrease the carbon footprint of the material

EXPERIMENTAL INVESTIGATION

The Powers Model [24] estimates that 0.4 is the cement ratio that reaches full hydration, we used this figure to determine the cement replacement to be used in our experiment.

The paste of our reference mortar was made with a w/c of 0.25, and successive additions of 5% silica fume were added to the mix up to a final addition of 15%. Another set of mixtures consisted in replacing 37.5% of the cement by volume by either limestone or quartz powder. The set of mixes are summarized in the Table 1. The mixes were divided in two groups A and B.

Group A:

- This set of mixtures intended to disclose if the unhydrated cement particles contributed to the strength. The mix A consisted in a mortar at a w/c of 0.25, mixes AL and AQ replaced 37.5% of cement's volume by Limestone or Quartz Powder in order to achieve the maximum degree of hydration which in theory is reached at a w/c of 0.4 in this cement. For example, the mix A consists in a mixture containing a w/c of 0.25 and an addition of 15% by weight of cement (woc) of silica fume, while the mix AL consists in replacing 37.5% of the cement of the A mix by limestone powder.

Group B

- This set of mixtures was done to define the threshold in which the silica fume can help to match the compressive strength and BER of cement-silica fume binary systems when using cement-filler replaced ternary systems. The mixes of the B set (B5, B10 and B15) are done at a w/c of 0.25 plus 5, 10 or 15% of silica fume, following that number a letter L or Q may follow indicating a replacement of 37.5% of the cement volume by either limestone or quartz powder respectively. For example, the mix B10 was made at a w/c of 0.25 having an addition of silica fume

of 10% while the mix B10Q is a modification of the B10 mix having 37.5% of the cement replaced by quartz powder.

Trial batches were made to determine the minimum dosage of the high range water reducing admixture (HRWRA) to obtain a target spread of around 310 mm ± 20 measured through the standard cone described in ASTM C 230 [25] without vibration. This target was decided to have a comparable air content between the mixes.

Each batch of mortar consisted in 2.5 liters, the spread value reported in Table 1 is the average of two measurements. Fresh stage unit weight and air content were determined according to the standard procedure described in ASTM C185. Mixing was performed in a 19-liters planetary mixer according to the following procedure:

1. All the powders followed by approximately 90 % of the mixing water were introduced to the mixer bowl. The remaining 10 % of water was used to dilute the superplasticizer admixture for a faster distribution within the mixture.
2. An initial mixing of 4 minutes at a speed of 104 rpm was performed for better dispersion of both silica fume and cement. Afterwards, the diluted superplasticizer admixture was added, and the mixing continued for 2 additional minutes. This delay of 4 minutes of the administration of the superplasticizer avoids the entrapping of the polycarboxylate chains inside the first products of hydration, helping to increase the spread without any further addition of superplasticizer [26].
3. From the sixth to eighth minute the speed was shifted to 194 rpm.
4. Finally, the mixing continues at a speed of 353 rpm for 5 minutes. The total mixing time was 15 minutes.

Table 1. Mixture Proportions.

Material, parameter or property	A	AL	AQ	B5	B5L	B5Q	B10	B10L	B10Q	B15	B15L	B15Q
W/C weight ratio	0.25	0.40	0.40	0.25	0.40	0.40	0.25	0.40	0.40	0.25	0.40	0.40
W/(HS+ Q or L) volumetric ratio	0.80	0.80	0.80	0.80	0.80	0.80	0.80	0.80	0.80	0.80	0.80	0.80
SF by weight of cement	0.00	0.00	0.00	0.05	0.08	0.08	0.10	0.16	0.16	0.15	0.24	0.24
Water (kg/m^3)	200	200	200	199	199	200	199	199	200	199	199	200
HS (kg/m^3)	800	500	500	796	499	500	796	499	500	796	499	500
L (kg/m^3)	0	250	0	0	250	0	0	250	0	0	251	0
Q (kg/m^3)	0	0	245	0	0	245	0	0	245	0	0	245
SF (kg/m^3)	0	0	0	40	40	40	80	80	80	120	120	120
Solids in HRWRA (kg/m^3)	12	5	5	12	7	7	12	7	7	12	7	7
Sand (kg/m^3)	1404	1430	1430	1362	1375	1379	1315	1328	1332	1268	1281	1284
Volumetric weight (kg/m^3)	2415	2385	2396	2421	2391	2391	2400	2370	2	2394	2361	2353
Air content before vibration (%)	1.6	0.4	0.1	1.7	0.1	0.1	2.1	0.6	0.2	1.6	0.4	0.8
Air content after vibration (%)	/	/	/	0.2	/	/	0.8	/	/	0.9	/	/
Mini cone Spread without vibration (cm)	32	29	31	33	31	33	32	32	33	31	33	33

The mortars were poured within 50 mm cubic molds (ASTM C 109), mixtures B5, B10 and B15 were vibrated for 75 seconds to attain a similar air content as the other mixes. Both pre and after vibration air content was recorded and can be consulted in Table 1. The samples were kept on a curing room at 100% relative humidity without immersion until the day of the test. The cubes were tested on compressive strength according to ASTM C109 at 7, 28 and 91 days and the bulk resistivity was measured with the RCON 2 device by Giatec at 1 KHz. In order to identify the crystalline phases, the state of hydration and the pozzolanic reaction of the paste fraction of mortars B15, B15L and B15Q. A paste reproduction of the mixtures was poured in plastic tubes and sealed for X ray diffraction characterization at the age of 91 days.

The preparation of the samples and the conditions for the XRD experiments are the following:

- The pastes were ground by hand with an agate mortar and pestle until all the material passed the sieve No. 30.
- Ten grams of the ground paste was submerged in a 100 ml isopropanol bath and stirred for 10 minutes.
- The suspension was then filtered to remove the highest possible amount of isopropanol.
- Ten milliliters of diethyl ether were added to wash the isopropanol while the sample remained on the filter paper and under vacuum to facilitate the isopropanol evaporation.
- The resulting solids were dried under vacuum for 30 minutes.
- For the final step, the sample was further ground until all the material passed the sieve No. 100.

The XRD patterns were acquired with a detector PixCel1D from Brucker under a continuous scan from 5 to 70 2θ, following the recommendations of [27], a Rietveld refinement of the anhydrous powders was performed according to procedure described in [28], the source of X-rays was a Cu filament, the generator had a current of 50 mA and 40 kV, the goniometer radius was 240 mm and the irradiated length was 10 mm. The amount of each phase was normalized with the external standard method using a corundum sample with known crystallinity of 98.2% that was calibrated with the NIST's corundum SRM 676a standard.

The powdered samples were backloaded and the scan was performed under the following conditions:

- Step size 0.0260 º 2θ from 5 to 70 2 2θ.
- Divergence slit: 1º
- Antiscatter slit: 1º
- Soller slit: 0.04 rad
- Rotation speed s/rev: 4
- Total time: 30 minutes

For the XRD pattern deconvolution the Rietveld refinement method was performed with the help of the software High Score Plus v 4.0. The Mass Attenuation Coefficient of the samples was calculated from the combined XRF chemical composition of the materials presented in each paste and corrected for CO_2 an H_2O content with the use of Thermogravimetric Analysis (TGA) conducted using a TA instrument model SDT-600.

It is suggested that the major contribution of silica fume to the concrete lies on the decrease of porosity on the Interfacial Transition Zone (ITZ) [29]. The effect of silica fume and fillers on the ITZ structuration was measured in a semi quantitative manner with the help of Back Scattered Electrons Imaging (BSEI) technique. The BSEI technique allows the study of the amount of hydrates fraction and sometimes some specific phases can be de-convoluted from the histogram of the image [30]. To get reliable results from this technique, a very good procedure of polishing has to be done.

To study the ITZ, 30 cm x 2.54 cm x 2.54 cm prims were casted and cured in a 100% RH room during 91 days after which a 3 mm thick slice was cut with a low speed diamond saw. The samples were analyzed with a Hitachi S-3400 N scanning electron microscope at 15 kV acceleration voltage and a 10 mm working distance. To stop the hydration of the slices, they were submerged during 2 weeks in an isopropanol bath inside a plastic tube. The quantity of isopropanol was approximately 50 times the volume of the slice. The slices were mounted on resin to make cylinders with a height of 2 cm. The polishing was done by hand with successive sandpapers starting with the no. 400 and ending with the no. 2000. The quality of the polishing was supervised with optical microscopy at each step. The polishing with each sandpaper lasted between one and two minutes, then the samples were washed in an ultrasonic bath with isopropanol for 2 minutes. For the final polishing, oil soluble diamond

suspensions were used, having 3 and 1 μm diamonds respectively, the diamond suspensions were spread in a low nap cloth, and then the samples were polished during one minute in each in order to reach a mirror like aspect, after which they were submitted to vacuum and coated with a carbon layer of 15 nm.

For this work, thirty images from polished samples were taken at a 400x magnification where aggregates having a diameter of 500 μm (average aggregate size of the sand) were found [31]. Before starting with the image acquisition, the samples remained inside the SEM chamber for an approximate of 2 hours in order to get a stable beam emission, which was checked with the probe current on a faraday cage. The processing of the images started with a flat field correction, followed by the application of a 3 pixels median filter.

To obtain the porosity and unhydrated material content as a function of the distance, first the histogram of a band of 80 μm around 30 aggregates was measured and averaged to find the threshold of both porosity and unhydrated material (Figure 1). The choosing of the porosity threshold was done with the criteria showed in [32]. The anhydrous threshold was defined as the point where the histogram was flat before the last peak. Once the thresholds were defined, binary images having only porosity or unhydrated material were produced, with that histograms of bands every 3 μm until 80 μm were obtained and the percentage of either porosity or unhydrated material quantified.

Finally, a quantitative analysis of the C-S-H composition of selected mixtures B15, B15L and B15Q was done with the help of the Quantitative Energy Dispersive X-ray Spectroscopy (QEDS). Spot analysis were performed in mortar samples after 91 days hydration at bands having a separation of 6 μm starting from a distance of 3 μm from the aggregate, the utilized Scanning Electron Microscope was a Hitachi S-3400 N equipped with an Oxford Inca Energy 250 energy-dispersive spectrometer (EDS). To cover 50 μm and have points at each 3 μm, the bands were intercalated to start at either 3 or 6 μm.

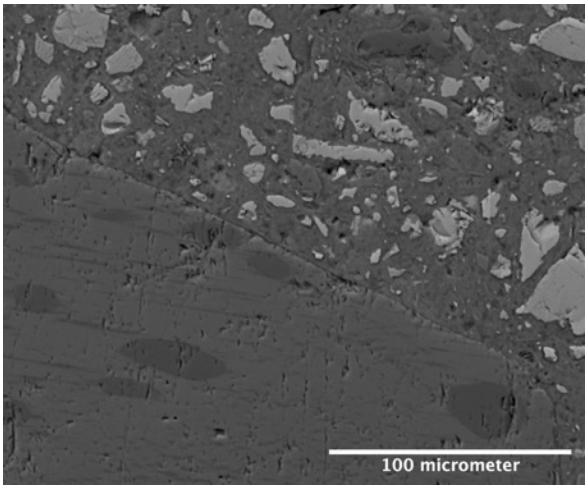
100 micrometer

a)

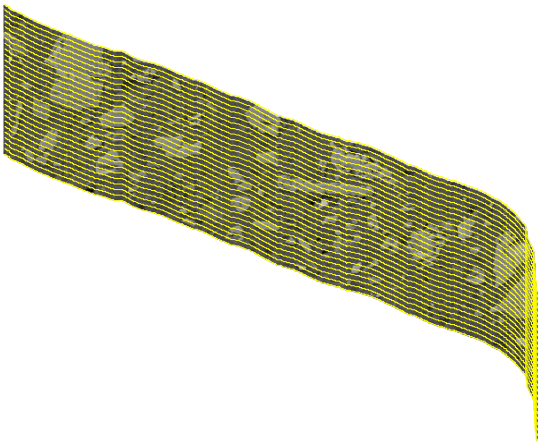

b)

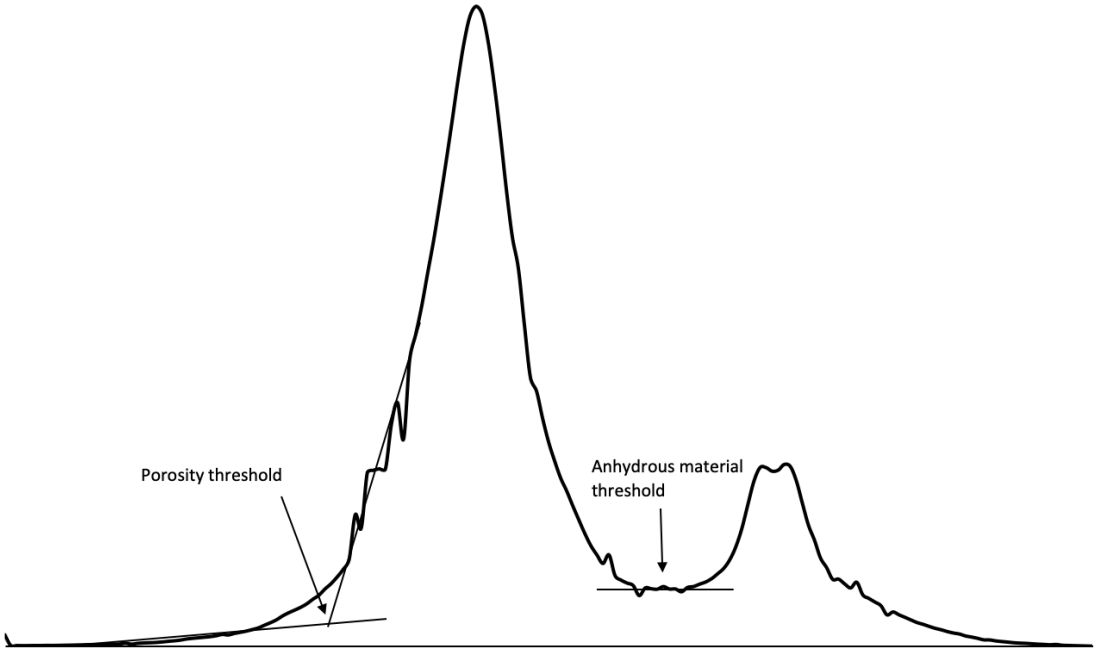
Porosity threshold
Anhydrous material
threshold

c)

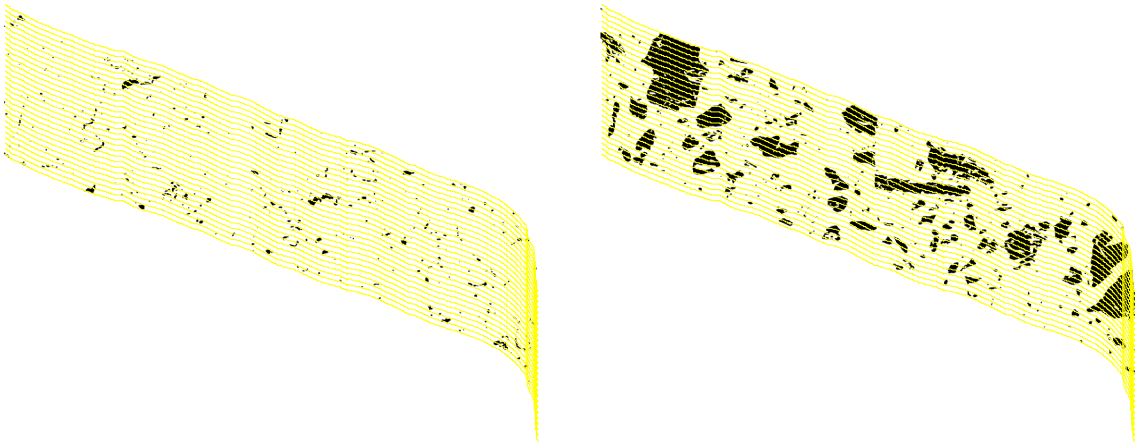

d) e)

Figure 1. Processing of the BSE images a) picture treated with a flat field correction and a median filter of 3 pixels b) segmentation of an 80 micrometer bands in smaller ones having a width of 3 micrometers c) averaged histogram of 30 80 micrometers bands around aggregates and determination of the thresholds for both apparent porosity and unhydrated material d) binary image having the threshold for porosity applied e) binary image having the threshold for unhydrated material applied.

The accelerating voltage was set to 15 kV, and the working distance at 10 mm. To obtain at least 100,000 counts, each spot analysis lasted 20 seconds, the interaction volume of the spot analysis under the conditions of this microscope was modeled previously using the CASINO software [33], the model indicated that for C-S-H the characteristic depth was between 1100 and 1700 nm, and for the clinker phases between 900 and 1000 nm and the radius range between 0.5 and 0.75 micrometers. Four fields were studied per mix at 400x having 1272 spot analyses per experiment (Figure 2).

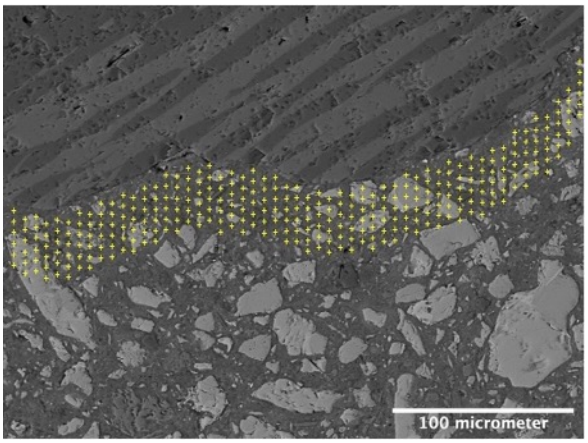

Figure 2. Example of the spot analysis for paste to define the composition of C-S-H

The spectra were post-processed with the NIST software DTSA-II that allows to obtain quantitative data from the information of previously measured standards with known chemical composition. The Duane-Hunt limit was used to exclude points where local charging could have taken place.

The standards were chosen to have a similar composition to the phases that are encountered in Portland cement pastes and were supplied by SPI supplies. The standards utilized were: C_2S for Ca and Si, C_3A for Al, olivine for Mg and Fe, anhydrite for S, orthoclase for K, tugtupite for Na and Cl, and sphene for Ti. The quantification process was verified by the deconvolution of the spectrum of kaersutite [34]. Compounds with more than one element were used to improve the quantitative result, it is expected that this measure could reduce the ZAF correction [35].

Bivariate histograms were made with the Si/Ca and Al/Ca ratios. The bivariate histograms were constructed with bins at 0.01, the result shows the areas with higher density of points, from this the composition of C-A-S-H was derived.

Materials

The materials used in this work were the following: A sulfate resistant Type HS cement (HS) with a Blaine fineness of 438 m^2/kg, and a density of 3.18 g/cm^3. A silica fume (SF) with a BET-surface of 18.66 m^2/g and a density of 2.20 g/cm^3. A policarboxylate based super plasticizer (SP) with a density of 1.09 g/cm^3 and an active agent content of 40%. A Quartz

Powder (Q) with a mean particle size of 19 μm and a density of 2.75 g/cm^3. A Limestone Powder (L) with a mean particle size of 17 μm and a density of 2.71 g/cm^3. A natural river sand with 5 mm maximum size, a density of 2.61 g/cm^3 and an absorption of 1.15 %.

The physical and chemical properties of the powders are summarized in the Table 2. To obtain the chemical composition the X-Ray fluorescence spectrometer used was an Axios Advanced by PANalytical. To obtain the particle size distribution a Mastersizer 2000 laser granulometer was used, results can be found in the Figure 3. The density of the powder was obtained through a Quantachrome Multi Pycnometer. The Blaine Fineness was measured with the Slimatic device by Intechlab, and the BET surface area was obtained with an ASAP 2020 Plus device by Micromeritics.

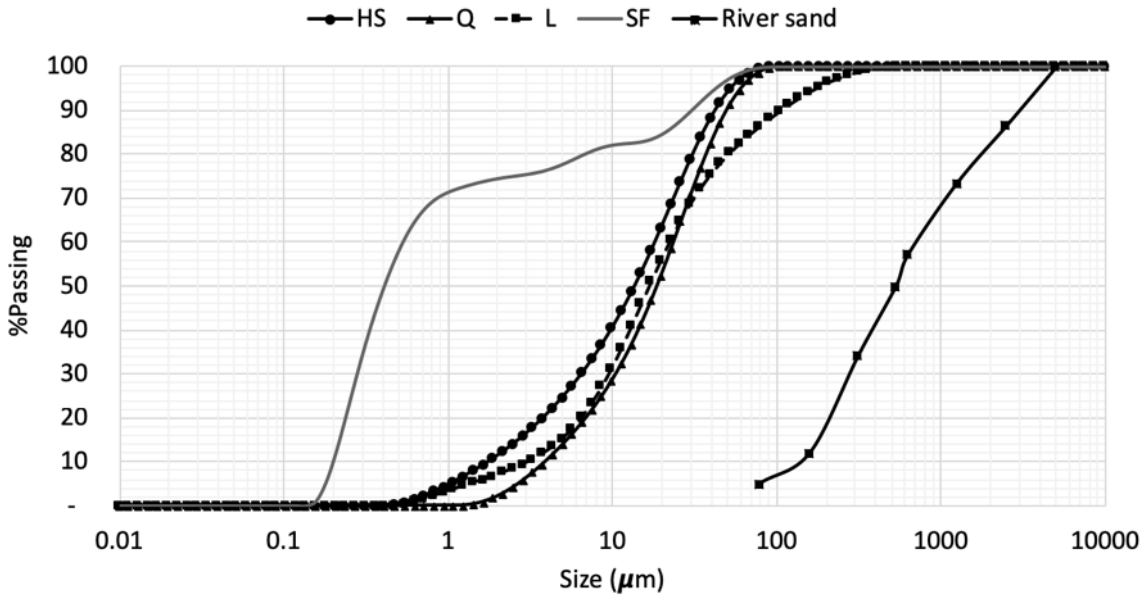

Figure 3**.** Particle size distribution of the materials used in this work.

The results are of the phase composition of the materials obtained through XRD are summarized in the Table 3.

Table 2. Physical and chemical properties obtained with X-Ray Fluorescence, pycnometry, blaine and BET tests, and laser granulometry

Property	Quartz Powder (QZ)	Limestone Powder (LS)	Silica fume (SF)	HS Cement (HS)
SiO_2 (wt%)	99.6	5.1	94.3	21.8
TiO_2 (wt%)	0.01	0.04	0	0.18
Al_2O_3 (wt%)	0.1	0.8	0.1	4
Fe_2O_3 (wt%)	0.02	0.27	0.06	3.14
Mn_2O_3 (wt%)	0.002	0.008	0.037	0.038
MgO (wt%)	0.1	1.3	0.3	1.9
CaO (wt%)	0	51.2	0.4	63.1
Na_2O (wt%)	0	0	0.18	0.05
K_2O (wt%)	0	0.34	0.58	0.56
P_2O_5 (wt%)	0	0.01	0.14	0.09
SO_3 (wt%)	0	0.06	0.28	2.37
SrO (wt%)	0	0.03	0	0.1
ZnO (wt%)	0	0	0.51	0.02
Loss on ignition (wt%)	0.1	40.9	3	2.6
Equivalent alkali (Na_2Oeq)	0	0.22	0.56	0.42
Specific gravity (g/cm^3)	2.75	2.71	2.2	3.18
Blaine surface m^2/kg				438
BET surface (m^2/g)			18.66	
Mean particle size, d50 (μm)	19	17	0.4	14

Table 3. Phase composition of the utilized powders

	Q	L	SF	HS
Phase	% anhydrous	% anhydrous	% anhydrous	% anhydrous
C_3S				51
C_2S				18
C_3A cubic				1
C_3A orthorhombic				2
Ferrite				10
Periclase				1
Gypsum				1
Bassanite				3
Cacite		76		5
Quartz	100	3		
Mossanite			1	
Cristobalite			1	
Dolomite		3		
Amorphous		19	98	7

EXPERIMENTAL RESULTS AND DISCUSSION

Compressive strength

Compressive Strength results at 7, 28 and 91 days, for mortars with and without cement replaced with inert fillers (L and Q) are presented in the Figure 4. Figure 4 shows in the X axis the amount of silica fume per cubic meter in the mortar, ranging from 0 to 120 kg/m^3, the mixes with labeled with a L or Q had 37.5% of cement's volume replaced by limestone (L) or quartz powder (Q). To allow an easy consult of the mixture proportioning (Table 1) of each mortar the code for each mix is written next to the compressive strength value.

The mixtures without silica fume (A, AL, AQ) were produced to test if the hardness of the unhydrated cement was contributing to the strength of the compound, it was assumed that the 37.5% cement replaced would leave no anhydrous clinker grains (this assertion was

further explored in the X-ray diffraction section of the results). It was clearly evident that at all ages the mix with pure cement (w/c 0.25) had higher strength, being in average 16, 18 and 12% stronger at the ages of 7, 28 and 91 days, respectively.

Given the large differences of hardness between calcite and quartz, 2 and 14 GPa respectively, a significant difference in strength was expected, but the differences shown between AL and AQ mixtures were only 4, 0, and 2% at 7, 28 and 91days, respectively. From this we may assume that although the cement does not react completely, almost all of the superficial area of the clinker particles reacts providing a strong bond between each other, in which the mechanical properties of the material itself plays a complimentary role.

The effect of the pozzolanic reaction of the silica fume in the compressive strength starts to be evident from the age of 28 days where the difference between filler-replaced and non-replaced mixes start to decrease until a similar strength is obtained at 120 kg/m^3 of silica fume where the quartz and pure cement mortars compressive strength are more comparable with the limestone replaced mortar result.

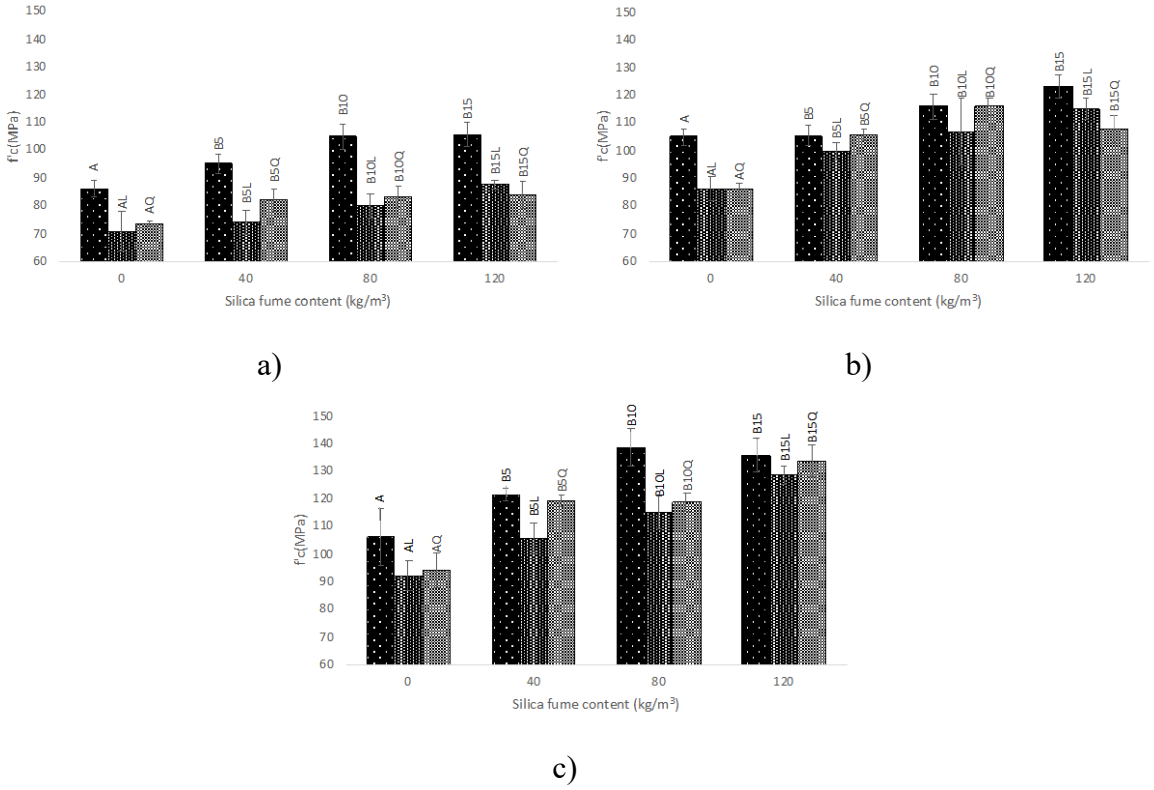

Figure 4. Compressive strength results for cement replaced and non-replaced mortar mixtures at different levels of silica fume additions and at different ages a) 7 days, b) 28 days and c) 91 days.

Mixtures with Q could successfully replace the cement within the range of silica fume additions that were studied (Figure 4c, 91 days), nevertheless, the limestone could only replace cement when the silica fume was present at least at 10% addition. Previously works have shown that systems having great amounts of silica fume can perform well with low quantities of cement [36]–[38], it has been attributed this phenomena to the enhanced pozzolanic reaction of the silica fume when the water availability increases leading to the formation of a low Ca/Si ratio C-S-H, and to the improvement of the ITZ by the addition of the silica fume that enhances the packing density.

Bulk Electrical Resistivity (BER)

The durability development was qualitatively followed through BER tests, **Figure 5** contains the thresholds to estimate the Risk of Chloride Ion Penetration that was established in the AASHTO T 350 standard, in order to use those thresholds a conversion between the surface resistivity in the standard and the Bulk Resistivity was done, the limits in terms of BER (High > 6, Moderate 6 ≤ 10.5, Low 10.5 ≤ 18.75, Very Low 18.75 ≤ 127 and Negligible > 127 Kohm·cm), were calculated through the procedure proposed by W. Morris et al. in 1996 [39], from the correspondent limits provided by AASHTO T358 for the Wenner surface electrical resistivity test (High > 12, Moderate 12 ≤ 21, Low 21 ≤ 37, Very Low 37 ≤ 254 and Negligible > 254 Kohm·cm). **Figure 5** a) and b) show the resistivity in function of the silica fume content and the type of mix in a similar way as what presented in the compressive strength at ages 7 and 28 days, respectively, whereas **Figure 5** c) shows additionally the compressive strength of the mortars at 91 days to illustrate the disconnection of the durability and mechanical parameters. The specimens were tested at 1 KHz after being cured in a humid chamber at 100% relative humidity.

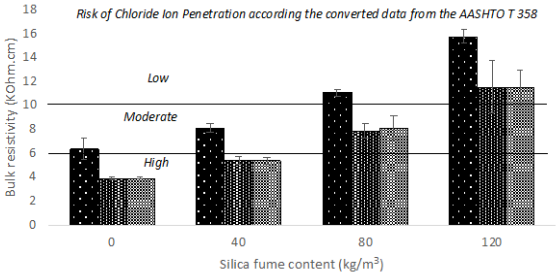

a)

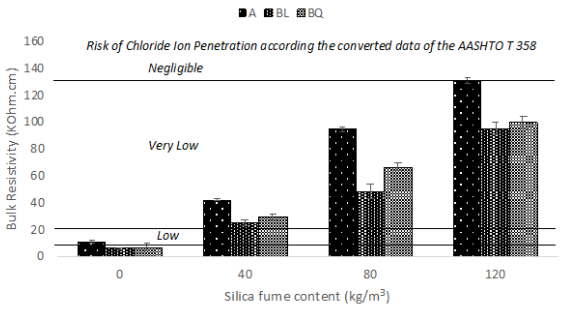

b)

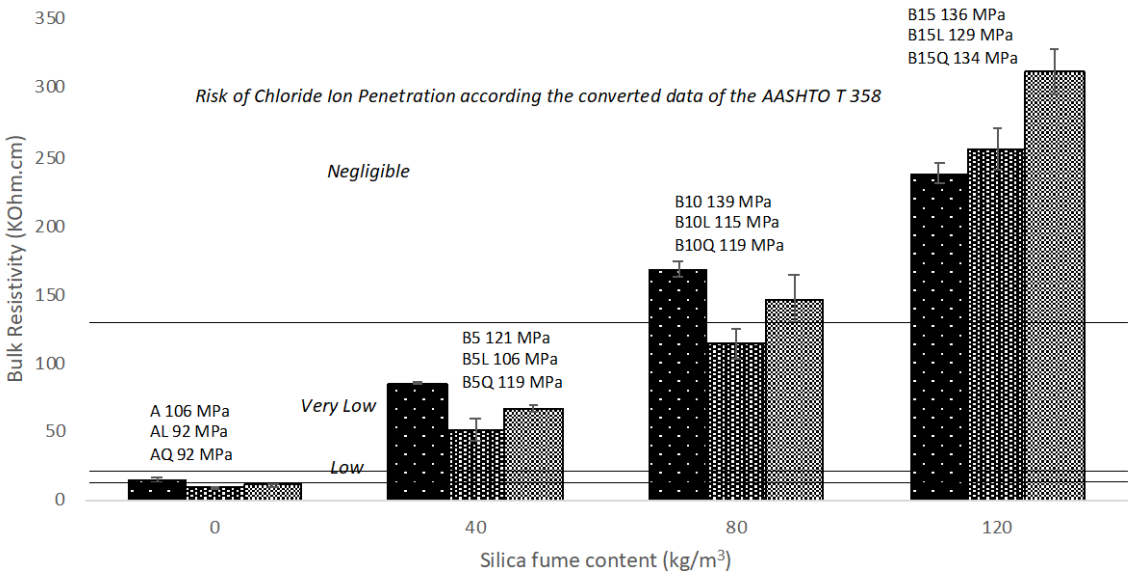

c)

Figure 5. Bulk electrical resistivity results for cement replaced and non-replaced mortar mixtures at different levels of silica fume addition with at different ages a) 7 days, b) 28 days and c) 91 days

From the analysis of the results of the Figure 5 c) at 91 days, a difference between Q and L mortars is evident at 120 kg/m^3 of silica fume, even though the compressive strength result presented in the previous section did not indicate a difference between the mortars.

While there is almost no difference between the mixtures with Q and L when there is no silica fume in the mix, a difference in the resistivity between the Q and L mortars increase as the time passes and the amount of silica fume augments. At 80 kg/m^3 addition of SF the mix with Q replacement at 91 days, sits within the negligible bracket alongside with the cement-silica fume sample; and at 120 kg/m^3 SF addition the resistivity developed is even higher, while

the L mortar shows a comparable resistivity as the silica-cement mix. Due to the BER being only a qualitative measurement of the permeability, the differences between the QZ and LS could not be big being both in the negligible risk bracket, nevertheless a possible explanation for this could be the reaction of the fines particles of quartz powder that could help to the production of a lower Ca/Si ratio C-S-H removing Ca^{+} from the pore solution as stated in [8], [40].

In the following sections the mixes B15, B15L and B15Q where the compressive strength was equivalent, and the resistivity was equal or exceeded the one from the binary cement-silica fume mixture, were studied under SEM with the BSEI technique to quantify the porosity and presence of unhydrated material within the ITZ, with XRD to study the phases present in the paste and to describe the pozzolanic reaction and finally with QEDS to show the changes of C-S-H composition with each mix design.

Back Scattered Electron Imaging

This work has the intent to define the conditions in which the unhydrated clinker content within a paste with non-reactive materials shows no performance compromises in both mechanical and durability parameters. This condition was met or surpassed at 120 kg/m^3 of silica fume in both compressive strength and electrical resistivity. In order to understand the phenomena, those mixes were studied under the SEM with the BSE detector. The BSE give an indication of the average atomic number; hence it can be utilized to define both unhydrated clinker phases (high average atomic number) as well as porosity (low average atomic number).

For the B15, B15L and B15Q mortars results of apparent porosity and unhydrated clinker as a function of the distance from the aggregate are presented in the Figure 6 as well as a bar indicating the standard deviation of each point. From the results presented in the Figure 6 the ITZ in both porosity and unhydrated clinker exists until 20 μm, the change between the ITZ an bulk paste was indicated inside this figure. The highest porosity value appears in the vicinity of the aggregate, having a value of around 8% for the mixtures B15 and B15L and a value of around 7% for the B15Q mix. The unhydrated clinker volume decreased by 15% when 37.5% cement was replaced by either Q or L, passing from about 25% to 10%. According to the Powers model it was expected that no clinker should have remained

unhydrated at a w/c of 0.40. Nevertheless, it is believed that the remaining unhydrated material could come from particles that are too big to hydrate within three months.

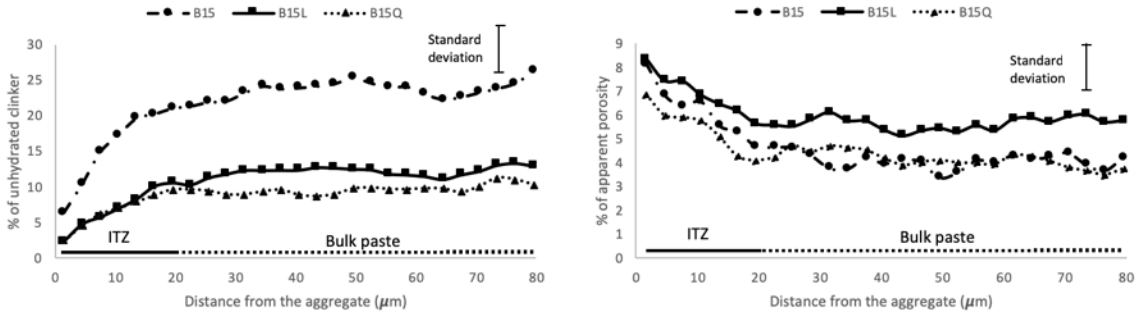

a) b)

Figure 6. Apparent porosity (a) and unhydrated clinker material (b) as function of the distance from the aggregate.

The tukey's range test was applied in two points of interest, at 1.5 and 40 μm, to study the differences in the vicinity of the aggregate and bulk paste respectively, the results can be found in the Table 4 and Table 5, this test allows the identification of homogenous groups within families of data, with this tool it was possible to define when the differences of porosity or anhydrous material was significant with a 95% level of confidence. The results of the statistical analysis indicate that the porosity in the vicinity of the aggregate can be consider as equals between each other, however, the porosity in the bulk paste of sample B15L sample's is higher than in samples B15 and B15Q.

Table 4. Tukey's range test for the anhydrous material in the vicinity of the aggregate and the bulk paste at 120 Kg/m^3 SF to define if the anhydrous materials among mixtures is equal at selected sites

	Unhydrated clinker volume in the vicinity of the aggregate (1.5 um)	Unhydrated clinker volume in the bulk paste (40.5 um)	
MIX	Homogenous groups	Homogenous groups	
B15	A	A	
B15Q	A		B
B15L	A		B

Table 5. Tukey's range test for the apparent porosity in the vicinity of the aggregate and the bulk paste at 120 Kg/m^3 SF to define if the apparent porosity among mixtures is equal at selected sites

	Porosity volume in the vicinity of the aggregate (1.5 um)	Porosity volume in the bulk paste (40.5 um)	
MIX	Homogenous groups	Homogenous groups	
B15	A	A	
B15Q	A	A	
B15L	A		B

As the compressive strength of the three samples was similar, the apparent limiting factor for the compressive strength is the porosity in the vicinity of the aggregate, while the porosity in both the vicinity of the aggregate and bulk paste could play a significant role in the resistivity of the material. Given that the B15L and B15 samples had the same resistivity, and B15Q sample presented higher resistivity, the results from the porosity seem contradictory, however, the water availability in samples B15L and B15Q could have led to a higher degree of hydration of the silica fume and to a different type of C-S-H with a lower Ca/Si ratio, this could originate that sample B15L maintained a low permeability even though its higher porosity and the sample B15Q sample had an even lower permeability.

X-ray diffraction.

A paste reproduction of the previously discussed three mixes was casted and studied with the XRD technique at an age of 91 days. The diffractograms were first deconvoluted using the Rietveld refinement and then a peak phase for C-S-H was added to the quantification to improve fitting, the quantities were normalized with the external standard method. The C-S-H phase pseudo mass was not calibrated due to its composition changing with the increase of pozzolanic addition, therefore the amount of C-S-H in each paste is only obtained by difference of the sum of all the phases identified in the XRD pattern.

The percentages of each phase normalized to the cement content in the paste are given in the Table 6, a ratio between the sum of the clinker phases (C_2S, C_3S, C_3A and C_4AF) in the unhydrated cement and the sum of the clinker phases presented in the hydrated pastes is presented in the Figure 7 as the cement's degree of hydration.

Table 6. Deconvolution of the X Ray Diffraction Spectra from the paste reproduction of the mortars B15, B15Q and B15L.

Phase	B15	B15Q	B15L
C_3S	14%	5%	5%
C_2S	9%	4%	3%
C_4AF	6%	3%	3%
Calcite	3%	1%	19%
Calcium Hydroxide	2%	1%	1%
Ettringite	2%	3%	3%
Quartz	0%	26%	1%
Bassanite	1%	1%	1%
Gypsum	0%	1%	1%
Amorphous content/C-S-H	62%	55%	62%

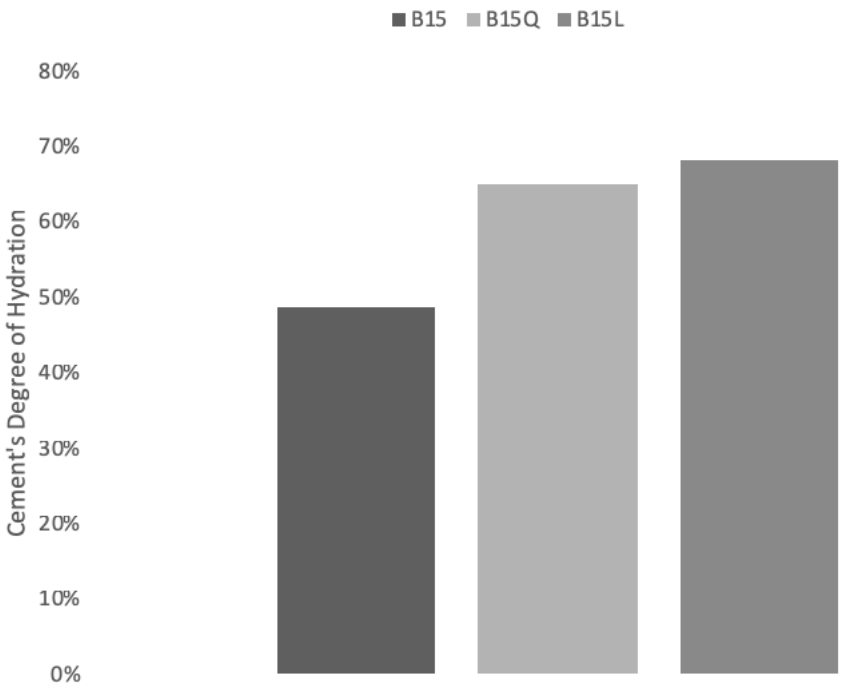

Figure 7. Degree of hydration of the cement in the paste reproduction of the mortars B15, B15Q and B15L

The following model of hydration of the silicates was used to estimate the calcium hydroxide production [41]:

$$C_3S + 5.3H \longrightarrow C_{1.7}SH_4 + 1.3CH \quad (1)$$

$$C_2S + 4.3H \longrightarrow C_{1.7}SH_4 + 0.3CH \quad (2)$$

The alite and belite content found in the hydrated pastes was subtracted from the amounts present in the anhydrous sample of cement to determine the reacted amount of the silicates. From that an estimation of the portlandite production was obtained by means of using the Equations 1 and 2. A difference between the theoretically produced portlandite and the amount present in the hydrated pastes was used to calculate the percentage of CH consumed in each mixture.

The 37.5% replacement in volume of the cement content increased the degree of hydration of the cement in 34 and 41% for the B15Q and B15L mixes respectively, passing for 49% to 65 and 68%. It can be inferred that the reaction of silica fume was as well enhanced by the replacement of cement with the change of the amount portlandite consumed that passed from 78% in the binary system silica fume-cement to 93% in both ternary systems.

From the resistivity tests (**Figure 5**) a hypothesis of the B15Q sample having a more pronounced pozzolanic reaction was made, the results in the Figure 8 indicate that the percentage of CH consumed per g of cement is higher in the filler replaced mixtures and slightly higher for the mixture B15Q. The increase in portlandite consumption led by the augmented water availability product of the increase of the w/c allows the silica fume to have an optimized performance on the ternary systems.

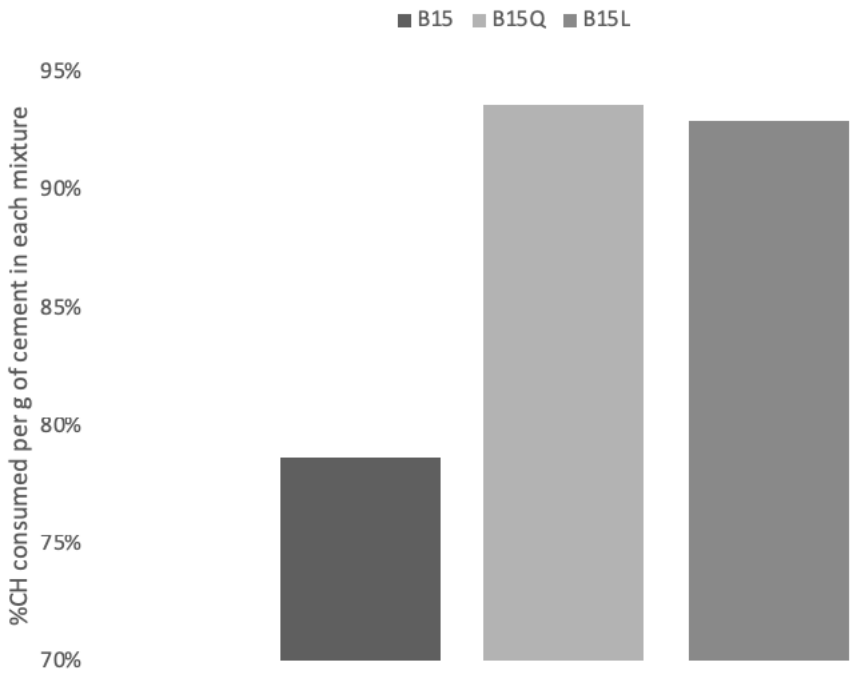

Figure 8. Calcium hydroxide consumed in the paste reproduction of the mortars B15, B15Q and B15L.

Quantitative Energy Dispersive X-ray Spectroscopy (QEDS)

The paste around the aggregates was investigated in layers of 3 μm. To cover 50 μm and have points at each 3 μm, the bands were intercalated to start at either 3 or 6 μm, the use of such distance between points was decided in order to not have intermixing of the information between lectures, as the radius on interaction is estimated at a range between 0.5 and 0.75 micrometers.

The use of standards allowed to have the percentage of each element in absolute terms which then are converted to oxides for each of the 1272 points per mixture. The difference between the sum of oxides (SOX) and 100% can be attributed to the water, CO_2, or porosity content of the studied spot being those elements of the composition of the hydrates that can not be reliably quantified with our SEM setup, in order to allow an approximate estimation of the amount of water in the C-A-S-H composition it was assumed as only water.

Bivariate histograms were made with the Si/Ca vs Al/Ca molar ratios (Figure 9), and SOX vs Si/Ca (Figure 10). The bivariate histograms were constructed with bins at 0.01, tie lines in the representation Si/Ca vs Al/Ca were made from the points of ettringite, aluminates and

calcium hydroxide to high density points in the cloud of composition in the range of C-S-H, the elemental ratios from the pure phases are the ones expressed in the Table 7.

The point of intersection of the three tie lines that appears in Figure 10 was assumed as the composition of the C-A-S-H of the mortar mixture. Such points were revised and averaged to obtain the sum of oxides of each C-A-S-H and indicated with a red dot in the Figure 10, along with its standard deviation. Relevant elemental ratios of the composition of each C-A-S-H were calculated as well as the ratio between water and Ca (Table 8).

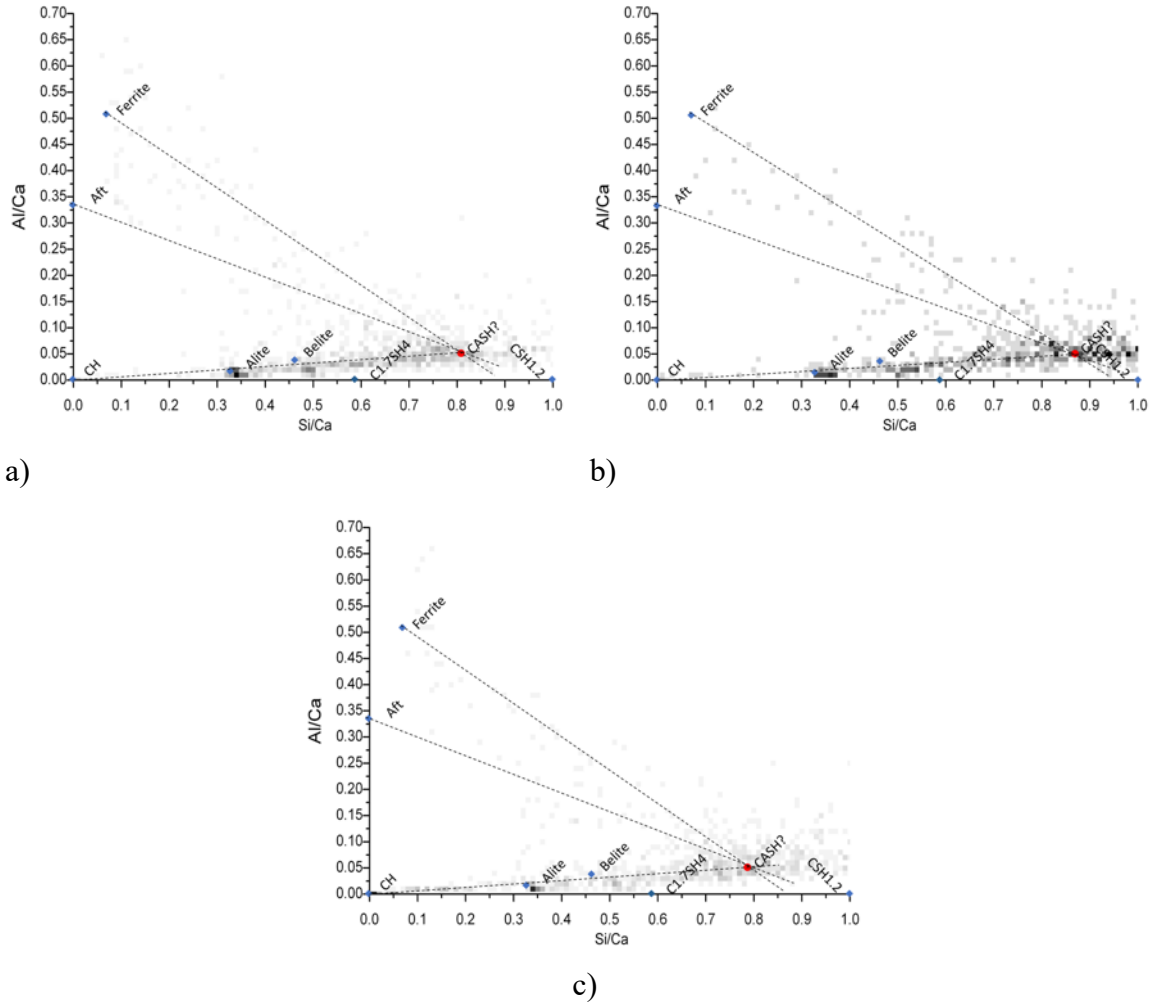

Figure 9. Bivariate histograms made from Si/Ca vs Al/Ca molar ratios of the paste adjacent to the aggregates of the mixes a) B15 b) B15Q c) B15L

Table 7. Elemental ratios and Sum of Oxides (SOX) of the phases pointed on the EDS bivariate histograms extracted from Taylor [42].

Phase	Si/Ca (molar)	Al/Ca (molar)	SOX (weigth)
Alite	0.33	0.02	1.00
Belite	0.46	0.04	1.00
Ferrite	0.07	0.51	1.00
Calcium Hydroxide (CH)	0.00	0.00	0.76
Calcium Carbonate (CC)	0.00	0.00	0.56
Etringite (Aft)	0.00	0.33	0.54
$C\text{-}S\text{-}H_{1.2}$ (C-S-H(I))	1.00	0.00	0.84
$C_{1.7}SH_4$ (C-S-H(II))	0.59	0.00	0.80

Table 8. Composition of the C-A-S-H expressed in elemental ratios for the mixes B15, B15Q and B15L.

Mix	Ca/Si	Al/Ca	S/Ca	Fe/Ca	H2O/Ca
B15	1.23 *±0.00*	0.05 *±0.00*	0.05 *±0.02*	0.02 *±0.02*	1.99 *±0.24*
B15Q	1.15 *±0.01*	0.05 *±0.00*	0.03 *±0.01*	0.02 *±0.01*	1.84 *±0.44*
B15L	1.20 *±0.01*	0.05 *±0.00*	0.03 *±0.01*	0.02 *±0.01*	2.00 *±0.31*

It is seen in Table 8 that for sample B15Q the Ca/Si ratio was the lowest encountered among the mixtures, probably due to some local defects on the quartz structure product of the grinding process which in turn could have led to a partial solubilization of it and a posterior incorporation of Si into the C-S-H, while both ternary systems have a lower Ca/Si ratio than the B15 mixture. The explanation of how cement-silica fume mixtures and filler-cement-silica fume mixtures can present similar compressive strengths and BER, could be related to an increase of pozzolanic activity together with the presence of higher amount of C-S-H. The ability of the silica fume to allow high replacements of cement by inert materials, in this case 37.5%, may be related to the production of low Ca/Si C-S-H, because such hydrates have longer chain length than the ones resulted from the Portland cement reaction [42] and will lead to higher strengths [23] and also to its ability to block the pores in the ITZ.

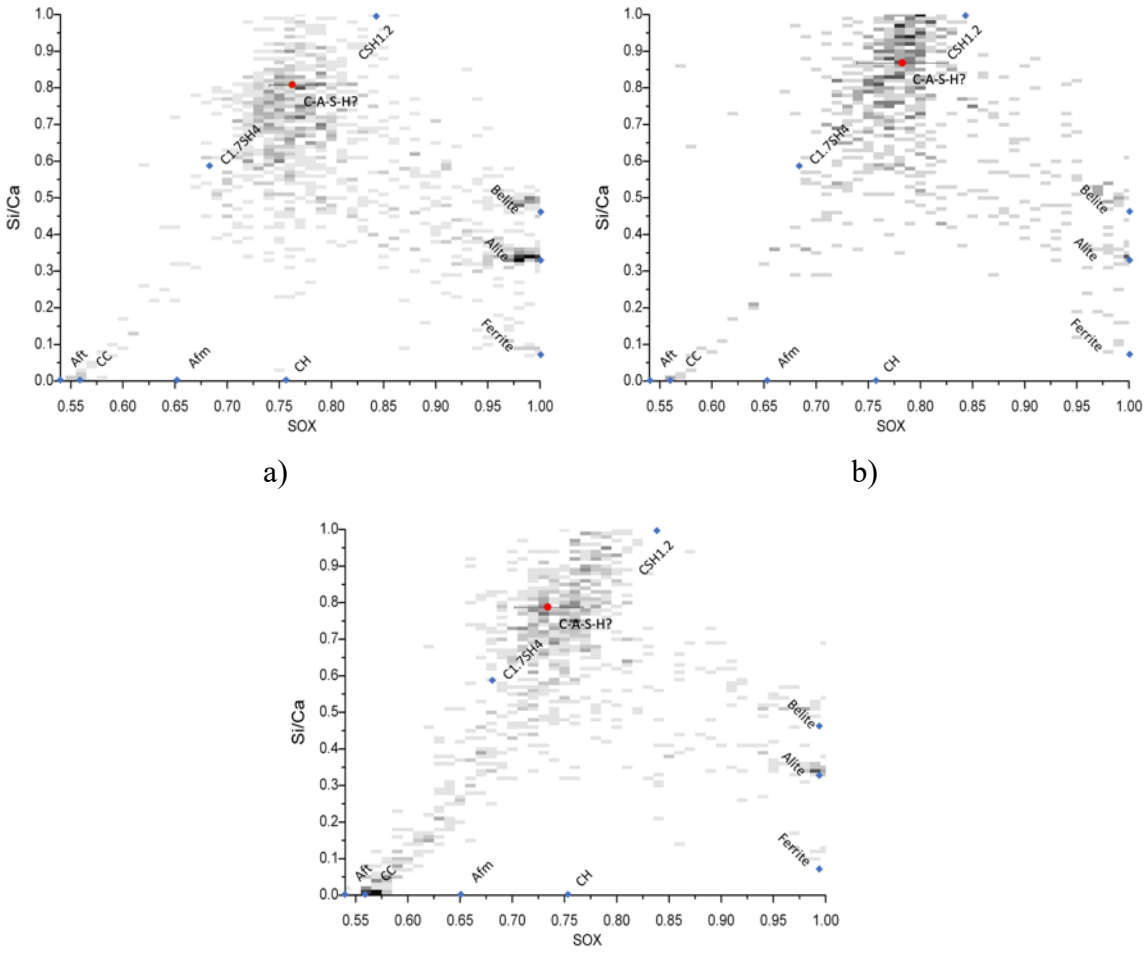

Figure 10. Bivariate histograms made from Si/Ca molar ratio vs the Sum of Oxides (SOX) of the paste adjacent to the aggregates of the mixes a) B15 b) B15Q c) B15L

Sustainability

This work has shown the mechanism upon which the silica fume can allow great cement replacements in UHPC systems. It was previously stated that the pozzolans are relatively more scarce than inert materials, with this type of mix design a broader number of materials will be available to replace cement and with that, more applications could be beneficiated by the durability and mechanical properties of UHPC, these mixes will not only be as reliable as regular UHPC but will have a smaller carbon foot print. An estimation of the ecological impact of the production of such mixes was done with regard to the global warming potential which is related to the equivalent CO_2 emissions per kg of a given material, in this case the

quantification was done with regard to a cubic meter of concrete based on the mix design and the global-warming-potential (GWP) of the raw materials shown in the Table 9.

Table 9. Global warming potential of the raw materials

Material	GWP (kg CO_2 /kg)
Cement[43]	0.951
Limestone Powder [43]	0.0172
Quartz Powder [43]	0.0234
Silica fume [44]	0.028
Plasticizer Policarboxilate [43]	0.944

Two parameters were calculated with the information contained in Table 1 and Table 9, the GWP per cubic meter (CO_2 kg/m^3) and the GWP normalized by strength (CO_2 kg/(m^3*MPa)) which shows the carbon footprint required to reach a given strength depending on the system, the two parameters are summarized in Figure 11 .

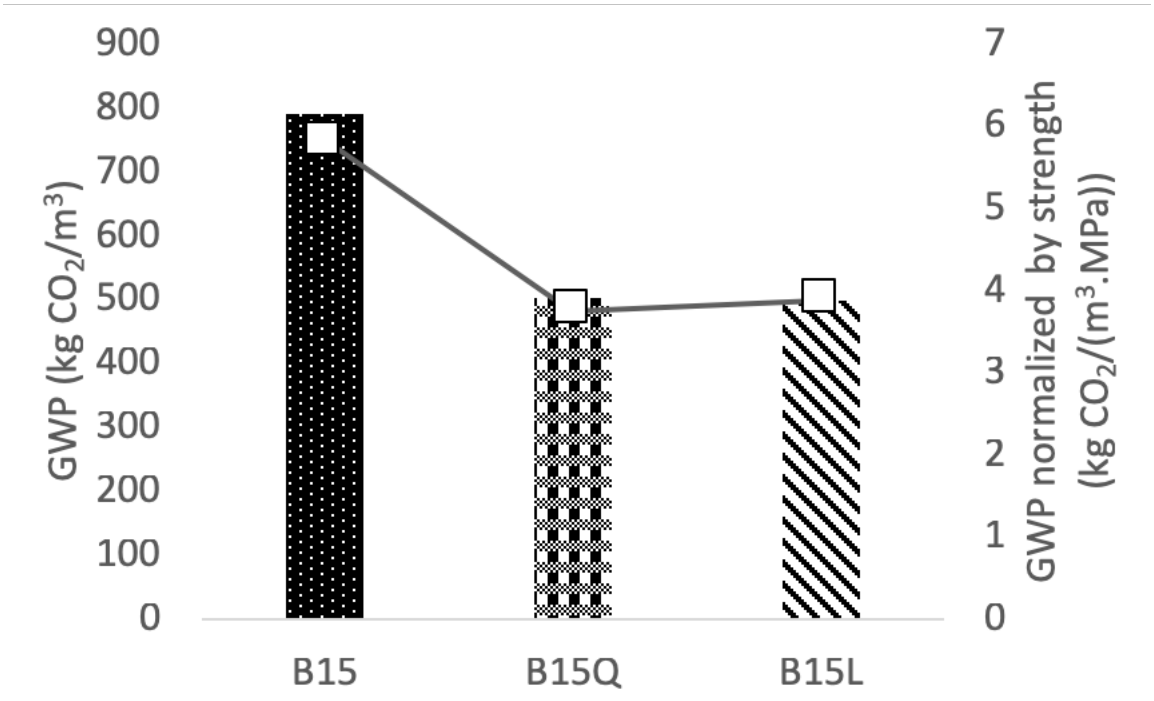

Figure 10. GWP and normalized GWP by strength for the mixes B15, B15Q and B15L.

The results of the GWP study shows a reduction in the CO_2 emission of 37% per cubic meter when 37.5% of the cement is replaced by both inert materials, and a 35% and 33% reductions of emission per cubic meter per MPa by the ternary systems containing Q and L, respectively. The tested durability parameter (BER) shows a similar or better performance between the mix with pure cement and silica fume and the ternary systems, this type of mix design should be seriously considered in the UHPC proportioning as it maintains performance and lower by a third the emissions to reach it

CONCLUSIONS

Based on the experimental results obtained in this research work, the following conclusions can be drawn:

- It was quantified with the use of the XRD that the degree of hydration of both cement and silica fume is enhanced on UHPC with the inclusion of mostly inert fillers
- The BSEI technique showed that when the ITZ porosity is adequate, the hardness of the anhydrous inclusions does not play the major role in the development of either durable or mechanical parameters
- The QEDS showed that the replacement of cement by inert fillers enhanced the silica fume reaction, allowing the silica fume to react with a bigger amount of calcium hydroxide and water yielding a lower Ca/Si ratio C-S-H with presumed better degree of polymerization.
- The relative amounts of silica fume in UHPC allows for high cement replacement due to various factors: As a filler the silica fume blocks physically the pores in the ITZ, and as supplementary cementitious material reacts with the portlandite to improve the C-S-H properties in both the ITZ and bulk paste.
- This combination of factors gave the ternary systems with lower cement amounts comparable mechanical and durability characteristics while lowering the carbon footprint 37% and in average 34% the emissions per MPa.

ACKNOWLEDGMENTS

The authors wish to express their gratitude and sincere appreciation to the different organizations that contributed in the development of this project, to the Consejo Nacional de Ciencia y Tecnología of Mexico (CONACYT), to the Facultad de Ingeniería Civil (FIC) of the Universidad Autónoma de Nuevo León (UANL) and to the Faculté de Genié of the University of Sherbrooke. Guillermo Hernández would like to specially thank William Wilson for his support in the microstructural characterization required in this work.

REFERENCES

[1] P. Richard and M. Cheyrezy, "Composition of reactive powder concretes," *Cem. Concr. Res.*, vol. 25, no. 7, pp. 1501–1511, 1995.

[2] O. M. Jensen and P. F. Hansen, "Water-entrained cement-based materials I . Principle and theoretical background," *Cem. Concr. Res.*, vol. 31, no. 4, pp. 647–654, 2000.

[3] Z. Yunsheng, S. Wei, L. Sifeng, J. Chujie, and L. Jianzhong, "Preparation of C200 green reactive powder concrete and its static-dynamic behaviors," *Cem. Concr. Compos.*, vol. 30, no. 9, pp. 831–838, 2008.

[4] S. L. Yang, S. G. Millard, M. N. Soutsos, S. J. Barnett, and T. T. Le, "Influence of aggregate and curing regime on the mechanical properties of ultra-high performance fibre reinforced concrete (UHPFRC)," *Constr. Build. Mater.*, vol. 23, no. 6, pp. 2291–2298, 2009.

[5] H. Yazıcı, M. Y. Yardımcı, S. Aydın, and A. Ş. Karabulut, "Mechanical properties of reactive powder concrete containing mineral admixtures under different curing regimes," *Constr. Build. Mater.*, vol. 23, no. 3, pp. 1223–1231, Mar. 2009.

[6] N. A. Soliman and A. Tagnit-Hamou, "Development of ultra-high-performance concrete using glass powder Towards ecofriendly concrete," *Constr. Build. Mater.*, vol. 125, pp. 600–612, 2016.

[7] G. Hernández Carrillo, A. Durán Herrera, and P. L. Valdez Tamez, "ULTRA HIGH PERFORMANCE CONCRETE (UHPC) WITH LOW SILICA FUME CONTENTS AND LIMESTONE AGGREGATES," *Proc. RILEM Int. Conf. Mater. Syst. Struct. Civ. Eng. Conf. Segm. Concr. with Suppl. Cem. Mater.*, pp. 349–358, 2016.

[8] J. E. Rossen, B. Lothenbach, and K. L. Scrivener, "Composition of C-S-H in pastes

with increasing levels of silica fume addition," *Cem. Concr. Res.*, vol. 75, pp. 14–22, 2015.

[9] S. L. Sarkar and P.-C. Aïtcin, "Dissolution rate of silica fume in very high strength concrete," *Cem. Concr. Res.*, vol. 17, no. 4, pp. 591–601, 1987.

[10] K. L. Scrivener, V. M. John, and E. M. Gartner, "Eco-efficient cements: Potential economically viable solutions for a low-CO2cement-based materials industry," *Cem. Concr. Res.*, no. February, 2018.

[11] M. Zajac, A. Rossberg, G. Le Saout, and B. Lothenbach, "Influence of limestone and anhydrite on the hydration of Portland cements," *Cem. Concr. Compos.*, vol. 46, pp. 99–108, 2014.

[12] G. Menéndez, V. Bonavetti, and E. F. Irassar, "Strength development of ternary blended cement with limestone filler and blast-furnace slag," *Cem. Concr. Compos.*, vol. 25, no. 1, pp. 61–67, 2003.

[13] A. Skaropoulou, G. Kakali, and S. Tsivilis, "Thaumasite form of sulfate attack in limestone cement concrete: The effect of cement composition, sand type and exposure temperature," *Constr. Build. Mater.*, vol. 36, pp. 527–533, 2012.

[14] S. Tsivilis, K. Sotiriadis, and A. Skaropoulou, "Thaumasite form of sulfate attack (TSA) in limestone cement pastes," *J. Eur. Ceram. Soc.*, vol. 27, no. 2–3, pp. 1711–1714, 2007.

[15] A. Skaropoulou, K. Sotiriadis, G. Kakali, and S. Tsivilis, "Use of mineral admixtures to improve the resistance of limestone cement concrete against thaumasite form of sulfate attack," *Cem. Concr. Compos.*, vol. 37, no. 1, pp. 267–275, 2013.

[16] Y. Wang, X. He, Y. Su, J. Huang, and B. Ma, "Effect of silica fume on the thaumasite form of sulfate attack on cement-based materials," *J. Wuhan Univ. Technol. Mater. Sci. Ed.*, vol. 32, no. 5, pp. 1108–1114, 2017.

[17] M. E. Broz, R. F. Cook, and D. L. Whitney, "Microhardness, toughness, and modulus of Mohs scale minerals," *Am. Mineral.*, vol. 91, no. 1, pp. 135–142, 2006.

[18] L. Sorelli, G. Constantinides, F. J. Ulm, and F. Toutlemonde, "The nano-mechanical signature of Ultra High Performance Concrete by statistical nanoindentation techniques," *Cem. Concr. Res.*, vol. 38, no. 12, pp. 1447–1456, 2008.

[19] W. Wilson, L. Sorelli, and A. Tagnit-Hamou, "Unveiling micro-chemo-mechanical

properties of C–(A)–S–H and other phases in blended-cement pastes," *Cem. Concr. Res.*, vol. 107, no. February, pp. 317–336, 2018.

[20] W. C. Oliver and G. M. Pharr, "An improved technique for determining hardness and elastic modulus using load and displacement sensing indentation experiments," *Journal of Materials Research*, vol. 7, no. 06. pp. 1564–1583, 1992.

[21] D. P. Bentz and P. C. Aitcin, "The Hidden Meaning of Water- Cement Ratio Distance between cement particles is fundamental," *Concr. Int.*, vol. 30, no. 5, pp. 51–54, 2008.

[22] R. F. Feldman and J. J. Beaudoin, "Microstructure and strength of hydrated cement," *Cem. Concr. Res.*, vol. 6, no. 3, pp. 389–400, 1976.

[23] W. Kunther, S. Ferreiro, and J. Skibsted, "Influence of the Ca/Si ratio on the compressive strength of cementitious calcium-silicate-hydrate binders," *J. Mater. Chem. A*, vol. 5, no. 33, pp. 17401–17412, 2017.

[24] O. M. Jensen and P. F. Hansen, "Water-entrained cement-based materials I . Principle and theoretical background," *Cem. Concr. Res.*, vol. 31, pp. 1–13, 2000.

[25] K. Wille, A. E. Naman, and G. J. Parra-Montesinos, "Ultra - High Performance Concrete with Compressive Strength Exceeding 150 MPa (22ksi) : A Simpler Way," *ACI Mater. J.*, vol. 108, no. 1, pp. 46–53, 2011.

[26] N. V Tue, J. Ma, M. Orgass, and E. Fehling, "Influence of addition method of superplasticizer on the properties of fresh UHPC," in *2nd International Symposium on Ultra High Performance Concrete*, 2008.

[27] R. Snellings, A. Bazzoni, and K. Scrivener, "The existence of amorphous phase in Portland cements: Physical factors affecting Rietveld quantitative phase analysis," *Cem. Concr. Res.*, vol. 59, pp. 139–146, 2014.

[28] K. Scrivener, R. Snellings, and B. Lothenbach, *A Practical Guide to Microstructural Analysis of Cementitious Materials*. 2016.

[29] K. L. Scrivener, A. Bentur, and P. L. Pratt, "Quantitative characterization of the transition zone in high strength concretes," *Adv. Cem. Res.*, vol. 1, no. 4, pp. 230–237, 1988.

[30] F. Deschner, B. Münch, F. Winnefeld, and B. Lothenbach, "Quantification of fly ash in hydrated, blended Portland cement pastes by backscattered electron imaging," *J. Microsc.*, vol. 251, no. 2, pp. 188–204, 2013.

[31] M. G. Alexander, *Engineering and Transport Properties of the Interfacial Transition Zone in Cementitious Composites*. RILEM Publications, 1999.

[32] K. L. Scrivener, "Backscattered electron imaging of cementitious microstructures: Understanding and quantification," *Cem. Concr. Compos.*, vol. 26, no. 8, pp. 935–945, 2004.

[33] W. Wilson, L. Sorelli, and A. Tagnit-Hamou, "Automated coupling of NanoIndentation and Quantitative Energy-Dispersive Spectroscopy (NI-QEDS): A comprehensive method to disclose the micro-chemo-mechanical properties of cement pastes," *Cem. Concr. Res.*, vol. 103, no. August 2017, pp. 49–65, 2018.

[34] W. Wilson, L. Sorelli, and A. Tagnit-Hamou, "Chemo-mechanical properties of cement matrices with fly ash and slag," *Am. Concr. Institute, ACI Spec. Publ.*, vol. 2017-Janua, no. SP 320, pp. 1–14, 2017.

[35] N. W. M. Ritchie, "Standards-Based Quantification in DTSA-II—Part II," *Micros. Today*, vol. 20, no. 01, pp. 24–28, 2012.

[36] D. Breton, "Low-heat high-performance," United States Patent 5531823, 1995.

[37] C. Vogt, "Ultrafine particles in concrete - Influence of ultrafine particles on concrete properties and application to concrete mix design," *Sch. Archit. Built Environ. Div. Concr. Struct.*, vol. PhD, p. 177, 2010.

[38] W. Huang, H. Kazemi-Kamyab, W. Sun, and K. Scrivener, "Effect of cement substitution by limestone on the hydration and microstructural development of ultra-high performance concrete (UHPC)," *Cem. Concr. Compos.*, vol. 77, pp. 86–101, 2017.

[39] W. Morris, E. I. Moreno, and A. A. Sagüés, "Practical evaluation of resistivity of concrete in test cylinders using a Wenner array probe," *Cem. Concr. Res.*, vol. 26, no. 12, pp. 1779–1787, 1996.

[40] H. Moosberg-Bustnes, B. Lagerblad, and E. Forssberg, "The function of fillers in concrete," *Mater. Struct.*, vol. 37, no. 266, pp. 74–81, 2004.

[41] P.-C. Aitcin, *Binders for Durable and Sustainable Concrete*. 2018.

[42] H. F. W. Taylor, *Cement chemistry*. 1990.

[43] H. S. Müller, M. Haist, and M. Vogel, "Assessment of the sustainability potential of concrete and concrete structures considering their environmental impact, performance

and lifetime," *Constr. Build. Mater.*, 2014.

[44] J. M. Khatib, *Sustainability of construction materials.*, 2nd ed. Elsevier, 2016.

6 *Filler effect on Cement-Limestone-Calcined clays UHPC based systems*

6.1 Introduction

The popularity of the ternary systems comprising cement-limestone-calcined clays has increased over the last years due to its ability to allow high cement replacements while increasing durability and lowering the carbon footprint. This kind of system is tested within this research program to explore if the performance is repeated at very low w/c of 0.25.

The first part of the work shows how the mechanical properties and durable parameters improve when adding metakaolin to a pure cement system, additions from 0 to 240 kg/m^3 where tested. Upon finishing the stage on the metakaolin improvements to the performance, the cement was replaced by limestone powder until reaching a w/c of 0.4 to enhance hydration and to prove that the formation of carboaluminates was the source of the performance on such systems. To discard the possibility of the limestone acting as mere filler a second set of mixes containing quartz powder instead of limestone were tested.

The results show that the metakaolin reaction is very fast staying dormant after 7 days. An unexpected outcome was obtained as the cement mixes replaced by either quartz or limestone reached similar performance in both durable and mechanical aspects, and little monocarboaluminate formation was observed.

Microstructural testing was done in order to describe the hydration mechanism and phase assemblage on the systems in order to explain the obtained results.

6.2 Paper 2 Effect of limestone and quartz fillers in UHPC with calcined clay

Guillermo Hernández-Carrillo [a)b)], Arezki Tagnit-Hamou[b)], Alejandro Durán-Herrera[a)]*

[a)] *Universidad Autónoma de Nuevo León, Facultad de Ingeniería Civil, Ave. Universitaria S/n, Ciudad Universitaria, 66450 San Nicolás de los Garza, N.L., México 66455*

[b)] *Université de Sherbrooke, Faculté de Genié, 2500 Boulevard de l'Université, Sherbrooke, QC J1K 2R1, Canadá*

Abstract

Ultra-high performance concrete (UHPC) is a material developed to maximize the engineering characteristics of hydraulic concrete, in terms of durability and mechanical properties, but the adoption of this technology in practice has not turned out as desired, mainly due to the high amounts of cement and silica fume required for its production, and for its consequences on both economic and ecological costs. As an option to improve the impact of UHPC, both on costs and on sustainability, this work evaluates four UHPC series with metakaolin additions of 5, 10, 15 and 20%, and the substitution of 37.5% of the Portland cement volume by limestone or quartz filler. The compressive strength, the bulk electrical resistivity and a set of tests for microstructural characterization (TGA, XRD and quantitative EDS) were utilized to better understand the role of calcite on the hydration and pozzolanic reactions in ternary Portland cement-matakaolin-limestone filler. Results indicate that the reaction of calcite is scarce and should be considered as a mere filler as no increase in AFm phases were found. Nevertheless, the ternary mixture with 15 % of metakaolin in addition to cement, and with 37.5 % of the Portland cement volume substituted by limestone filler, was the one that presented the best performance in terms of compressive strength and bulk electrical resistivity. The results of the microstructural characterization indicate that the high kaolin content in the metakaolin, originated the most significant hydration and pozzolanic reactions development between the ages of 7 and 28 days, as between 28 and 91 the reaction remained dormant. In general, the whole set of results included in this work indicate that

limestone filler don't act as better filler than other kind of powders when used in ternary Portland cement-metakaolin- filler systems.

Keywords: ultra-high performance concrete, metakaolin, limestone filler, C-A-S-H, monocarboaluminate.

Introduction

Ultra High Performance Concrete (UHPC) is a material developed to maximize the engineering characteristics of hydraulic concrete, in terms of durability and mechanical properties, but even though the significance that this development represents for the concrete construction industry, the adoption of this technology in practice has not turned out as desired, mainly due to the high amounts of cement and silica fume required for its production [1], and for its consequences on both economic and ecological costs.

In contrast, a remarkable benefits of UHPC that counteract the negative impact on both economic and ecological costs, are associated with its ultra-high mechanical properties and durability; first because for a specific application and in relation to a conventional concrete, in the structural design, these characteristics will lead to structural elements of smaller dimensions and, consequently, they will require a smaller volume of concrete for their construction, and second, because its superior durability will increase the potential service life of structures that in service will be subject to environmental conditions that typically cause the deterioration of concrete elements built with conventional concrete.

Nowadays, the production of Portland cement contributes 10% of anthropogenic emissions [2], although this contribution could be considered constant, due to the increase in the demand for concrete that is expected in the immediate future (especially in the developing countries), the net contribution (in terms of tons of CO_2 / ton of cement) coming from the cement industry, will be increased proportionally to the consumption of this material. However, this negative impact on sustainability can also be counteracted through a greater use of UHPC in the practice of concrete construction.

One option that could contribute to this objectives is the substitution of cement by reactive fillers, and even more so because substitutions of up to 20 % by mass, in concretes with w/c of 0.35 have shown negligible effect on the diffusion coefficient of chloride ions, resulting

advantageous because the more costly unreacted cement is being replaced by limestone filler, in this regard, the limestone replacement for cement in low w/cm concretes appears to be one viable, but currently underutilized, option [3].

In order to search for an alternatives to reduce the negative impacts (both in costs and sustainability), attributable to the high consumption of cement and silica fume demanded by the UHPC, it has been reported that metakaolin could be an appropriate alternative to silica fume in UHPC [4], in this work, four binary cementitious combinations of Portland cement and metakaolin were produced to evaluate the effect of the metakaolin as a supplementary cementitious material and matrix densification enhancer in UHPC, in combination with a limestone or quartz powder dosed in substitution of a fixed volume of the cement.

For cementitious systems like the ones studied in this work, it has been reported that the formation of carboaluminates resulting from the reaction of limestone, calcined clays and Portland cement can be the source that leads to the improvement of concrete properties [5]. However, the low solubility of calcite and the low availability of water in UHPC concretes can interfere with the formation of these phases, so in order to evaluate the influence of either the solubility of the calcite and/or its filler effect, the experimental work in this investigation consisted of the determination of the compressive strength and the bulk electrical resistivity, as well as the characterization of thermal, chemical and microstructural properties evaluated by thermogravimetric analysis (TGA), quantitative X-Ray Diffraction analysis (QXRD), and Quantitative Energy Dispersive Spectroscopy (QEDS).

Experimental Investigation

Materials

The materials used in the research were as follows:

- An ASTM C 1157 Type HS cement (HS), with a Blaine fineness of 438 m^2/kg, a mean particle size of 14 µm and a density of 3.18 g/cm^3.
- An ASTM C 618 Metakaolin (MK), with a BET-specific surface area of 10.66 m^2/g, a mean particle size of 14 µm and a density of 2.59 g/cm^3.
- An ASTM C 994 Type A Polycarboxylate based high range water reducer or superplasticizer (HRWRA), with a density of 1.09 g/cm^3 and an active agent content of 40%.

- Quartz Powder (Q) with a mean particle size of 19 µm and a density of 2.75 g/cm^3.
- Limestone Powder (L) with a mean particle size of 17 µm and a density of 2.71 g/cm^3.
- An ASTM C 33 natural river sand with 5 mm maximum size, a density of 2.61 g/cm^3 and an absorption of 1.15 %.

Figure 1 presents the particle size distribution of the cement, the metakaolin, the limestone and the quartz powders, and the natural river sand. Table 1 summarizes the powders chemical and physical properties, and with the exception of the natural river sand and the quartz powder that is 100 % quartz, Table 2 summarizes the normalized chemical phase composition for HS, MK and L.

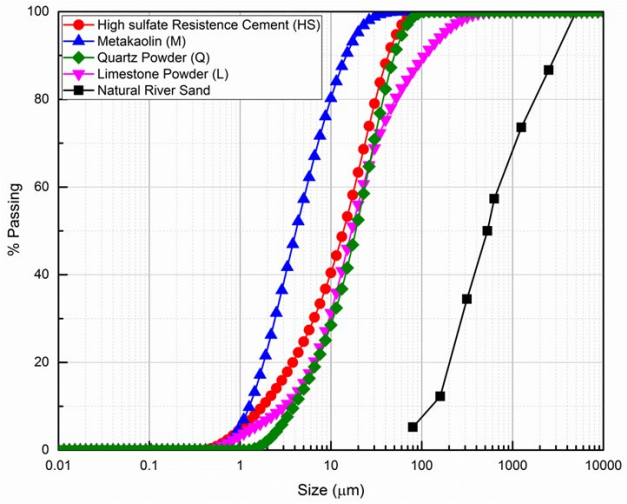

Figure 1 Particle size distribution of HS, MK, Q, L and the natural river sand.

Table 1 Physical and chemical properties for HS, MK, Q and L, obtained by X-Ray fluorescence, pycnometry, air permeability (Blaine), BET tests, and laser granulometry.

Oxide amount or property (wt %)	Cementitious Materials		Powders	
	HS	MK	Q	LS
SiO_2	21.8	52.1	99.6	5.10
TiO_2	0.18	1.6	0.01	0.04
Al_2O_3	4.00	44.4	0.10	0.80
Fe_2O_3	3.14	0.4	0.02	0.27
Mn_2O_3	0.038	-----	0.002	0.008
MgO	1.90	0.10	0.10	1.30
CaO	63.10	-----	-----	51.20
Na_2O	0.05	0.10	-----	-----
K_2O	0.56	0.10	-----	0.34
P_2O_5	0.09	-----	-----	0.01
SO_3	2.37	-----	-----	0.06
SrO	0.10	-----	-----	0.03
ZnO	0.02	-----	-----	-----
Loss on ignition	2.60	1.0	0.10	40.90
Equivalent alkali (Na_2Oeq)	0.42	0.20	-----	0.22
Density, g/cm^3	3.18	2.59	2.75	2.71
Blaine surface, m^2/kg	438.00	-----	-----	-----
BET surface, m^2/g	-----	10.66	-----	-----
Mean particle size (d50), µm	14.00	4.10	19.00	17.00

Table 2 Normalized chemical phase composition for HS, MK, Q and L

Chemical phase (wt %)	HS	MK	Q	L
C_3S	52	-----	-----	-----
C_2S	18	-----	-----	-----
C_3A cubic	1.0	-----	-----	-----
C_3A orthorhombic	2.0	-----	-----	-----
Ferrite	10	-----	-----	-----
Periclase	1.0	-----	-----	-----
Gypsum	1.0	-----	-----	-----
Bassanite	3.0	-----	-----	-----
Calcite	5.0	-----	-----	75
Quartz	-----	-----	100	3.0
Anatase	-----	2.0	-----	-----
Dolomite	-----	-----	-----	3.0
Amorphous	7.0	98	-----	19

Mixture proportions

Power´s model is a simple approach for estimating the relative volumes of hydration products, porosity, and chemical shrinkage present in Portland cement paste as a function of its starting water-to-cement ratio (w/c) and current degree of hydration. It forms an important link between cement composition, microstructure, and performance, necessary for modeling cement-based systems [6]. Through this model [7] the estimated w/c to maximize cement hydration is around 0.4.

For this research work, four base mix designs with a w/c of 0.25, a cement consumption of 800 kg/m^3, a target flow of 250 ± 50 mm, and metakaolin additions of 5, 10, 15 and 20% were used to evaluate the reaction of limestone powder in a binary Portland cement-metakaolin UHPC cementitious system, and to confirm if the reaction of the limestone powder have the potential to detonate improvements in concrete performance. For this purpose and for each of the four base mix designs, two additional mixtures were produced,

in which the cement volume was replaced by 37.5 % of either limestone or quartz powder, and at the same time the cement content was decreased to 500 kg/m^3 in order to reach a w/c of 0.40 for a fixed water dosage of 200 kg/m^3.

To reach the target flow of 250 ± 50 mm, measured through the standard cone described in ASTM C 230 [8], a SP-HRWRA polycarboxylate based admixture was used. Nevertheless, the mixtures with an addition of 20% MK did not reach such level of fluidification without a slight vibration.

The proportions for the four series of mixtures evaluated in this work, as well as some fresh stage properties determined by duplicate are reported in Table 3, where in the nomenclature used to distinguish the different mixtures, the number indicates the percentage of metakaolin dosed in addition to the cement content (5, 10, 25 and 20 %), and the letter at the end of some nomenclatures indicates the volume of cement substituted by limestone (L) or quartz (Q) powder. In all the nomenclatures M indicates metakaolin. As an example, mixture M15 is a mixture with 15% of metakaolin in addition to the cement mass, while the mixture M15L has the same amount of metakaolin but additionally a volume substitution of 37.5% of the cement by limestone powder.

The reductions of unit weight reported in Table 3 for mixtures with L or Q, are attributed to the differences between the density of the cement (3.18) and the limestone (2.75) or quartz powders (2.71). In this Table, the results of air content indicate that the compaction by vibration could eliminate the entrapped air by extracting from concrete between 10 and 30 liters of air, this level of compaction also influenced the unit weight and exhibits a very dense cementitious matrix.

Table 3. Proportions and fresh stage properties for the mixtures evaluated in this work

Material, parameter or property	Mixtures											
	M5	**M5L**	**M5Q**	**M10**	**M10L**	**M10Q**	**M15**	**M15L**	**M15Q**	**M20**	**M20L**	**M20Q**
W/C weight ratio	0.25	0.40	0.40	0.25	0.40	0.40	0.25	0.40	0.40	0.25	0.40	0.40
MK by weight of cement	0.05	0.08	0.08	0.1	0.16	0.16	0.15	0.24	0.24	0.2	0.32	0.32
Water (kg/m^3)	199	199	200	199	199	200	199	199	200	200	200	200
HS (kg/m^3)	797	499	500	797	499	500	798	499	500	800	500	500
L (kg/m^3)	---	250	---	---	250	---	---	251	---	---	256	---
Q (kg/m^3)	---	---	245	---	---	245	---	-	245	---	---	259
MK (kg/m^3)	40	40	40	80	80	80	120	120	120	160	160	160
Solids in HRWRA (kg/m^3)	12	9	9	12	9	9	12	9	9	14	11	11
Sand (kg/m^3)	1369	1377	1381	1328	1336	1339	1287	1296	1298	1239	1246	1246
Unit weight (kg/m^3)	2436	2407	2399	2421	2390	2397	2424	2380	2378	2352	2330	2318
Air content before vibration (%)	1.0	1.0	1.0	2.0	1.0	1.0	2.0	2.0	2.0	3.0	2.0	3.0
Air content after vibration (%)	0.0	0.0	0.0	0.0	0.0	0.0	0.0	0.0	0.0	2.0	0.0	0.0
Mini cone Spread without vibration (cm)	30	32	33	28	31	33	27	30	32	24	28	27

To mix the ingredients and produce the twelve mixtures evaluated in this work, a 19-litre planetary mixer was used, to make individual concrete batches of 2.5 liters through the mixing procedure described below.

- Approximately, ninety percent of the water volume and all the other ingredients were added to the bowl.
- The initial mixing consisted of 4 minutes at 104 rpm, during this time is believed that the aggregates play a role at breaking powders conglomerates.
- After the initial mixing, the mixer was turned off for a period of one minute. The SP-HRWRA was mixed in the remaining volume of water to facilitate its homogenization with the other ingredients when pouring it into the mixing bowl at the end of the rest period. The delayed dosage of the admixture avoids the entrapment of the polycarboxylate chains within the first cement hydration products and improves its performance [9].
- From minute sixth to tenth the speed of the mixer was shifted to 194 rpm.

- Finally, mixing continues at a speed of 353 rpm for 5 minutes, for a total mixing time of 15 minutes.

Test methods

For the chemical and physical characterization of the powdered materials, the following analytical techniques and equipment's were used:

- Elemental chemical composition - PANalytical X-Ray Fluorescence Sprectometer, model Axios.
- Particle Size Distribution - Malvern Mastersizer 2000.
- Density - Quantachrome,Multi Pycnometer.
- Blaine Fineness - Slimatic by Interlab.
- BET specific surface area - Micromeritics ASAP 2020 Plus.

In order to identify the crystalline phases and the amorphous content of the powders, XRD patterns were acquired with a PixCel1D detector form Bruker under a continuous scan from 5 to 70 2θ. Rietveld refinement of the anhydrous powders was performed according to the recommendations and procedures described by R. Snellings et al. and K. Scrivener et al. [10, 11]. The amount of each phase was normalized through the external standard method, using for this purpose a corundum sample with known crystallinity of 98.2 %, that was calibrated with the NIST's corundum SRM 676a standard. Results are summarized in the Table 4.

For each mixture reported in Table 3, compressive strength was determined according to ASTM C 109, for which three (3 specimens) were casted, cured in a standard curing room ($T = 23 \pm 2$ °C, RH ≥ 95 %, not immersed in water) until the scheduled testing age, and tested at the ages of 7, 28 and 91 days. At the same ages, these specimens were also used to determine the bulk electrical resistivity (BER), according to the test procedure described in ASTM C 1876 and using for this purpose the equipment Giatec RCON 2 with a frequency 1 KHz.

Table 4 Phase distribution obtained through the Rietveld refinement method for the paste fractions of mixtures M15, M15L and M15Q, after 91 days of standard curing.

Phase	Mixtures		
	M15	M15L	M15Q
C_3S	15.0%	6.0%	7.0%
C_2S	6.0%	3.0%	4.0%
C_4AF	3.0%	2.0%	2.0%
Calcite	3.0%	20.0%	1.0%
Calcium Hydroxide	5.0%	3.0%	3.0%
Ettringite	4.0%	3.0%	3.0%
Quartz	-----	-----	25.0%
Bassanite	-----	1.0%	-----
Gypsum	1.0%	1.0%	1.0%
Monocarbonate	0.00%	0.10%	0.20%
Amorphous content/C-S-H	62.0%	62.0%	53.0%

To identify the most sensitive phases to the reactions due to the interaction of the different species present in the study mixtures, and to quantify or qualify their concentrations, thermogravimetric an X-Ray diffraction (XRD) analysis were performed in the paste fraction of the mixtures that presented similar compressive strengths at the age of 91 days. The thermogravimetrica analysis (TGA) were conducted using a TA instrument model SDT-Q600.

The flowability level (spread) was measured through the set of flow table and circular truncated cone specified in ASTM C 230, but without the impacts of the flow table established by the standard procedure described in ASTM C 1437. The fresh stage air content and unit weight were determined through the standard procedure describer in ASTM C 185.

Prismatic mortar bars with a square section of one inch and a length of 30 cm, were casted and cured under standard conditions for 91 days, subsequently several 3 mm thick slices were cut form the specimens with a low-speed diamond saw, and prior their image analysis to perform quantitative energy-dispersive X-Ray spectroscopy analysis (QEDS), the slices were immersed in isopropanol for 2 weeks to stop the hydration process. For the QEDS analysis, the samples were dried and mounted in resin, followed by polishing the surface and a later application of a 15 nanometers layer of carbon, in order to be analyzed with a Hitachi S-3400 N scanning electron microscope, for which the acceleration voltage and the working distance were set at 15 kV and 10 mm, respectively.

Experimental Results and Discussion

Compressive strength

For the four concrete series evaluated in this work, and for the ages of 7, 28 and 91 days, Figure 2 shows the compressive strength developments for mixtures MK, MKL and MKQ, as a function of the addition of metakaolin. (5, 10, 25 and 20%).

In the upper part of Figure 2 we can see that for MK mixtures and for the three ages for which the compressive strength is reported, the additions of metakaolin greater than 5% do not modify the compressive strength, which suggests that in concretes with additions of 10, 15 and 20%, the metakaolin is acting mainly as a filler. With compressive strengths of 109, 129 and 132 MPa at the ages of 7, 28 and 91 days, the best performance for MK mixtures was presented by the mixture with a metakaolin addition of 10%.

In this same Figure, we can see that for the four metakaolin additions (5. 10, 15 and 20%) and in relation to the results obtained for the MK mixtures, in the MKL and MKQ mixtures, the substitutions of 37.5% of the volume of cement by limestone or quartz powder, led for MKL mixtures to reductions of the compressive strength of 20.2, 11.9, 6.5 and 4.9, and 14.4, 14.4, 1.6 and 10.9 at the ages of 7 and 91 days respectively, as well as that for the MKQ mixtures with reductions of compressive strength of 15.4, 8.3, 1.9 and 5.8, and 11.2, 7.8, 0.8 and 5.9 at the ages of 7 and 91 days respectively. Based exclusively on the compressive strength, and on the results obtained at the age of 91 days, MKL and MKQ mixtures with 15% metakaolin, are the ones that contribute the most to reduce the ecological impact of the material, since with a replacement of 37.5% by volume of the cement by limestone or quartz

powder, the strengths were practically equal to those corresponding to the MK mixture (1.6% reduction for the MKL mixture and 0.8% reduction for the MKQ mixture).

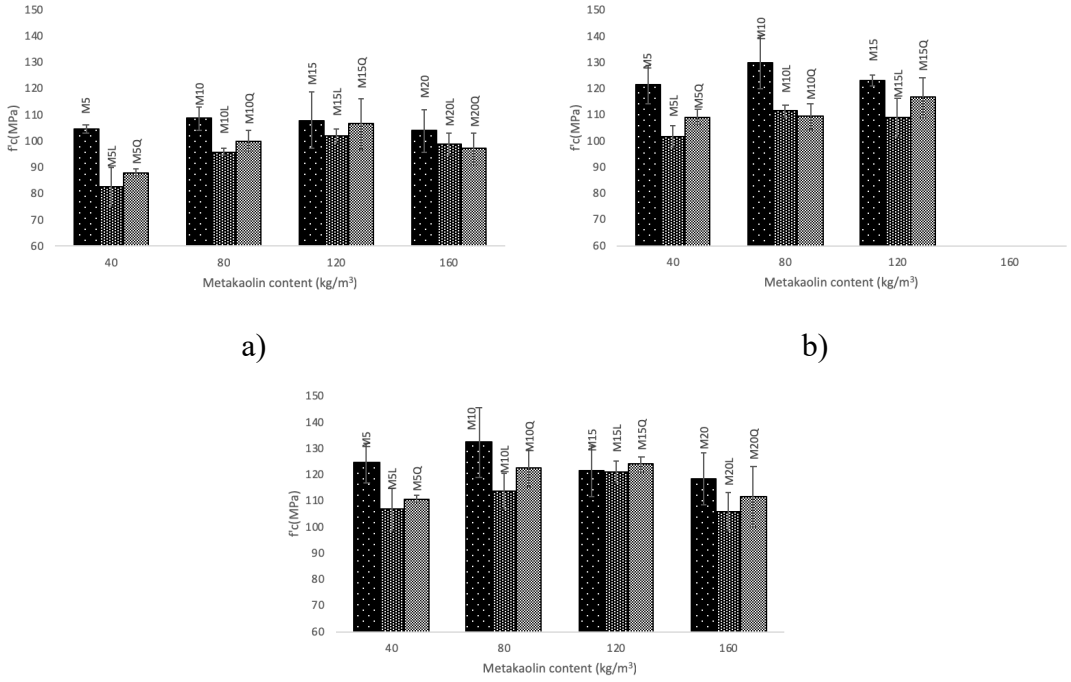

Figure 2 Compressive strength results for cement replaced and non-replaced mortar mixtures at different levels of metakaolin additions and at different ages a) 7 days, b) 28 days and c) 91 days.

In comparison with the compressive strengths results of mixtures MK, it was expected that in mixtures MKL the potential reaction between metakaolin and limestone powder could generate similar or superior strengths as a result of the presence of carboaluminate hydration products [5], but the results obtained for mixtures MKQ suggest that in the MKL mixtures the reaction between metakaolin and limestone powder did not occur or that it was incipient, as well as that in low w/c systems the filler effect of limestone powder is more dominant.

Bulk Electrical Resistivity (BER)

As an estimation of the potential concrete durability, cubic standard specimens were used to determine the BER according to the standard procedure described in ASTM C 1876, and to evaluate also the probability of chloride ion penetration through the AASHTO T358 (Standard Method of Test for Surface Resistivity Indication of Concrete's Ability to Resist Chloride Ion Penetration) qualitative classification, but througth the limits in terms of BER (High > 6, Moderate 6 ≤ 10.5, Low 10.5 ≤ 18.75, Very Low 18.75 ≤ 127 and Negligible > 127 Kohm·cm), that were calculated through the procedure proposed by W. Morris et al. in 1996 [12], from the correspondent limits provided by AASHTO T358 for the Wenner surface electrical resistivity test (High > 12, Moderate 12 ≤ 21, Low 21 ≤ 37, Very Low 37 ≤ 254 and Negligible > 254 Kohm·cm).

For mixtures MK5, Mk10, MK15 and MK20, the BER results reported in Figure 3, up to an age of 91 days, suggest that the additions of metakaolin provide the most beneficial matrix densification, for these mixtures the BER values at an age of 7 days were 13.5, 23.0, 30.0 and 28.0 kohm.cm, respectively, corresponding to a low (10.5 ≤ 18.75 kohm·cm) or very low (18.75 ≤ 127 kohm·cm) probability of chloride ion penetration. For mixtures MK5, MK10 and MK15, the development of BER between the ages of 7 and 28 days were 1.05, 3.38 and 2.86 kohm-cm/day, corresponding for this period to a net BER development of 45.8, 58.2 and 41.7 %, respective to the BER value obtained at 91 days, this performance indicate that the matrix densification is more significant in this period. The development of BER between the ages of 28 and 91 days was less significant with values of 0.20, 0.44 and 0.86 kohm·cm/day, and contributes with 26.0, 23.0 and 37.5 % of the total BER obtained at 91 days. For mixtures MK5, MK10, MK15 and MK20 the BER results at 91 days were 48, 122, 144 and 130 kohm·cm, corresponding to a very low (18.75 ≤ 127 kohm·cm) or negligible probability of chloride ion penetration (>127 kohm·cm). The abrupt and most significant level of densification that the mixtures MK5, MK10 and MK15 developed during the first 28 days was 74.0, 77.0 and 62.5 % (including the 28.1, 18.9 and 20.8 % developed the first 7 days, respectively) of the 100 % developed at 91 days is attributed to the to the high reactivity of metakaolin. Even though mixture MK15 presented the highest BER at 91 days (14

kohm·cm), mixture MK10 was the one that developed the highest level of densification during the first 28 days (77.0 %).

The volume substitution of 37.5 % of cement by either L or Q originated a significant BER reductions. At the ages of 7/28/91 days, the results of BER for mixtures M5L, M10L, M15L and M20 were lower than the ones presented by the correspondent mixtures M5, M10, M15 and M20 by 29.6/22.5/25.0 %, 8.7/46.3/23.8 %, 23.3/42.2/42.4 % and 32.1/(n/a)/47.4 % respectively, and at the same ages, the reductions for mixtures M5Q, M10Q, M15Q and M20Q were 40.7/35.2/29.2 %, 43.5/47.3/36.9 %, 40.0/51.1/45.8 % and 35.7/(n/a)/48.5 % respectively. The lower reactivity shown by the previous results is due to the significant reduction of the cement that also caused reductions in the development of BER between the ages of 7 and 28 days and between the ages of 28 and 91 days (7-28/28-91, in kohm-cm/day), for mixtures M5L, M10L and M15L, the development of BER was 0.86/0.13, 1.40/0.67 and 1.38/0.49 kohm-cm/day, and for mixtures M5Q, M10Q and M15Q the development of BER was 0.71/0.17, 1.74/0.44 and 1.24/0.54 kohm-cm/day respectively. Although at the age of 7 days the mixtures with L or Q presents a moderate ($6 \leq 10.5$ Kohm·cm) or low ($10.5 \leq 18.75$ Kohm·cm) ability to resist chloride Ion Penetration, in the short term, all these mixtures improve their level of densification and present a very low ($18.75 \leq 127$ Kohm·cm) permeability that will be improve as time passes, as illustrated by the development of BER for the periods of 7 to 28 days and 28 to 91 days. To compliment these results and, at the same time, to confirm if the contribution of L to the densification of the cementitious matrix was merely as a filler or if it reacts in the presence of metakaolin, sections 3.3, 3.4 and 3.5 present the results of the following microstructural analysis: termogravimetric analysis, X-Ray diffraction and X-Ray spectroscopy.

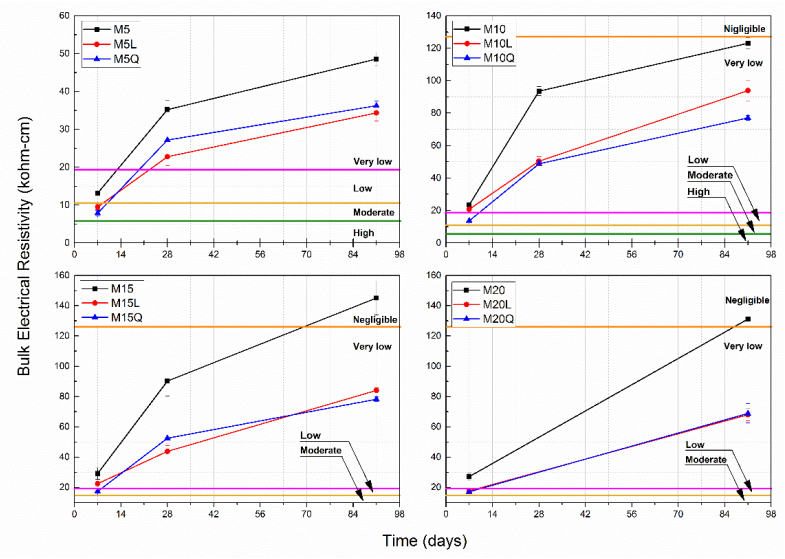

Figure 3 Bulk electrical resistivity results at ages between 7 and 91 days for concretes with metakaolin (M) and limestone (L) or quartz (Q) powders. A qualitative indication of the probability of chloride ion penetration, calculated for the BER results from those reported in AASHTO T358 is also included.

Thermogravimetric Analysis

These analyses were performed on paste fractions reproduced from the proportions of mixtures that presented similar compressive strengths at 91 days, M15, M15L and M15Q. For this purpose, the pastes were pulverized until the whole powder passes the sieve with a nominal opening of 150.0 µm (No. 100) and subsequently the solvent exchange method with isopropanol and diethyl ether was used to freeze the hydration process. The tests were carried out on 50 mg samples with a ramp of 10ºC/minute within a temperature range of 25 to 1000 ºC and a nitrogen flow of 50 ml/min.

The derivative thermogravimetric curves (DTG) for this paste fractions appears in Figure 4 and evidence that the amount of calcium hydroxide and monocarbonate is almost the same, regardless of the substitution of cement by limestone powder. The presence of monocarbonate in the paste fraction of mixture M15Q is attributed to the presence of calcite in the cement.

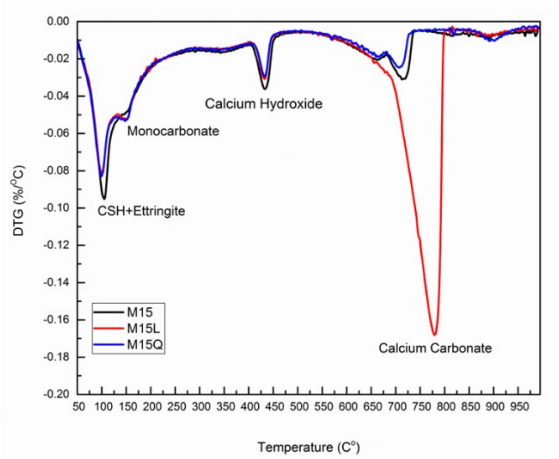

Figure 4 Derivative of the Thermogram for the paste fractions of mixtures M15, M15L and M15Q at 91 days.

From the TGA analysis, the calcium hydroxide (CH) content was obtained through the tangent method, and the bound water (Bw) regarded as the mass between 35 °C and 1000 °C the minus the amount of carbon dioxide resulting from by the decarbonation of carbonate minerals. The changes of CH and Bw normalized to the amount of cement in the sample and in relation to time are summarized in Figure 5, this figure illustrates the progress in cement hydration and the reaction of metakaolin as the amount of CH decreases.

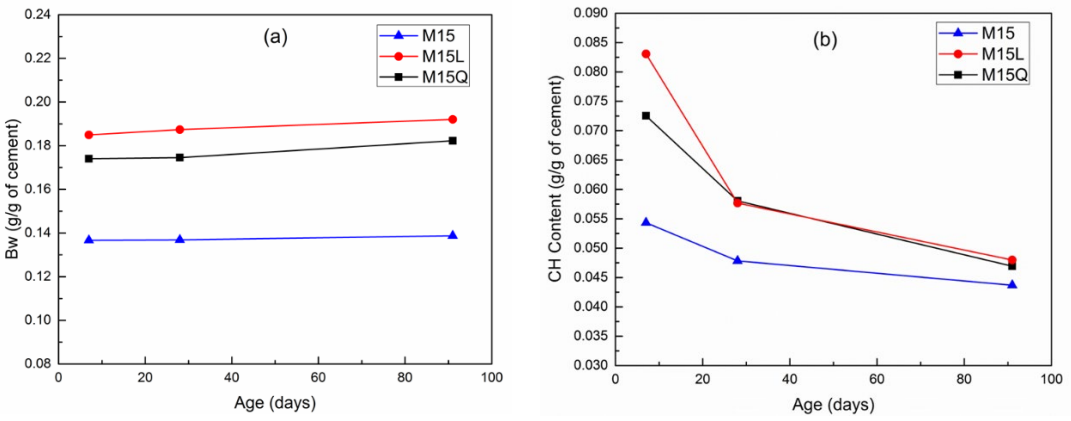

Figure 5 Development of bound water a) and calcium hydroxide content b) between 7 and 91 days for mixtures M15, M15L and M15Q

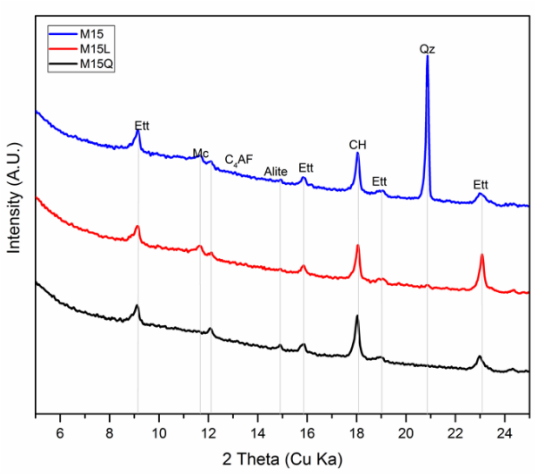

Figure 6 Mineral phases identified by XRD, in the paste fraction of mixtures M15, M15L and M15Q, after 91 days standard curing (ettringite: Ett, monocarbonate: Mc, tricalcium silicate: Alite, tretracalcium ferroaluminate: C_4AF, calcium hydroxide: CH, and quartz: Qz).

In Figure 5a, it can be observed that the substitution of cement by L or Q increases Bw by 0.04 and 0.03 g/g at an age of 7 days, and that slightly increases to 0.05 and 0.04 g/g at an age of 91 days [13], indicating a higher hydration level in mixtures M15L and M15Q, showing that the replacement of cement by fillers significantly increases the hydration degree. On the other hand, results indicate that in mixture M the hydration level remained the same between 7 and 91 days. At a macro level, these results are in agreement with the compressive strength results reported in Figure 2.

Regarding the reactivity of MK, Figure 5b shows that the development of the pozzolanic reaction if this supplementary cementitious material mainly occurs between the ages of 7 and 28 days, since after 28 days the reaction remains mostly dormant. Even though it has been stated that in comparison with other fillers, in cementitious systems with limestone filler the CH consumption increases as the limestone addition increases [4], in our case, this assertion is not valid because the sample with quartz presented almost the same calcium hydroxide content between the ages of 28 and 91 days. The reduction in the pozzolanic activity of MK between the ages of 28 and 91 days may be due to the fact that the MK used in this work has a high amount of kaolin [14].

X-Ray Diffraction

In a Portland cement system with a filler, the hydration level will increase as the amount of bound water increases and the phase dissolution can be monitored through an XRD analysis to identify the mineral phases that are present in the sample, the Figure 6 shows qualitatively the phases found in pastes fractions of mixtures M15, M15L and M15Q. As products of hydration it was possible to identify ettringite, monocarbonate and calcium hydroxide. Unlike what was reported in other works that used this technique to evaluate the hydration activity of Portland cement based systems with limestone filler [5, 15, 16], in the samples evaluated in this work at 91 days the presence of the phase hemicarbonate or strätlingite was not found.

To quantify the amount of the mineral phases reported in the difractograms of Figure 6, the High Score Plus software was used to perform the Rietveld refinement to the information provided by the XRD difractograms, including the determination of the background trough the bending factor functions of the software. In order to increase the robustness of the Rietveld refinement, a previous refinement of the anhydrous cement was performed to define the unit cell constants, and the profile variables that remained constant in the refinement of the hydrated samples [11]. Only the scale factor of the clinker phases was allowed to variate, and in the case of the hydration products the unit cell was restricted to a variation of 1% and the profile parameter *w* was restricted to oscillate between 0.0001 to 0.2. Once the Rietveld refinement was finished the results were corrected by the Mass Attenuation Coefficient and normalized using the G factor method [17].

Additionally, to the mineral phases identified in Figure 6, the presence of the following phases was also detected and quantified through the Rietveld refinement method: belite (C_2S), calcite, basanite, gypsum and amorphous content (C-S-H). The results of the refinement that appears in Table 4 confirm the very little amount of the monocarboaluminate phase identified also by the TGA analysis. As reported previously from thermodinamical modelling and mass balance analysis [18], the results indicate that the reaction degree of limestone is minimum, still in conditions in which there is sufficient amount of aluminate, calcium and water, the production of such phase is scarce [16].

The degree of hydration was calculated according to Equation 1 with the difference in the concentration of the phases in the hydrated and unhydrated Portland cement (C_3S, C_2S, C_3A and C_4AF), the results are presented in the Figure 7.

$$DOH = \frac{(C_3S,C_2S,C_3A \text{ and } C_4AF)_{anhydrous} - (C_3S,C_2S,C_3A \text{ and } C_4AF)_{sample}}{(C_3S,C_2S,C_3A \text{ and } C_4AF)_{anhydrous}} \quad \text{Eq. (1)}$$

Where:

DOH: Degree of hydration of the cement

$(C_3S, C_2S, C_3A \text{ and } C_4AF)_{anhydrous}$: Is the sum of clinker phases in the anhydrous cement.

$(C_3S, C_2S, C_3A \text{ and } C_4AF)_{sample}$: Is the sum of clinker phases in the hydrated sample.

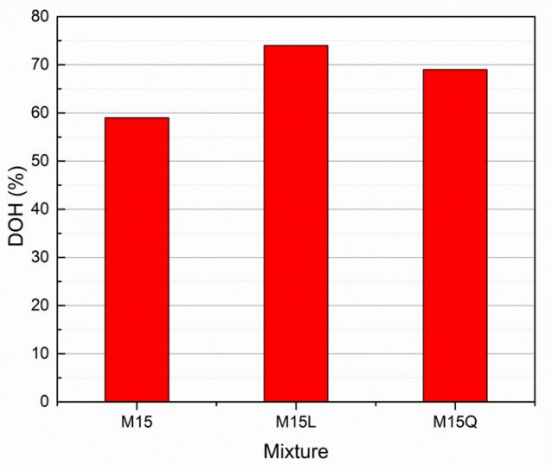

Figure 7 Cement's Degree of Hydration at 91 days for paste fractions of samples M15, M15L and M15Q.

Figure 7 clearly evidence the improvement in terms of hydration degree when fillers are used in a Portland cement based cementitious system, as the paste fractions for mixtures M15L and M15Q presented higher hydration degrees (74 and 69% respectively) in comparison with the one obtained for the paste fraction of mixture M15 (59 %). From these results we can also highlight that in this comparison, the metakaolin addition and the low w/c ratio decreased the degree of hydration of the portland cement, and that the substitution of 37.5 % of the cement volume by L or Q fillers practically led to complete hydration of all cement. In this

regard . when cements with a scarce amount of C_3A are combined with metakaolin, they will present a low performance (decreased dissolution and hence low mechanical performance), attributed to a rapid decrease in the alkalinity of the pore solution, which is not present in systems made exclusively with Portland cement [15]. However, due to rheological and workability issues, in UHPC mixtures it is always recommended to use cements with low amounts of aluminates and to define the most compatible polycarboxylate admixture (structure and dosage) [19].

Finally, an indirect measurement of the pozzolanic reaction was performed by determining the amount of calcium hydroxide consumed in the paste. For this purpose, first the Ca/Si ratio of the C-S-H was determined through Equation 2 as a function of the Alite dissolution and of the calcium hydroxide production, on paste fractions without metakaolin and with w/c of 0.25 and 0.4, that previously to the analysis remain under standard cured for 91 days [20]. The Ca/Si ratios obtained for pastes with w/c of 0.25 and 0.4 were 1.85 and 2.01 respectively.

$$\frac{Ca}{Si} = 3 - \frac{\%CH * \%C_3S}{mwCH * mwC_3S} \qquad \text{Eq. (2)}$$

Where:

Ca/Si: Is the calcium to silica ratio of the C-S-H that results from the reaction of Alite

%CH: Is the weight in percentage of calcium hydroxide normalized for the cement content in the sample.

mwCH: Is the molar weight of calcium hydroxide.

$\%C_3S$: Is the weight in percentage of the C_3S that reacts and normalized for the cement content in the sample.

mwC_3S: Is the molar weight of the C_3S.

This Ca/Si ratios were used to estimate trough Equations 3 and 4, the amount of calcium hydroxide produced in the reaction

$$\%CH_{0.25} = \%C_3S * \frac{mwCH}{mwC_3S} * (3 - \frac{Ca}{Si} for\ 0.25\ mix(1.85)) \qquad \text{Eq. (3)}$$

$$\%CH_{0.40} = \%C_3S * \frac{mwCH}{mwC_3S} * (3 - \frac{Ca}{Si} for\ 0.4\ mix(2.01)) \quad \text{Eq. (4)}$$

Where:

$\%CH_{0.25}$= Is the estimated percentage of calcium hydroxide resulting from the hydration of the Alite in the cement, for a paste fraction with a w/c of 0.25 analyzed after 91 days of standard curing.

$\%CH_{0.4}$= Is the estimated percentage of calcium hydroxide resulting from the hydration of the Alite in the cement, for a paste fraction with a w/c of 0.40 analyzed after 91 days of standard curing.

Finally, the consumed CH was obtained by the following Equation.

$$\%CH_c = \frac{\%CH_{0.40 or\ 0.25} - \%CH}{\%CH_{0.40\ or\ 0.25}} \quad \text{Eq. (5)}$$

Where

%CHc: Is the estimated consumed CH

$\%CH_{0.4\ or\ 0.25}$ = As described before, is the estimated CH production. The result obtained for paste with a w/c of 0.25 were used to calculate the 91 day theoretical CH content for mixture M15, and the result obtained for a paste with a w/c of 0.40 were used to calculate the 91 day theoretical CH contents for mixtures M15L and M15Q.

In order to be able to compare the consumed CH in the three mixtures, the value was normalized dividing the consumed CH by the 91-day theoretical CH, to obtain a percentage which is presented in the Figure 8. Results indicate that with the cement replacement by L or Q, the portlandite consumption increases 15%. The almost equal performance presented by mixtures M15, M15L and M15 Q in terms of compressive strength is attributed to the increase of both, the hydration degree and the portlandite consumption.

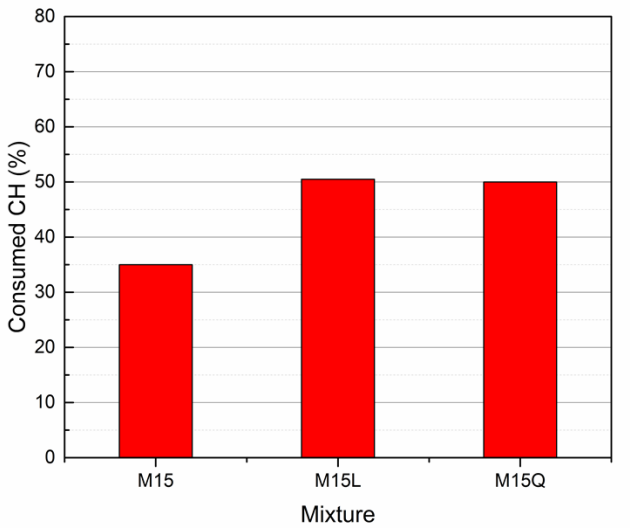

Figure 8 Consumed Calcium Hydroxide in the paste fraction of mixtures M15, M15L and M15Q after 91 days of standard curing.

X-Ray Spectroscopy

In a binary Portland cement-metakaolin based cementitious system one of the reaction products will be the Calcium-aluminum-silicate-hydrates (C-A-S-H). To determine the composition of this hydrate, bars of UHPC with dimensions of one square inch and a length of 10 inches were casted and standard cured for 91 days. From this specimens, slices of 3 mm thick were cut with a diamond saw and stored immersed in isopropanol for two weeks to remove as much free water as possible. Then the samples were dried by the solvent exchange method, and after they were mounted in resin, polished, and coated with a 15 nm carbon layer. Finally, the samples were introduced to a scanning electronic microscope (SEM) equipped capable to perform Quantitative Energy-Dispersive X-Ray Microanalysis (QEDS).

To perform quantitative measurements in the cement paste, standards were used for every relevant element within the cement paste: C_2S for Ca and Si, C_3A for Al, olivine for Mg and Fe, anhydrite for S, orthoclase for K, tugtupite for Na and Cl, and sphene for Ti. The obtained spectra were post-processed with the NIST software DTSA-II, that allow us to obtain quantitative data from the information of previously measured standards with a known chemical composition. The Duane-Hunt limit was used to exclude points where local

charging could have taken place. The investigation was performed in the paste around the aggregates in layers of 3 μm, for a total thickness of 50 μm within the paste around the aggregate particle (Figure 9).

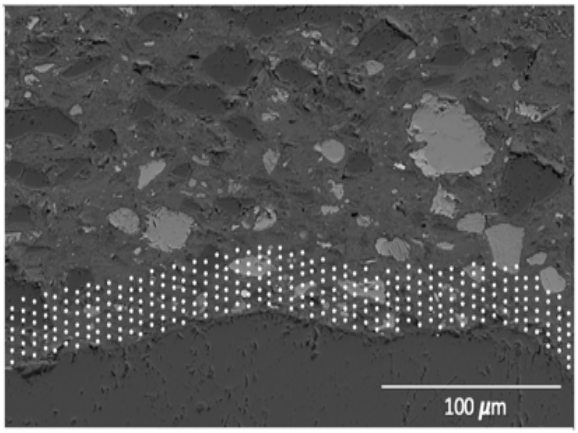

Figure 9 Example of the spot analysis on the paste to define the C-A-S-H composition.

For this purpose, bivariate histograms were constructed with the Si/Ca vs Al/Ca molar ratios (Figure 10). The red dots in the intersection are representative of the C-A-S-H composition, and its average elemental ratios are summarized in Table 5. The different molar ratios reported in Table 5 shows very similar C-A-S-H compositions among the mixtures evaluated through this analysis, and also that in comparison with the typical Al/Ca ratio for ordinary Portland cement (0.05) [21], the ternary Portland cement-filler-metakaolin cementitious systems and the binary cement-metakaolin system presented AL/Ca ratios of 0.20 or higher. it is noted the great aluminum incorporation in the C-A-S-H passing from the 0.05 Al/Ca ratio in normal OPC pastes to more than 0.2. This heavy Al incorporation results from the high kaolinite content in our calcined clay [22]. Wrapping up the results, we could see that the limestone filler is not specially more beneficial when used in conjunction with calcined clays in low water/cement environments, further evaluation with other type of fillers must be done to expand the metakaolin based ternary systems to not only calcite. Nevertheless, the use of any kind of fillers enhance the hydration degree in systems with very low water availability.

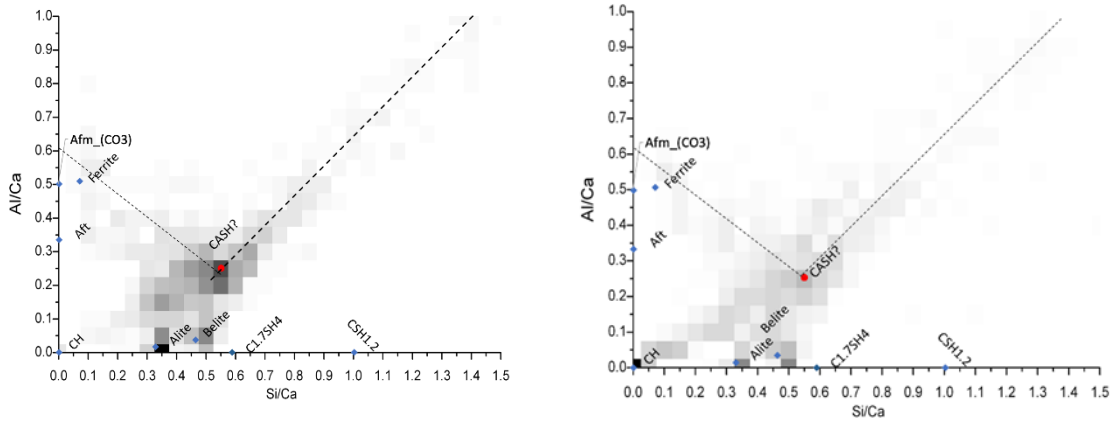

a) b)

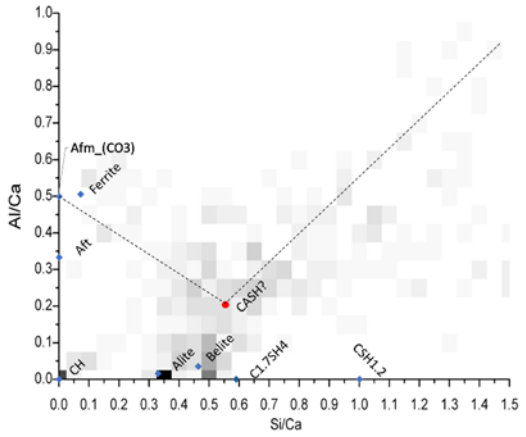

c)

Figure 10 Bivariate Histograms for the definition of C-A-S-H composition for mixtures M15 a) M15L b) and M15Q c) after 91 days of standard curing.

Table 5 C-A-S-H composition for mixtures M15, M15L and M15Q after 91 days of standard curing.

Mixture	Ca/Si	Al/Ca	S/Ca	Fe/Ca
M15	1.82 *±0.05*	0.25 *±0.01*	0.06 *±0.01*	0.03 *±0.02*
M15L	1.82 *±0.05*	0.25 *±0.02*	0.04 *±0.02*	0.03 *±0.03*
M15Q	1.80 *±0.05*	0.20 *±0.04*	0.03 *±0.01*	0.04 *±0.06*

Conclusions

Based on the results and commentaries of this work, the following conclusions can be drawn:

1. In terms of compressive strength and sustainability, the UHPC that presented the best performance was the one with a metakaolin addition of up to 15 % by mass of cement of metakaolin and with a substitution of 37.5 % of the cement volume by either limestone or quartz filler. Higher additions of metakaolin are ineffective.
2. As a durability index, the bulk electrical resistivity indicates that metakaolin additions between 10 and 20 % by mass of the cement significantly improves the ability of these concretes to resist chloride ion penetration and reach the maximum the highest level of imperviousness considered in AASHTO T358 (negligible for BER > 127 Kohm·cm), since an age of 70 days or later.
3. Results of TGA revealed that the hydration of both cement and metakaolin is very active between 7 and 28 days, and dormant at later ages, as well as that the substitution of cement by limestone or quartz fillers (37.5 % by volume), improves the hydration reaction and as a result of the significant cement reduction that also decreased the amount of portlandite by 15 %.
4. XRD results indicate that the low water-cement ratio and the high reactivity of metakaolin didn't allow the formation of monocarboaluminate.
5. From the QEDS it was possible to quantify the increased aluminum incorporation at 15% MK passing from a normal C-A-S-H Al/Ca ratio of 0.05 to 0.20. Both quartz and limestone filler replaced samples yield the same type of C-A-S-H.

References

[1] G. Benjamin A., “Material Property Characterization of Ultra-High Performance Concrete,” FHWA, no. FHWA-HRT-06-103, p. 186, 2006.

[2] K. L. Scrivener, V. M. John, and E. M. Gartner, “Eco-efficient cements: Potential, economically viable solutions for a low-CO2, cement-based materials industru,” 2016.

[3] Dale P. Bentz, A Edgardo F., Irassar B., Brooks Bucher C., and W. Jason Weiss C, Limestone Fillers to Conserve Cement in Low w/cm Concretes: An Analysis Based on Powers’ Model, Concrete International, vol. 31, No. 11 and 12, pp. 41-46 and 35-39, 2009.

[4] W. Huang, H. Kazemi-Kamyab, W. Sun, and K. Scrivener, “Effect of replacement of silica fume with calcined clay on the hydration and microstructural development of eco-UHPFRC,” *Mater. Des.*, vol. 121, pp. 36–46, 2017.

[5] M. Antoni, J. Rossen, F. Martirena, and K. Scrivener, “Cement substitution by a combination of metakaolin and limestone,” *Cem. Concr. Res.*, vol. 42, no. 12, pp. 1579–1589, 2012.

[6] Elizabeth I. Nadelman and Kimberly E. Kurtis, “Application of Powers’ model to modern portland and portland limestone cement pastes”, Journal of the American Ceramic Society, vol. 100, no. 9, pp. 4219-4231, 2017.

[7] O. M. Jensen and P. F. Hansen, “Water-entrained cement-based materials I . Principle and theoretical background,” *Cem. Concr. Res.*, vol. 31, pp. 1–13, 2000.

[8] K. Wille, A. E. Naman, and G. J. Parra-Montesinos, “Ultra - High Performance Concrete with Compressive Strength Exceeding 150 MPa (22ksi) : A Simpler Way,” *ACI Mater. J.*, vol. 108, no. 1, pp. 46–53, 2011.

[9] N. V Tue, J. Ma, M. Orgass, and E. Fehling, “Influence of addition method of superplasticizer on the properties of fresh UHPC,” in *2nd International Symposium on Ultra High Performance Concrete*, 2008.

[10] R. Snellings, A. Bazzoni, and K. Scrivener, “The existence of amorphous phase in Portland cements: Physical factors affecting Rietveld quantitative phase analysis,” *Cem. Concr. Res.*, vol. 59, pp. 139–146, 2014.

[11] K. Scrivener, R. Snellings, and B. Lothenbach, *A Practical Guide to Microstructural*

Analysis of Cementitious Materials. 2016.

[12] W. Morris, E. I. Moreno, and A. A. Sagüés, "Practical evaluation of resistivity of concrete in test cylinders using a Wenner array probe," *Cem. Concr. Res.*, vol. 26, no. 12, pp. 1779–1787, 1996.

[13] W. Huang, H. Kazemi-Kamyab, W. Sun, and K. Scrivener, "Effect of cement substitution by limestone on the hydration and microstructural development of ultra-high performance concrete (UHPC)," *Cem. Concr. Compos.*, vol. 77, pp. 86–101, Mar. 2017.

[14] François Avet and Karen Scrivener, "Investigation of the calcined kaolinite content on the hydration of Limestone Calcined Clay Cement (LC3)," *Cem. Concr. Res.*, vol. 107, pp. 124–135, 2018; doi.org/10.1016/j.cemconres.2018.02.016

[15] M. Cyr, M. Trinh, B. Husson, and G. Casaux-Ginestet, "Effect of cement type on metakaolin efficiency," *Cem. Concr. Res.*, vol. 64, pp. 63–72, 2014.

[16] G. Puerta-Falla, M. Balonis, G. Le Saout, N. Neithalath, and G. Sant, "The influence of metakaolin on limestone reactivity in cementitious materials," *RILEM Bookseries*, 2015.

[17] Y. P. Stetsko, N. Shanahan, H. Deford, and A. Zayed, "Quantification of supplementary cementitious content in blended Portland cement using an iterative Rietveld-PONKCS technique," *J. Appl. Crystallogr.*, vol. 50, pp. 498–507, 2017.

[18] F. Avet, X. Li, and K. Scrivener, "Determination of the amount of reacted metakaolin in calcined clay blends," *Cem. Concr. Res.*, vol. 106, no. February, pp. 40–48, 2018.

[19] Johannes Arend, Alexander Wetzel and Bernhard Middendorf, Fluorescence Microscopic Investigations of the Retarding Effect of Superplasticizers in Cementitious Systems of UHPC, Materials, 13, 1057, 13 pp., 2020; doi:10.3390/ma13051057

[20] J. I. Escalante-Garcia, G. Mendoza, and J. H. Sharp, "Indirect determination of the Ca/Si ratio of the C-S-H gel in Portland cements," *Cem. Concr. Res.*, vol. 29, no. 12, pp. 1999–2003, 1999.

[21] W. Wilson, J.M. Rivera-Torres, L. Sorelli, A. Durán-Herrera, A. Tagnit-Hamou; "The micromechanical signature of high-volume natural pozzolan concrete by combined statistical nanoindentation and SEM-EDS analyses"; Cement and Concrete Research,

Volume 91, pp. 1–12, 2017.

[22] F. Avet, E. Boehm-Courjault, and K. Scrivener, “Investigation of C-A-S-H composition, morphology and density in Limestone Calcined Clay Cement (LC3),” *Cem. Concr. Res.*, vol. 115, no. July 2018, pp. 70–79, 2019.

7 Conclusions in English

- Ultra High Performance Concrete is a mix of both physical and chemical phenomena.
- Whitin the work it was explained that due to the very low water/cement ratio and pozzolanic additions on UHPC the cement can not completely react allowing the concrete designer to optimize costs and improve the sustainability of the product by adding large quantities of fillers.
- In both MK and SF systems it was shown that after certain pozzolanic addition there are no more evident benefits, we attribute this to the physical distribution of the pozzolan and to the water availability
- Very little differences on hydration, mechanical and durable properties of the mixtures when the filler was varied from a soft material to a harder one. The description of this behavior can broaden the combinations of materials to yield low cost and acceptable UHPC mixes around the world
- The use of microstructural characterization not only allows understanding but shows a clear dependency between the hydration and the macroscopic performance.
- Ternary blends of the kind of this document can be the foundation for new more durable and possibly cheaper cements, (products like this are already on the Canadian market).

8 Conclusions en français

- Le béton à ultra-hautes performances est un mélange de phénomènes physiques et chimiques.

- Dans le cadre de ce travail, il a été expliqué qu'en raison du très faible rapport eau/ciment et des ajouts pouzzolaniques sur le BUHP, le ciment ne peut pas réagir complètement, ce qui permet au concepteur du béton d'optimiser les coûts et d'améliorer la durabilité du produit en ajoutant de grandes quantités de charges.

- Dans les systèmes MK et SF, il a été démontré qu'après certains ajouts pouzzolaniques, il n'y a plus d'avantages évidents, nous attribuons cela à la distribution physique de la pouzzolane et à la disponibilité de l'eau.

- Très peu de différences sur l'hydratation, les propriétés mécaniques et durables des mélanges lorsque la charge est passée d'un matériau mou à un matériau plus dur. La

description de ce comportement peut élargir les combinaisons de matériaux pour produire des mélanges de BUHP acceptables et à faible coût dans le monde entier.

- L'utilisation de la caractérisation microstructurale permet non seulement de comprendre mais aussi de montrer une dépendance claire entre l'hydratation et la performance macroscopique.
- Les mélanges ternaires du type de ceux présentés dans ce document peuvent être à la base de nouveaux ciments plus durables et peut-être moins chers (des produits de ce type sont déjà sur le marché canadien).

9 Recommendations for future work

The present work showed alternatives of mix design for UHPC showing that high strengths can be achieved by either silica fume or metakaolin. Furthermore, the project showed that the filler effect plays a really important role in performance characteristics of the material.

-Recommendations:

- To explore binary matrices with pozzolanic materials under the same parametric study
- To study the pozzolanic reaction with the x ray diffraction technique to see if it is possible to separate the reaction of high pozzolanic materials from the regular pozzolans.
- To study the C-A-S-H distribution within the matrix
- Add thermodynamic modeling to the study
- Replace metakaolin by less reactive calcined clays
- To study different durable parameters of this kind of concrete like, sulfate resistance, chloride permeability, carbonation, resistance to freez-thaw cycles.
- To study the possibility of making such compounds with alkali activated cements.

10 Annexes

10.1 Evidence of the submission of paper No. 1

Manuscript ID M-2021-062 - Manuscript Receipt Acknowledgment

AS **ACI Structural and Materials Journals <onbehalfof@manuscriptcentral.com>** Ayer a las 22:03

Para

16-Feb-2021

Dear Mr. Guillermo Hernández-Carrillo

Thank you for submitting the manuscript titled, "Optimization of UHPC by the use of limestone and quartz fillers," for possible publication in the ACI Journals. Please refer to Manuscript ID M-2021-062 in all correspondence regarding this manuscript.

If the manuscript is found to comply with the ACI Publications Policy and the ACI Author Guidelines, it will be peer reviewed to determine its suitability for publication. The peer review process is expected to last three to six months.

To view the status of your manuscript, please visit your Author Center at https://na01.safelinks.protection.outlook.com/?url=https%3A%2F%2Fmc.manuscriptcentral.com%2Faci&data=04%7C01%7C%7Cf9c81645b32b44dca04808d8d2f90625%7C84df9e7fe9f640afb435aaaaaaaaaaaa%7C1%7C0%7C637491314274638488%7CUnknown%7CTWFpbGZsb3d8eyJWIjoiMC4wLjAwMDAiLCJQIjoiV2luMzI submitted manuscripts are listed in the "Submitted Manuscripts" folder under "My Manuscripts."

Please return the completed Copyright Transfer Form found under the Instructions & Forms tab at the top right corner of https://na01.safelinks.protection.outlook.com/?url=https%3A%2F%2Fmc.manuscriptcentral.com%2Faci&data=04%7C01%7C%7Cf9c81645b32b44dca04808d8d2f90625%7C84df9e7fe9f640afb435aaaaaaaaaaaa%7C1%7C0%7C637491314274638488%7CUnknown%7CTWFpbGZsb3d8eyJWIjoiMC4wLjAwMDAiLCJQIjoiV2luMzI and return it to ACI. By signing the form, the author(s) are certfying that the manuscript:

(a) is presented for ACI's exclusive use;
(b) has not been published previously;
(c) is not under consideration for publication elsewhere.

If there are any changes in your e-mail address or other contact information, please log in to Manuscript Central at https://na01.safelinks.protection.outlook.com/?url=https%3A%2F%2Fmc.manuscriptcentral.com%2Faci&data=04%7C01%7C%7Cf9c81645b32b44dca04808d8d2f90625%7C84df9e7fe9f640afb435aaaaaaaaaaaa%7C1%7C0%7C637491314274638488%7CUnknown%7CTWFpbGZsb3d8eyJWIjoiMC4wLjAwMDAiLCJQIjoiV2luMzI and edit your user information as appropriate under the "Edit Account" tab in the top right corner.

Thank you for submitting your manuscript for possible publication in the ACI Journals.

Sincerely,
Ms Angela Matthews
Journals.Manuscripts@concrete.org

10.2 Evidence of the submission of paper No. 2

Technical Paper MTENG-12278 sent to Editor - [EMID:9b9eb16e034c4942]

JO **em.jrnmteng.0.70bbcd.4557600f@editorialmanager.com <em.jrnmteng.0.70bbcd.4557600f@editorialmanager.com>** en nombre de **Journal of Materials in Civil Engineering <em@editorialmanager.com>** Ayer a las 23:39

Para Guillermo Hernández-Carrillo

You are being carbon copied ("cc:\d") on an e-mail "To" "Alejandro Duran-Herrera"
CC: "Guillermo Hernández-Carrillo" ; , "Arezki Tagnit-Hamou" arezki.tagnit-hamou@usherbrooke.ca

Dear Alejandro Duran-Herrera,

Your submission, entitled "Effect of limestone and quartz fillers in UHPC with calcined clay," has been assigned manuscript number MTENG-12278 and has been forwarded to the Editor to begin the review process.

You may check the progress of your submission by logging onto editorial management system at https://www.editorialmanager.com/jrnmteng/.

Thank you for submitting your work to this journal.

Sincerely,

Journal of Materials in Civil Engineering

In compliance with data protection regulations, you may request that we remove your personal registration details at any time. (Use the following URL: https://www.editorialmanager.com/jrnmteng/login.asp?a=r). Please contact the publication office if you have any questions.